MichiganTech
Create the Future

Dissertations, Master's Theses and Master's Reports - Open

Dissertations, Master's Theses and Master's Reports

2009

Estimation of the flammability zone boundaries with thermodynamic and empirical equations

Travis Joseph Hansen
Michigan Technological University

Recommended Citation

Hansen, Travis Joseph, "Estimation of the flammability zone boundaries with thermodynamic and empirical equations", Master's Thesis, Michigan Technological University, 2009.
https://doi.org/10.37099/mtu.dc.etds/7

ESTIMATION OF THE FLAMMABILITY ZONE BOUNDARIES WITH THERMODYNAMIC AND EMPIRICAL EQUATIONS

By Travis Joseph Hansen

A Thesis Submitted in Partial Fulfillment of the Requirements for the Degree of

Master of Science

Chemical Engineering

MICHIGAN TECHNOLOGICAL UNIVERSITY

2009

This thesis (Estimation of the Flammability Limit Boundaries with Thermodynamic and Empirical Equations) is hereby approved in partial fulfillment of the requirements for the degree of Master of Science in the field of Chemical Engineering.

Department of Chemical Engineering

Michigan Technological University

_____

Thesis Advisor   Dr. Daniel A. Crowl

_____

Department Chair   Dr. Komar Kawatra

_____

Date

I would like to thank my advisor Dr. Daniel Crowl for his input on this research project and his technical expertise. Also, his excellent recommendation letters are greatly appreciated.

I would also like to acknowledge my thesis committee: Dr. Jason Keith and Dr. Jeffrey Naber.

I would like to thank my fellow graduate students for keeping me entertained over the past two years. More importantly, I would like to thank my officemates, Juan and Michael, for listening to my commentary.

Finally, I would like to thank Gabrielle and my family. Without them, I don't know what I would do.

Table of Contents

List of Figures

x

List of Tables

xiii

List of Abbreviations, Subscripts, Superscripts, and Greek Letters

<u>Abbreviations</u>

C – a constant

C_{st} – stoichiometric volume % fuel in air

C_p – heat capacity in J mol^{-1} K^{-1}

$\bar{C}_p$ – average heat capacity in J mol^{-1} K^{-1}

dof – degrees of freedom

F_o – F-test statistic

$F_{0.05,v_1,v_2}$ – the F-value for $\alpha = 0.05$ and v_1 and v_2 degrees of freedom

ΔG – Gibb's energy

ΔH – enthalpy

$\Delta \bar{H}$ – enthalpy in J mol^{-1}

LFL – lower flammability limit

LOC – limiting oxygen concentration

LOL – lower oxygen concentration

MS – mean-squared

n – number of moles

N_c – number of carbon atoms

R – ideal gas constant

R^2 – regression coefficient

ΔS – entropy

SS – sum of squares

t – student's t-value

t_o – t-test statistic

T – temperature

UFL – upper flammability limit

UOL – upper oxygen limit

$X_{n \times m}$ – a matrix of fitting data

$y_{n \times m}$ – a matrix of data to be fit

y_i – mole fraction of component i

z – oxygen stoichiometric coefficient

<u>Subscripts</u>

ad – adiabatic

c – combusted

f – fuel

i – initial

j – a component

L – lower

m × *n* – in reference to a matrix of *m* × *n* size

p – products

r – reaction or reactant

U – upper

UFBI – upper flammability boundary intercept

UFL,O_2 – oxygen content at the UFL

UOLI – upper oxygen limit intercept

v – number of carbon atoms in a hydrocarbon

w – number of hydrogen atoms in a hydrocarbon

x – number of oxygen atoms in a hydrocarbon

y – number of nitrogen atoms in a hydrocarbon

<u>Superscripts</u>

T – transposed

<u>Greek Letters</u>

α – a heat capacity parameter associated with the fuel content

β – a heat capacity parameter associated with the oxygen content

$\hat{\beta}_{n \times m}$ – a matrix of fitting coefficients

ν – degrees of freedom

γ – a heat capacity parameter associated with inert species

ψ – fraction of groups present for a contribution method

Abstract

The flammability zone boundaries are very important properties to prevent explosions in the process industries. Within the boundaries, a flame or explosion can occur so it is important to understand these boundaries to prevent fires and explosions. Very little work has been reported in the literature to model the flammability zone boundaries. Two boundaries are defined and studied: the upper flammability zone boundary and the lower flammability zone boundary. Three methods are presented to predict the upper and lower flammability zone boundaries:

- The linear model

- The extended linear model, and

- An empirical model.

The linear model is a thermodynamic model that uses the upper flammability limit (UFL) and lower flammability limit (LFL) to calculate two adiabatic flame temperatures. When the proper assumptions are applied, the linear model can be reduced to the well-known equation $y_{LOC} = zy_{LFL}$ for estimation of the limiting oxygen concentration. The extended linear model attempts to account for the changes in the reactions along the UFL boundary. Finally, the empirical method fits the boundaries with linear equations between the UFL or LFL and the intercept with the oxygen axis.

Comparison of the models to experimental data of the flammability zone shows that the best model for estimating the flammability zone boundaries is the empirical method. It is shown that is fits the limiting oxygen concentration (LOC), upper oxygen limit (UOL), and the lower oxygen limit (LOL) quite well. The regression coefficient values for the fits to the LOC, UOL, and LOL are 0.672, 0.968, and 0.959, respectively. This is better than the fit of the "zy_{LFL}" method for the LOC in which the regression coefficient's value is 0.416.

1 Introduction and Literature Review

1.1 The Flammability Zone Boundaries

An explosion is a rapid, chemical release of energy from the oxidation of a fuel. In order for an explosion to occur, three elements must be present: a fuel, an oxidizer, and an ignition source. Experience has shown that it is impractical to eliminate ignition sources, so to prevent explosions the goal is to eliminate flammable mixtures (Crowl and Louvar 2001). To avoid flammable mixtures, the flammability zone boundaries must be studied and understood.

The flammability zone boundaries are very important properties of combustible materials. Beyond the flammable boundaries, a flame cannot propagate so it is essential to keep industrial process vessels from containing fuel-oxygen-nitrogen mixtures in the flammability zone. There are two flammability zone boundaries: the upper flammability zone boundary and the lower flammability zone boundary. The upper flammability zone boundary is the boundary in the fuel rich area of the limit. It is named as it is because it contains the upper flammability limit (UFL), where the upper flammability limit is the maximum fuel concentration that can burn in air (Crowl and Louvar 2001). The lower flammability zone boundary is in the oxygen rich area of the limit and contains the lower

flammability limit (LFL). The lower flammability limit being the minimum fuel

concentration that can burn in air (Crowl and Louvar 2001).

Often these points are reported in fuel-oxygen-nitrogen systems. Fuel-air mixtures are

often of concern because air is most frequently used as an oxidizer and nitrogen as an

inert gas. However, some sources do report the limits with as gas such as carbon dioxide

(Coward and Jones 1952; Zabetakis 1965; NFPA 1994) because it can be a convenient

inert gas when a source such as a combustion engine or boiler is near.

Another very important flammability property is the limiting oxygen concentration

(LOC). Typically, the point where the upper and the lower flammability zone boundaries

intersect is the limiting oxygen concentration. The limiting oxygen concentration is also

defined as lowest oxygen concentration where combustion can occur (Crowl and Louvar

2001). If the oxygen concentration is brought below this value, then the possibility of an

explosion is eliminated. This reason makes the LOC essential knowledge for inerting and

purging operations.

The final important points along the flammability zone boundaries are the lower and

upper oxygen limits. The lower oxygen limit (LOL) is the lowest fuel concentration in

pure oxygen that combusts and the upper oxygen limit (UOL) is the maximum fuel

concentration in pure oxygen that combusts. These two points are where the upper and

lower flammability zone boundaries intersect the nitrogen axis (Crowl and Louvar 2001).

Pure oxygen conditions are rarely seen in industrial settings but are important to complete

mapping of the flammability zone.

The flammability limits, the limiting oxygen concentration, and the oxygen limits are the

most important points along the flammability zone boundary. Often when flammability

data is reported, these parameters are given (Coward and Jones 1952; Zabetakis 1965;

Kutcha 1985; Lewis and von Elbe 1987; NFPA 1994; Lide 2006). The importance of

these locations on the flammability boundaries is shown when trying to estimate the

entire flammability zone. An accurate estimate of the flammability zone can be made

with these five points. A line is draw between the UOL and the UFL, then to LOC, from

the LOC to the LFL, and finally ending at the LOL. However, since the boundaries are

not truly linear, this is only an approximation.

1.2   Plotting of the Flammability Zone

The flammability zone data can be plotted using multiple techniques. The simplest way

to plot this data is on a rectilinear plot with oxygen concentration on the x-axis and the

fuel concentration on the y-axis. This is very convenient way to examine the limiting

oxygen concentration (Britton 2002) and is simple with the aid of spreadsheet programs

like Excel® or MathCAD®. For this style to be used, it must be understood that there is still nitrogen present in the mixture and is solved for by subtracting the fuel and oxygen concentrations in mole fractions from one. Figure 1.1 is an example of a rectilinear plot for hydrogen.
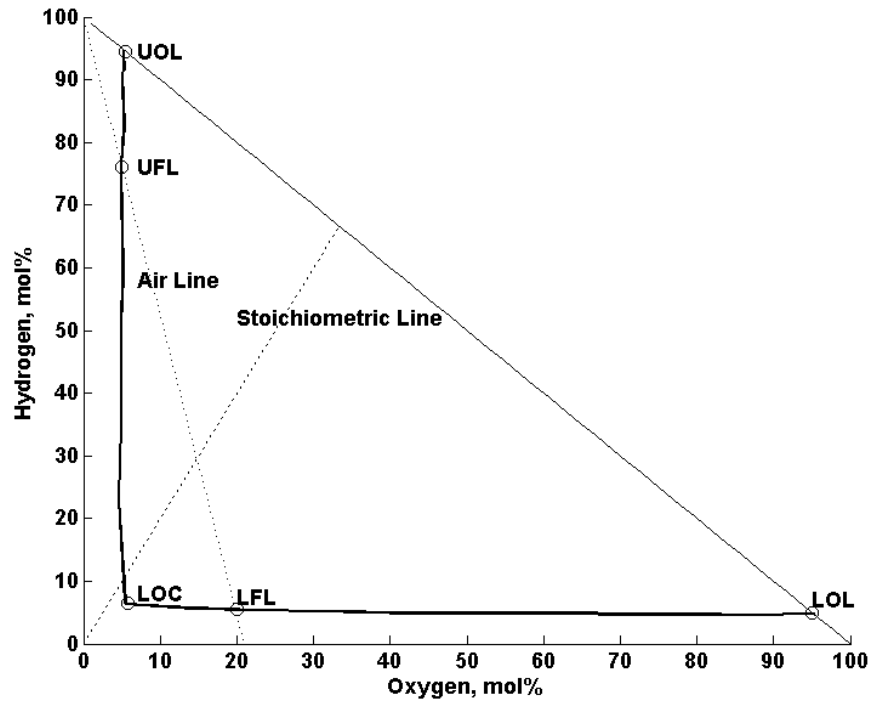
Figure 1.1:   The flammability boundary of hydrogen (Jo and Crowl 2006) plotted with the UOL, LOL, LOC, UFL, and LFL.

The stoichiometric line on the diagram represents all the stoichiometric combinations of fuel and oxygen on the graph. The air line is a line that represents all possible the fuel and air combinations.

Several other approaches have been taken to plot the flammability zone. In Coward and

Jones's Bulletin 508 (Coward and Jones 1952), the flammability zone is plotted as the

ratio of inert gas to flammable gas versus the percent flammable gas plus diluents.

Zebatakis (Zabetakis 1965) plotted the added inert gas versus the flammable gas in air.

The percent air is determined by the following equation:

$$\% \, air = 100\% - \% \, fuel - \% \, inert \qquad (1.1)$$

These methods can be quite confusing and are used because plotting all three components

(fuel, oxygen, and nitrogen) on a three-axis diagram can be difficult. However, with

better computer programs and computing power, plotting on three axis diagrams is

relatively simple.

The most straight-forward and informative method is to use a three-axis or triangle

diagram to plot the flammability data. Small amounts of data in Zebatakis's paper

(Zabetakis 1965) were plotted in this manner. More recently large amounts of data was

plotted by Mashuga and Crowl on triangle diagrams to show complete data sets

(Mashuga 1999; Mashuga and Crowl 1999). Crowl and Louvar even have a set of rules

for plotting on triangle diagrams (Crowl and Louvar 2001). The triangle diagram will be

used throughout this paper to plot flammability data.

The triangle diagram is convenient to use because it lists all three components on one diagram. Figure 1.2 is an example of the flammability limit boundary plotted on a triangle diagram and the upper oxygen limit (UOL), lower oxygen limit (LOL), upper flammability limit (UFL), lower flammability limit (LFL), and limiting oxygen concentration (LOC) are indicated:
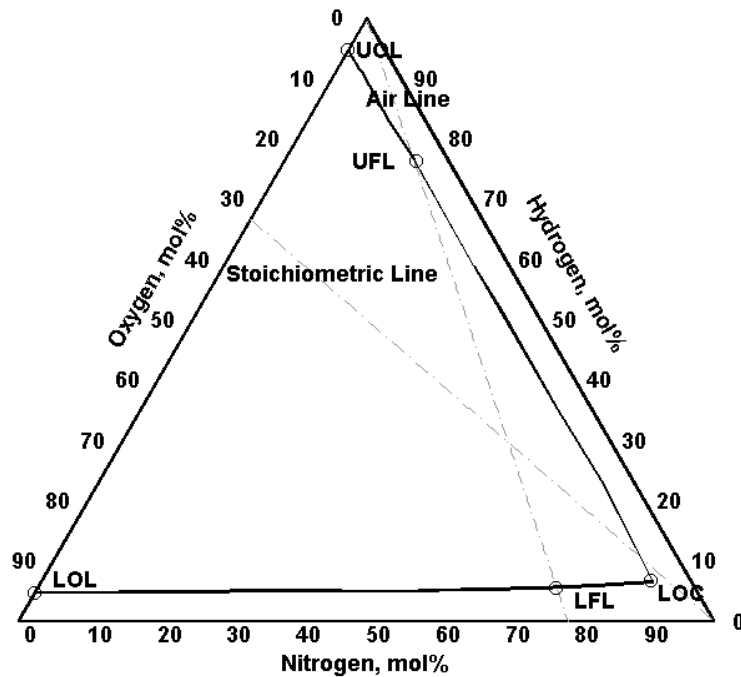
Figure 1.2:   The flammability boundary of hydrogen (Jo and Crowl 2006) plotted on a
              triangle diagram with the UOL, LOL, LOC, UFL, and LFL.

1.3   Theory of the Flammability Limits

The exact mechanism on why the flammability zone boundaries occur is not completely understood. However, it is understood to be associated with the lack of adequate energy to propagate the flame through a well-mixed gas of a fuel, an oxidizer, and an inert gas. Lewis and Von Elbe (Lewis and von Elbe 1987) contend that propagation of the flame is caused by a small number of free radicals caused by previous reactions. This is opposed to combustion caused by increasing the temperature of the molecules at the flame front to their ignition temperature. It is believed that conduction and radiation is simply too inefficient to explain the results observed in the laboratory (Lewis and von Elbe 1934; Lewis and von Elbe 1987). The propagation reaction is then terminated by collision with a solid object such as a wall or the radicals are completely oxidized (Glassman 1987).

However, the heat capacity of the inert gas and combustion products has been shown experimentally to have a great effect on the flammability limits (Coward and Jones 1952).   Gases with higher heat capacities (such as CO_2) have a higher LFL than gases with lower heat capacities (such as N_2). This opposes the idea that the propagation of the flame and the flammability limits are simply dependent on the chemical kinetics. It seems reasonable to assume that the inert gases present absorb energy present in the system to prevent free radicals from forming.

A final interesting aspect of flame propagation along the limits is that it has been observed that gaseous mixtures at the LFL do not have enough energy to raise the temperature of the surrounding gases to an ignition temperature. This can be explained by two phenomena. First, Goldmann (Goldmann 1929; Coward and Jones 1952) suggested that this is caused by the diffusion of the flammable gas faster into the mixture than any other gas. This increases the release of energy along the limit and broadens the flammability zone. This case is also encouraged by the fact that flammability limits vary with upward and downward propagation in a tube (Coward and Jones 1952). Since upward propagation limits are typically lower than downward propagation limits, it shows that the hydrogen is diffusing faster when it becomes more buoyant. However, this phenomenon could also be explained by the free radical theory (Lewis and von Elbe 1934). The case is that free radicals are influenced by diffusion rates, too.

It is thought that all of these factors have an influence on the flammability limits and the ability for a flame to propagate. However, a complete theory has yet to be established that explains and predicts the entire process occurring at the flammability limits. So, the flammability limits are a complicated process that involves chemical kinetics, heat transport, and mass transport that has yet to be fully explained.

1.4 Experimental Data and Correlations

Since the flammability limits are not easily explained and predicted, the use of experimental data and correlations to predict them is often used instead. Experimental data is typically the most accurate but expensive. Correlations can be easy to use but also can be prone to error. Since experimental data is preferred over correlations, previous work in this field will be discussed first.

1.4.1 Experimental Flammability Data

Experimental data on the flammability of gases has been collected since the 1800s on some of the lower hydrocarbons. The purpose of the data was to determine safe levels of these flammable compounds to prevent explosions in mines. Le Chatelier's work is an example of these early studies (Le Chatelier 1891; Mashuga and Crowl 2000). He used a long, narrow glass tube that was filled with the gaseous mixture under water. The mixture was lit from the top and if the mixture burned all the way to the bottom, it was considered flammable. Other early work was performed on gases such as marsh gas, coal gas, and hydrogen (Perman 1911).

Burgess and Wheeler determined the flammability limits for methane, ethane, propane, n-butane, n-pentane, and isopentane (Burgess and Wheeler 1911). A glass sphere with platinum electrodes was used to determine if the mixture was flammable. Observation of

the flame was the criteria used for determination of ignition. The sphere was chosen

because they questioned if tube walls had an effect on the flammability limits.

An early large collection of experimental data was put together by Coward and Jones in

1952 (Coward and Jones 1952). In Coward and Jones' work, an upward propagation of

the flame in a tube was used to determine if the mixture was flammable. They defended

this method because the upward propagation method gave lower values for the

flammability limits. A flammable mixture is defined in their paper as a mixture that can

support a self-propagating flame through an infinite distance. They present the

flammable limits for large number of gases with various inert gases.

Zabetakis presented a large amount of flammability data in his 1965 work (Zabetakis

1965). The flammability data was collected using a 2-inch diameter glass tube and a

spark ignition system. The apparatus was a bureau of mines standard. He provided data

for many compounds that included the flammability limits, the limiting oxygen

concentration, and the boundary points in between the flammability limits and the

limiting oxygen concentration.

Again, it was recognized that the walls of a flame tube may have an effect on the

flammability limits by conducting energy through the walls of the tube and effectively

reducing the flammability zone. In order to avoid the effect of the walls, a closed sphere was developed with a central ignition (Burgess, Furno et al. 1982). This sphere was very large (12 feet in diameter) and used a combination of visual recognition of a flame, pressure rise, and analysis of the products to determine if the mixture was flammable. This work was done for the single gases of methane, hydrogen, and carbon monoxide and also for mixtures of these gases.

More recent studies are using smaller closed spheres or similar shapes. Mashuga and Crowl (Mashuga and Crowl 1999) used a 20 liter sphere to determine the entire flammability zone of methane, ethylene, and 50% methane and 50% ethylene mixture. They used a 7% pressure rise criteria and 10 Joule fuse wire ignition to determine if the mixture was capable of supporting flames. The 7% pressure rise is in accordance with the ASTM standard E 918-83 (ASTM 1992). This apparatus has also been used to determine the flammability zone of hydrogen (Jo and Crowl 2006) and various liquid fuels with humidity (Brooks 2001).

Cashdollar, Zlochower et al. (Cashdollar, Zlochower et al. 2000) have provided data from similar apparatuses to determine the flammability limits and other burning characteristics. They used a 20-liter vessel and a 120-liter sphere in their experiments. A center ignition with spark and a pyrotechnic ignition system were used to determine the flammability characteristics and limits for deuterium, hydrogen, and methane.

It is know that several factors other than shape can affect the flammability limits.

Wierzba and Ale (Wierzba and Ale 1999) have shown that time in the reactor does have

an effect on the flammability limits. The walls seem to provide a surface for the oxygen

to react so the flammability zone is decreased. It has also been known that temperature

and pressure affect the flammability limits. With increasing temperature and pressure the

fuel and oxygen become more reactive and the flammability zone widens (Zabetakis

1965; Crowl 2003).

Many factors can affect the experimental values of the flammability limits. The shape of

the apparatus has been questioned as a potential source of error in the measurement of the

flammability zone boundaries. Another variable to consider is the residence time of the

fuel in the reactor. It has been shown that the flammability zone is reduced with

increased time in the reactor. Finally, higher temperatures and pressures are known to

widen the flammability zone. When using flammability data, one must consider all of

these factors to evaluate the quality of data and how it applies to that particular situation.

1.4.2 Methods to Estimate Flammability Properties

Many methods to estimate flammability properties have been proposed. The majority of

these methods are correlations that use thermodynamic properties such as the heat of

combustion or the elements within the molecules. Some of these methods will be discussed in this section.

The focus of the majority of the efforts in estimating flammability zone has been to predict the upper and lower flammability limits. An early correlation proposed by Jones (Jones 1938) used the stoichiometric oxygen concentration to estimate the value of the LFL and UFL:

$$y_{LFL} = \frac{0.55 C_{st}}{100} \qquad (1.2)$$

$$y_{UFL} = \frac{3.50 C_{st}}{100} \qquad (1.3)$$

These are quick and simple relationships to evaluate these properties.

Shimy (Shimy 1970) proposed a few correlations dependent on the amount of carbon and hydrogen in the molecules of the particular fuel. The correlations are also divided into different fuel groups of paraffinic hydrocarbons and olefins, isomers, the benzene series, and alcohols.

A more complicated group contribution method was proposed by High and Danner (High and Danner 1987). The correlation is dependent upon the number of carbon atoms (N_c)

in the skeleton of the fuel being examined. The following is the correlation they

proposed:

$$UFL = \exp(3.817 - 0.2627 N_c + 1.02 \times 10^{-2} {N_c}^2 + \sum_{j=1}^{24} h_j \psi_j) \qquad (1.4)$$

The h-values are determined from a chart provided by the authors and ψ_j is the fraction of

the groups.

Two correlations were proposed by Suzuki and Koide (Suzuki 1994; Suzuki and Koide

1994). These correlations relate the heat of combustion (ΔH_c) of the fuel to the UFL and

LFL. The following are the correlations that the proposed:

$$y_{LFL} = \left(\frac{-3.42}{\Delta H_c} + 0.569 \Delta H_c + 0.0538 \Delta H_c^2 + 1.80 \right) \frac{1}{100} \qquad (1.5)$$

$$y_{UFL} = (6.30 \Delta H_c + 0.567 \Delta H_c^2 + 23.5) \frac{1}{100} \qquad (1.6)$$

These correlations showed good fits to the experimental data.

An attempt at correlating the flammable limits to the heat of combustion is provided by

Britton (Britton 2002). He used the heat of combustion divided by the stoichiometric

oxygen coefficient (z) to predict the LFL and LOC:

$$LFL = \frac{Constant}{\frac{\Delta H_c^2}{z}} \qquad (1.7)$$

$$LOC = \frac{Constant}{(\frac{\Delta H_C}{z})^2}$$
(1.8)

A reasonable fit was shown with this method.

The most used correlation to predict the limiting oxygen concentration is a very simple (Crowl and Louvar 2001):

$$y_{LOC} = z y_{LFL}$$
(1.9)

This equation's simplicity is its most appealing attribute.

Correlations typically provide a simple, easy-to-use method for estimated these values. This is why many of these equations appear in literature and engineering textbooks on explosion prevention.

1.4.3 Other Methods to Estimate the Flammability Zone

Two methods have been proposed that are more theoretical methods of solving for the flammability zone. These methods are the Gibb's energy (ΔG) minimization techniques and flame modeling.

The most recent technique used to predict flammability properties is a Gibb's energy

minimization technique. This method was first proposed by Melhem (Melhem 1997). It

uses a constant flame temperature coupled with an energy balance and a component

balance to solve for fuel, oxygen, and inert concentrations of the initial mixture.

Lagrangian coefficients are used to reduce the degrees of freedom and minimize the

systems Gibb's energy.

Several authors have used this method to predict flammability properties. Mashuga and

Crowl (Mashuga and Crowl 1999) use this method to predict the entire flammability zone

boundary for methane, ethylene, and a 50% methane and 50% ethylene mixture. They

used a flame temperature of 1200 K because CO_2 seems to begin forming in significant

concentrations at this temperature.

Razus, Molarne, et al. (Razus, Molnarne et al. 2004; Razus, Molnarne et al. 2006) have

used calculated adiabatic flame temperatures and an equilibrium program to determine

the LOC for flammable compounds. A correlation related the temperature at the LFL to

the LOC.

Finally, Vidal, Wong, et al. (Vidal, Wong et al. 2006) use an adiabatic flame temperature

of 1600 K and the SuperChems[TM] program to predict the lower flammability limit for a

large collection of compounds. They have shown that the temperature of 1600 K works well for this application.

One final approach to determining the flammability limits will be discussed. This method involves modeling the flame from ignition to termination. It was first proposed by Lewis and von Elbe (Lewis and von Elbe 1934; Lewis and von Elbe 1987). However, the results were never very accurate. Recently, Van der Schoor, Hermanns, et al. (Van der Schoor, Hermanns et al. 2007) modeled flames as a sphere. They stated that if the flame propagated 100 mm or more it was considered flammable. These models showed an improvement in the accuracy but still a difference was present between the experimental data and the numerical solutions.

These two methods are ways to obtain an estimate for the flammability limits. All the methods have shown reasonable estimates but none are truly theoretical methods. They all require some assumed constant or value to obtain a solution. The Gibb's energy method requires a threshold temperature that may or may not be accurate and the flame modeling requires more complex calculations along with an arbitrary distance of propagation.

2   Purpose and Goals

The purpose of this research is to model the flammability zone boundaries in a fuel, oxidant, and inert system, to provide a means to reduce the amount of experimental work required to define the flammability zone boundaries, and to extend the range of existing experimental data. The model can also be applied to identify inconsistencies in the data and to improve the quality of experimental data.   Very little previous work by other investigators on this issue has been identified in the literature.

The model will be developed using the most common data that are readily available for combustible gases. For the case presented in this thesis, this means the upper and lower flammability limits. The method will also assume that thermodynamic data, such as heat capacities and heats of reaction are readily available for the pure species.

The model will also be applied to estimate the flammability parameters that are most commonly used in industry to prevent explosions: the limiting oxygen concentration and the upper and lower limits in pure oxygen.

Three approaches will be used to model the flammability zone boundaries.   The first approach will use an energy balance and an adiabatic flame temperature to define the boundary. The second approach will use a more detailed kinetic model. The third approach will be empirical. Comparison to experimental data and a statistical analysis of the results will be used to determine the appropriateness of the models.

3   Experimental Flammability Data

The flammability data collected from the literature for this work is listed in Appendix I:
Experimental Flammability Data.

Experimental data was collected from several sources: Mashuga (1999), Jo and Crowl
(2006), Coward and Jones (1952), NFPA 68 (1994), Zabetakis (1965), and Lide (2006).
The most abundant data available are values for the upper flammability limit and lower
flammability limit; however, there is only a limited amount of data available for other
flammability properties, such as the limiting oxygen concentration, upper oxygen limit,
and lower oxygen limit. The accuracy of the experimental data used to compare the
results of the modeling exercises performed in the results section is uncertain. This is due
to the limited amount of data, the lack of a standard experimental method, and poor
reporting of data accuracy and precision.

Experimental data for the upper oxygen limit, lower oxygen limit, and the limiting
oxygen concentration is only available in limited quantities. This is largely because
conducting the experiments to determine the entire flammability zone is expensive and
time consuming. The data in appendix I are collected from a multitude from of

investigators using a variety of experimental procedures. It is not clear how this will affect the conclusions drawn in this study.

Finally, the definition of the limiting oxygen concentration is difficult to apply experimentally. The most common definition of the limiting oxygen concentration is the lowest concentration of oxygen in a fuel, oxygen, and nitrogen mixture in which combustion or an explosion can occur.   Another, more practical definition could be used and often is: the intersection of the upper and lower flammability zone boundaries. This location on a flammability triangle can be referred to as the "nose" section of the flammability zone. Often, both of these definitions are correct for a flammable gas. However, in some cases, these points do not coincide and this can cause confusion. An example of this is the flammability data for dichloromethane. The experimental limiting oxygen concentration of dichloromethane is 19 mol% oxygen in a fuel-oxygen-nitrogen system (Lewis and von Elbe 1987). However, the upper flammability limit is listed as 23 mol% fuel (Lide 2006) with an oxygen concentration of 16.2 mol% oxygen at the UFL and the LFL is listed as 13 mol% fuel with an oxygen concentration of 18.3 mol%. Figure 3.1 shows these points along the flammability zone boundary:
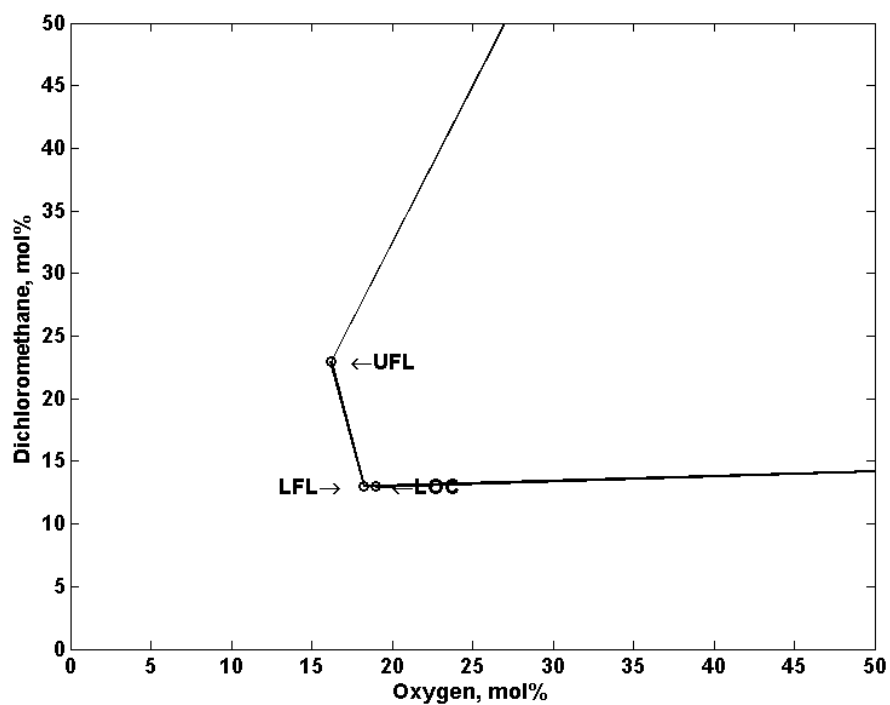
Figure 3.1:   The nose section of the flammability zone boundary for dichloromethane.

These values are clearly less than the limiting oxygen concentration, so what value is truly the LOC? Dichloromethane was excluded from the data set for this study because of this reason. The intersection definition of the LOC will be used in this study.

# 4	The Linear Model

## 4.1	The Adiabatic Energy Balance

Beyond the flammability zone boundaries on a fuel-oxygen-inert diagram, no reaction

can occur. If the ignition at the boundaries is assumed to be adiabatic then a simple

energy balance can be used to represent the reaction (Mashuga and Crowl 2000):

$$\Delta \overline{H} = 0 \qquad\qquad (4.1)$$

For this assumption, the ignition is used to estimate the behavior of the explosion and the

volume of the ignition is assumed to be very small compared to the total volume of the

explosion. It is assumed that there is no heat loss and the volume of the system is

expanded so the pressure remains constant. This expansion occurs because of the heat

generated in the reaction and the formation of the product gases. The gas is also assumed

to behave as an ideal gas. If this energy balance is applied to the entire flammability

range then this range is assumed to be a series of constant temperature lines up to and

including the flammability limit boundary with the temperature the highest towards the

center. If all of these lines were placed onto a single flammability triangle, it would look

similar to a "contour map." Figure 4.1 shows a "contour map" of the flammability zone.
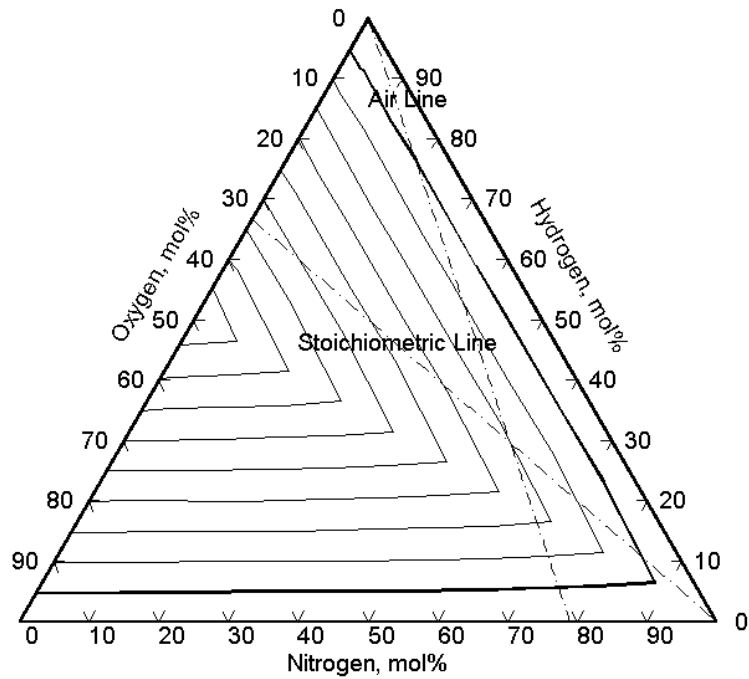
Figure 4.1:   A "contour map" of the flammability region for the hydrogen-oxygen-
nitrogen system.

The flammability boundary is at the edge of the contours and this boundary is composed
of two lines:

1. A line that represents the upper flammability zone boundary and passes
    through the upper flammability limit, and

2. Another line that represents the lower flammability zone boundary and passes
    through the lower flammability limit.

The reaction along the upper flammability zone boundary is almost entirely oxygen-limited while the reaction along the lower flammability is almost entirely fuel-limited. However, the boundaries can change from fuel-limited to oxygen-limited or from oxygen-limited to fuel-limited near the stoichiometric line.   The goal of this section is to introduce a thermodynamic-based model of the flammability zone boundaries.

4.2   Modeling the Flammability Zone Boundaries as Linear Expressions

In order to model the flammability zone boundary, the adiabatic energy in equation 4.1 is applied. The energy balance can be split up in two steps because enthalpy is a state function. The first represents a constant pressure release of energy from the reaction and the second represents a constant pressure increase in temperature of the products of the reactions. The energy balance is now written as the following:

$$n_{f,c} \Delta \overline{H}_r + \sum_j n_j \, \Delta \overline{H}_j = 0 \tag{4.2}$$

For an ideal gas, $\Delta \overline{H}_j = \int_{T_i}^{T_{ad}} C_{p,j} dT$ (Sandler 2006) and is substituted into equation 4.2.

$$n_{f,c} \Delta \overline{H}_r + \sum_j \, n_j \int_{T_i}^{T_{ad}} C_{p,j} dT = 0 \tag{4.3}$$

The following is defined as an average heat capacity:

$$\bar{C}_{p,j} = \frac{\int_{T_i}^{T_{ad}} C_{p,j} dT}{T_{ad} - T_i} \tag{4.4}$$

To allow the separation of variables, it is convenient to substitute $\bar{C}_{p,j}(T_{ad} - T_i)$ for $\int_{T_i}^{T_{ad}} C_{p,j} dT$ and equation 4.5 is the result of this treatment.

$$n_{f,c} \Delta \bar{H}_r + \sum_j n_j \bar{C}_{p,j}(T_{ad} - T_i) = 0 \tag{4.5}$$

In order to complete this analysis, a specific reaction must be considered. For the first case, the reaction along the lower flammability zone boundary is used. Along the lower flammability zone boundary, the reaction is fuel limited, so, for a carbon, hydrogen, oxygen, and nitrogen fuel, the combustion reaction is the following:

$$C_v H_w O_x N_y + z O_2 \rightarrow v C O_2 + \frac{w}{2} H_2 O + \frac{y}{2} N_2 \tag{4.6}$$
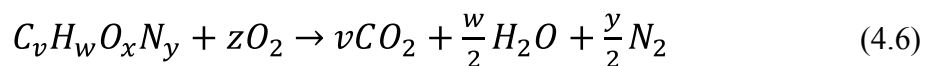
Where:

$$z = v + \frac{w}{4} - \frac{x}{2} \tag{4.7}$$

For one mole of fuel and fuel-oxygen-nitrogen system, equation 4.5 becomes:

$$y_f \Delta \bar{H}_r + ((y_{O_2} - z y_f) \bar{C}_{p,O_2} + v y_f \bar{C}_{p,CO_2} + \frac{w}{2} y_f \bar{C}_{p,H_2O}$$

$$+ \left(1 - y_{O_2} - y_f + \frac{y}{2} y_f\right) \bar{C}_{p,N_2})(T_{ad} - T_i) = 0 \tag{4.8}$$

If

$$\alpha_L = v\bar{C}_{p,CO_2} + \frac{w}{2}\bar{C}_{p,H_2O} + \frac{y}{2}\bar{C}_{p,N_2} - z\bar{C}_{p,O_2} - \bar{C}_{p,N_2} \qquad (4.9)$$

$$\beta_L = \bar{C}_{p,O_2} - \bar{C}_{p,N_2} \qquad (4.10)$$

$$\gamma_L = \bar{C}_{p,N_2} \qquad (4.11)$$

Then equation 4.8 becomes:

$$y_f\Delta\bar{H}_r + (\alpha_L y_f + \beta_L y_{O_2} + \gamma_L)(T_{ad} - T_i) = 0 \qquad (4.12)$$

Equation 4.12 can be solved for y_f.

$$y_f = \frac{\beta_L(T_{ad} - T_i)}{-\Delta\bar{H}_r - \alpha_L(T_{ad} - T_i)}y_{O_2} + \frac{\gamma_L(T_{ad} - T_i)}{-\Delta\bar{H}_r - \alpha_L(T_{ad} - T_i)} \qquad (4.13)$$

Equation 4.13 has the form of $y = mx + b$ and can be used as a linear model of the lower flammability zone boundary.

In order to solve for the adiabatic flame temperature, an iterative solution must be used for equation 4.13 because values of the heat capacities are also dependent on the temperature. MathCAD® is a convenient program for this solution. See Appendix II for an example MathCAD® spreadsheet. Since the adiabatic flame temperature calculation can be solved for all mixtures in a reaction system, a point that is known to be reactive is

chosen along the limit. The lower flammability limit is chosen since it is a value that is readily available for most systems and, if it is not available, it can be obtained most easily through a series of experiments. Figure 4.2 is an example of hydrogen-oxygen-nitrogen system LFL boundary plotted using an adiabatic flame temperature of 639 K.
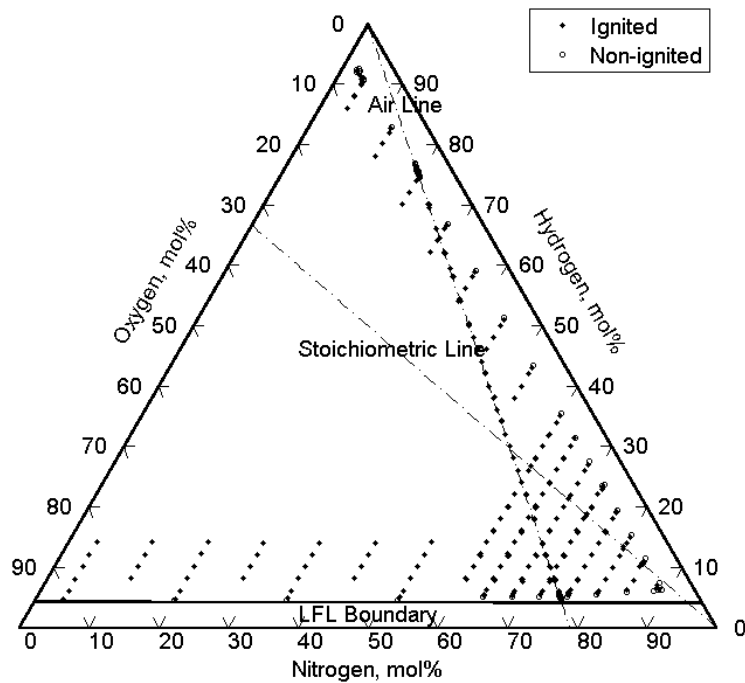
Figure 4.2:   The lower flammability zone boundary plotted against hydrogen data (Jo and Crowl 2006) with an adiabatic flame temperature of 639 K and LFL of 4.2%.

A similar treatment can be applied to estimate the upper flammability limit boundary. For this second case, the reaction in equation 4.6 is used again. Since the reaction is

oxygen limited in this case, the following parameter is used for one mole of the initial fuel-oxygen-nitrogen mixture:

$$n_{f,c} = \frac{1}{z} y_{O_2} \qquad (4.14)$$

It is also assumed that the fuel remaining in the system is unreacted and this results in the following terms:

$$\alpha_U = \bar{C}_{p,f} - \bar{C}_{p,N_2} \qquad (4.15)$$

$$\beta_U = \frac{v}{z} \bar{C}_{p,CO_2} + \frac{w}{2z} \bar{C}_{p,H_2O} + \frac{y}{2z} \bar{C}_{p,N_2} - \frac{1}{z} \bar{C}_{p,f} - \bar{C}_{p,N_2} \qquad (4.16)$$

$$\gamma_U = \bar{C}_{p,N_2} \qquad (4.17)$$

Combining equations 4.5, 4.14, 4.15, 4.16, and 4.17 and rearranging to solve for y_f results in the following equation:

$$y_f = \frac{-\frac{1}{z}\Delta \bar{H}_r - \beta_U (T_{ad} - T_i)}{\alpha_U (T_{ad} - T_i)} y_{O_2} - \frac{\gamma_U}{\alpha_U} \qquad (4.18)$$

This equation can be used to estimate the upper flammability zone boundary. The same procedure used for the lower flammability limit boundary can be applied to determine the upper flammability boundary. The upper flammability limit for hydrogen used was 76.1% and this gives an adiabatic flame temperature of 1123 K. Figure 4.3 is a plot of both boundaries for hydrogen.
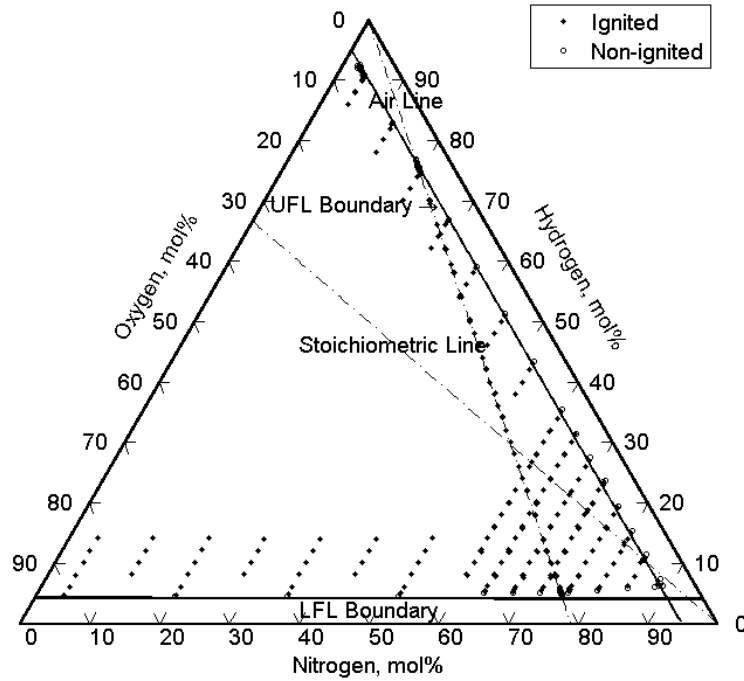
Figure 4.3:   The upper and lower flammability zone boundary plotted against

hydrogen data (Jo and Crowl 2006) with an adiabatic flame temperature of

1123 K and a UFL of 76.1%.

4.2.1 Estimation of the Limiting Oxygen Concentration

The reaction in equation 4.6 was chosen in order to estimate the limiting oxygen

concentration (LOC). To derive an equation to estimate the LOC, it must be assumed

that the LOC occurs at the intersection of UFL boundary and LFL boundary lines.

Equations 4.13 and 4.18 are equated, separate adiabatic temperatures are assigned for the

upper and lower flammability zone boundaries, and $y_{O_2} = y_{LOC}$:

$$\frac{\beta_L(T_{ad,L}-T_i)}{-\Delta\bar{H}_r-\alpha_L(T_{ad,L}-T_i)}y_{LOC} + \frac{\gamma_L(T_{ad,L}-T_i)}{-\Delta\bar{H}_r-\alpha_L(T_{ad,L}-T_i)} =$$

$$\frac{-\frac{1}{z}\Delta\bar{H}_r-\beta_U(T_{ad,U}-T_i)}{\alpha_U(T_{ad,U}-T_i)}y_{LOC} - \frac{\gamma_U}{\alpha_U} \tag{4.19}$$

The equation is rearranged and solved for y_{LOC}:

$$y_{LOC} = \frac{\gamma_L\alpha_U+\gamma_U\left(\frac{-\Delta\bar{H}_r}{T_{ad,L}-T_i}-\alpha_L\right)}{\left(\frac{1}{z}\frac{-\Delta\bar{H}_r}{T_{ad,U}-T_i}-\beta_U\right)\left(\frac{-\Delta\bar{H}_r}{T_{ad,L}-T_i}-\alpha_L\right)-\beta_L\alpha_U} \tag{4.20}$$

Equation 4.20 is a functional equation that can be used to estimate the limiting oxygen concentration. However, a few assumptions can be made to simplify this equation. Since the two lines converge at the limiting oxygen concentration, it can be assumed that at the intersection $\gamma_U = \gamma_L = \gamma$ and $T_{ad,U} = T_{ad,L} = T$ and equation 4.20 becomes:

$$y_{LOC} = \frac{\gamma_L\left(\frac{-\Delta\bar{H}_r}{T_{ad}-T_i}+\alpha_U-\alpha_L\right)}{\left(\frac{1}{z}\frac{-\Delta\bar{H}_r}{T_{ad}-T_i}-\beta_U\right)\left(\frac{-\Delta\bar{H}_r}{T_{ad}-T_i}-\alpha_L\right)-\beta_L\alpha_U} \tag{4.21}$$

When the magnitudes of the terms are examined, β_U is insignificant when compared to $\frac{1}{z}\frac{-\Delta\bar{H}_r}{T_{ad}-T_i}$ and $\beta_L\alpha_U$ is small when compared to $\left(\frac{1}{z}\frac{-\Delta\bar{H}_r}{T_{ad}-T_i}-\beta_U\right)\left(\frac{-\Delta\bar{H}_r}{T_{ad}-T_i}-\alpha_L\right)$.

These terms are excluded from the equation to result in:

$$y_{LOC} = \frac{\gamma\left(\frac{-\Delta\bar{H}_r}{T_{ad}-T_i}+\alpha_U-\alpha_L\right)}{\left(\frac{1}{z}\frac{-\Delta\bar{H}_r}{T_{ad}-T_i}\right)\left(\frac{-\Delta\bar{H}_r}{T_{ad}-T_i}-\alpha_L\right)} \tag{4.22}$$

The LFL boundary line has a slope very close to zero, thus equation 4.23 is assumed:

$$y_{LFL} = \frac{\gamma}{\frac{-\Delta \bar{H}_r}{T_{ad}-T_i}-\alpha_L} \qquad (4.23)$$

Therefore, equation 4.23 can be substituted into equation 4.22 and the following is obtained:

$$y_{LOC} = z y_{LFL} \frac{(\frac{-\Delta \bar{H}_r}{T_{ad}-T_i}+\alpha_U-\alpha_L)}{\left(\frac{-\Delta \bar{H}_r}{T_{ad}-T_i}\right)} \qquad (4.24)$$

$\alpha_U - \alpha_L$ is small when compared to $\dfrac{-\Delta \bar{H}_r}{T_{ad}-T_i}$ so those terms can be excluded and this

results in the following:

$$y_{LOC} = z y_{LFL} \qquad (1.9)$$

This procedure has been shown to produce a simple equation that has already been in use for many years (Crowl and Louvar 2001). This derivation has simply validated it.

4.2.2 Estimation of the Pure Oxygen Limits

The methodology will be used to develop equations for the pure oxygen limits. First, the fuel value at the point at which the upper flammability limit zone intercepts the inert gas axis is defined as the upper oxygen limit. Also, the fuel value at the point at with the lower flammability limit boundary intercepts the inert gas axis is defined as the lower oxygen limit. When these lines intercept the inert axis, this implies that no inert gas is present in the system.

For the LOL, equation 4.13 is adapted by removing the nitrogen terms resulting in the following equation:

$$y_f = \frac{\beta_L(T_{ad,L}-T_i)}{-\Delta\bar{H}_r - \alpha_L(T_{ad,L}-T_i)}y_{O_2} \tag{4.25}$$

Where:

$$\alpha_L = v\bar{C}_{p,CO_2} + \frac{w}{2}\bar{C}_{p,H_2O} + \frac{y}{2}\bar{C}_{p,N_2} - z\bar{C}_{p,O_2} \tag{4.26}$$

$$\beta_L = \bar{C}_{p,O_2} \tag{4.27}$$

In this case, $y_f = y_{LOL}$ and $y_{O_2} = 1 - y_{LOL}$. This is substituted into equation 4.25 and solved for y_{LOL}.

$$y_{LOL} = \frac{\beta_L}{\frac{-\Delta\bar{H}_r}{T_{ad,L}-T_i}-\alpha_L+\beta_L} \tag{4.28}$$

Equation 4.28 can be used to calculate the lower oxygen limit using the adiabatic flame temperature at the LFL; however, a few assumptions can be made to simplify it. If β_L is considered insignificant when compared to $\frac{-\Delta\bar{H}_r}{T_{ad}-T_i} - \alpha_L$ and the heat capacity of oxygen is approximately equal to the heat capacity of nitrogen then the equation will reduce down to the following when equation 4.23 is incorporated:

$$y_{LOL} = y_{LFL} \tag{4.29}$$

This equation is consistent with experimental data that the lower flammability zone boundary is a line with a slope of zero.

33

The same treatment is performed for the upper oxygen limit using equation in which the

nitrogen terms are removed from equation 4.18.

$$y_f = \frac{-\frac{1}{z}\Delta\bar{H}_r - \beta_U(T_{ad,U} - T_i)}{\alpha_U(T_{ad,U} - T_i)} y_o \quad (4.30)$$

Where:

$$\alpha_U = \bar{C}_{p,f} \quad (4.31)$$

$$\beta_U = \frac{v}{z}\bar{C}_{p,CO_2} + \frac{w}{2z}\bar{C}_{p,H_2O} + \frac{y}{2z}\bar{C}_{p,N_2} - \frac{1}{z}\bar{C}_{p,f} \quad (4.32)$$

$y_f = y_{UOL}$ and $y_{O_2} = 1 - y_{UOL}$ are substituted into equation 4.30 and it is solved for

y_{UOL}.

$$y_{UOL} = \frac{\frac{\Delta\bar{H}_r}{T_{ad,U} - T_i} + z\beta_U}{\frac{\Delta\bar{H}_r}{T_{ad,U} - T_i} + z(\beta_U - \alpha_U)} \quad (4.33)$$

Equation 3.34 can be used to estimate the upper oxygen limit and no further

simplifications should be made. The temperature used in the solution of equation 4.33

should be an adiabatic flame temperature at the UFL. The results section will further

evaluate the accuracy of the equations 4.13 and 4.18.

4.3   Results for the Linear Model

In order to evaluate the linear model, the adiabatic flame temperatures at the upper

flammability limit must be solved for using the energy balance described in theory

section. The complete combustion reaction described earlier was used to solve for the

temperatures at the UFL and LFL:

Table 4.1:   Adiabatic flame temperatures for a complete combustion reaction at the

upper flammability limit and the lower flammability limit.

Compound	ΔH_r[1] kJ mole^{-1}	Adiabatic Flame Temperature	
		UFL (K)	LFL (K)
Hydrogen	-237.4	1123	687
Deuterium	-237.4	1159	695
Ammonia	-339.7	2058	1722
Hydrogen Sulfide	-504.2	1320	731
Methane	-818.7	2085	1450
Carbon Monoxide	-283	1349	1367
Methanol	-707.8	1507	1656
Carbon Disulfide	-1062.6	1320	731
Acetylene	-1236	729	1302
Ethylene	-1332.4	1609	1341
Ethane	-1468.7	2001	1535
Dimethyl Ether	-1430.1	1504	1536
Ethanol	-1333.2	607	1521
Methyl Formate	-964.7	1888	1848
Chloroethane	-1322.2	1801	1645
1,2-Dichloroethane	-1141	1686	2094
1,1,1-trichloroethane	-1007	1577	2042
Cyclopropane	-1998.5	2090	1645
Propene	-1959	2101	1624
Propane	-2750.2	1982	1530
Acetone	-1743.7	1868	1700
Methyl Acetate	-1494	1563	1570
1,3-Butadiene	-2409	1972	1676
1-Butene	-2600.6	1839	1727
Isobutene	-2594.1	1949	1597
Isobutane	-2747.9	1912	1640
n-Butane	-2750.2	1905	1702

Table 4.1 (continued): Adiabatic flame temperatures for a complete combustion reaction

at the upper flammability limit and the lower flammability limit.

Divinyl Ether	-2285	1349	1431
Butanone (MEK)	-2381.2	2027	1272
Diethyl Ether	-2649.7	943	1635
1-chlorobutane	-2581.8	1765	1574
Isobutyl formate	-2740	1793	1770
3-methyl-1-Butene	-3149	1849	1636
Isopentane	-3383.3	1893	1902
n-Pentane	-3389.8	1850	1668
Benzene	-3210.3	2097	1581
n-Hexane	-4030.3	1720	1612
Toluene	-3835.1	1924	1701
n-Heptane	-4671	1769	1780
Styrene	-4263	1959	1640
Ethylbenzene	-4387	1905	1338
Methylstyrene	-4869	1939	2627

Data from [1](Yaws 2003).

Using the adiabatic flame temperatures and equations 4.13 and 4.18, the UOL, the LOL,

and the LOC were estimated where the UOL is the UFL boundary interception of the

nitrogen axis, the LOL is the LFL boundary interception of the nitrogen axis, and the

LOC is the interception of the UFL and LFL boundaries. The following are the results of

the limiting oxygen concentration with $y_{LOC} = zy_{LFL}$ (Crowl and Louvar 2001) included

for comparison:

Table 4.2:   Estimates of the limiting oxygen concentration using the "zy_{LFL}" method
and the linear method and the absolute difference of the experimental
values and estimated values which are listed in Appendix I.

	zy_{LFL}	|Experimental - Estimate|	Linear Model	|Experimental - Estimate|
Hydrogen	0.0242	0.0248	0.0520	0.0030
Hydrogen Sulfide	0.0645	0.0105	0.1020	0.0270
Methane	0.097	0.0190	0.1570	0.0410
Carbon Monoxide	0.0625	0.0075	0.0600	0.0050
Methanol	0.1095	0.0095	0.0960	0.0040
Carbon Disulfide	0.036	0.0140	0.0890	0.0390
Acetylene	0.065	0.0030	0.0260	0.0360
Ethylene	0.0786	0.0144	0.1000	0.0070
Ethane	0.105	0.0050	0.1480	0.0380
Dimethyl Ether	0.099	0.0060	0.0960	0.0090
Ethanol	0.105	0.0000	0.1180	0.0130
Methyl Formate	0.114	0.0110	0.1170	0.0140
1,2-Dichloroethane	0.186	0.0560	0.1400	0.0100
1,1,1-trichloroethane	0.1925	0.0525	0.1380	0.0020
Cyclopropane	0.108	0.0070	0.1470	0.0320
Propene	0.108	0.0070	0.1510	0.0360
Propane	0.105	0.0100	0.1470	0.0320
Acetone	0.12	0.0050	0.1350	0.0200
Methyl Acetate	0.1085	0.0015	0.1080	0.0020
1,3-Butadiene	0.11	0.0050	0.1360	0.0310
1-Butene	0.096	0.0190	0.1400	0.0250
Isobutene	0.108	0.0120	0.1400	0.0200
Isobutane	0.117	0.0030	0.1430	0.0230
n-Butane	0.1235	0.0035	0.1430	0.0230
Butanone (MEK)	0.11	0.0000	0.1280	0.0180
Diethyl Ether	0.114	0.0090	0.0520	0.0530
1-chlorobutane	0.1125	0.0275	0.1310	0.0090
Isobutyl Formate	0.13	0.0050	0.1320	0.0070
3-methyl-1-Butene	0.1125	0.0025	0.1320	0.0170
Isopentane	0.112	0.0080	0.1370	0.0170
n-Pentane	0.12	0.0000	0.1370	0.0170
Benzene	0.105	0.0090	0.1510	0.0370
n-Hexane	0.114	0.0060	0.1240	0.0040

Table 4.2 (continued): Estimates of the limiting oxygen concentration using the "zy_{LFL}" method and the linear method and the average difference of the experimental values and estimated values which are listed in Appendix I.

Toluene	0.126	0.0310	0.1480	0.0530
n-Heptane	0.132	0.0170	0.1310	0.0160
Styrene	0.11	0.0200	0.1380	0.0480
Ethylbenzene	0.084	0.0010	0.1340	0.0490
Methylstyrene	0.2185	0.1285	0.1490	0.0590
Average Difference		0.028		0.031
95% Confidence Interval		0.063		0.068
R^2		0.415		0.151

The "zy_{LFL}" method has a 95% confidence interval on the mean of $y_{LOC} \pm 0.063$ and the linear method has a 95% confidence interval on the mean of $y_{LOC} \pm 0.068$. The R^2 value of the "zy_{LFL}" method is 0.415 and for the linear method is 0.151. The fit of the linear method is less appropriate than the "zy_{LFL}" method.

The following are the estimates made for the upper oxygen limit and the lower oxygen limit by the linear method. The methods are not compared to any previous method since none exist.

Table 4.3:   Estimates of the upper oxygen limit and the lower oxygen limit using the

linear method and absolute differences of this method and experimental

data which are listed in Appendix I.

| | | Linear Method | | |
Compound	UOL	|Experimental - Estimated|	LOL	|Experimental - Estimated|
Hydrogen	0.950	0.010	0.049	0.000
Deuterium	0.948	0.002	0.050	0.001
Ammonia	0.801	0.011	0.154	0.004
Methane	0.727	0.076	0.050	0.001
Carbon Monoxide	0.940	0.000	0.125	0.030
Acetylene	0.955	0.025	0.027	0.001
Ethylene	0.776	0.030	0.027	0.002
Ethane	0.629	0.046	0.031	0.001
Chloroethane	0.720	0.020	0.041	0.001
Cyclopropane	0.590	0.070	0.025	0.000
Propene	0.583	0.053	0.025	0.004
Propane	0.548	0.028	0.022	0.001
Isobutane	0.497	0.017	0.018	0.000
n-Butane	0.498	0.008	0.018	0.000
Divinyl Ether	0.714	0.136	0.017	0.001
Diethyl Ether	0.767	0.053	0.020	0.000
Average Difference		0.040		0.015
95% Confidence Interval		0.13		0.020
R^2		0.882		0.954

The R^2 values show a rather good fit for both of these estimates. The estimate for the

UOL has a 95% confidence interval on the mean of $y_{UOL} \pm 0.13$ and the LOL has a 95%

confidence interval on the mean of $y_{LOL} \pm 0.020$.

4.4   Discussion of the Linear Model and its Results

The linear model presented in this paper is a thermodynamic model of the flammability zone boundary. It was assumed that the flammability zone boundary was adiabatic flame with a constant flame temperature throughout the entire boundary. The appropriateness of the two major assumptions will be explored in order to justify the modeling of the limit in this manner.

4.4.1 The Thermodynamic Assumptions

In previous studies, an adiabatic assumption has been used to estimate flammability relationships. Mashuga and Crowl used this assumption to derive Le Chatelier's mixing law of the flammability limits and to estimate the entire flammability zone boundary (Mashuga and Crowl 1999; Mashuga and Crowl 2000). Wierzba, Shrestha, and Karim (Wierzba, Shrestha et al. 1994; Shrestha, Wierzba et al. 1995; Wierzba, Shrestha et al. 1996) suggested using a similar energy balance to the one used in this thesis to determine a relationship for the change in flammability limits with temperature.

The adiabatic energy balance is used because it estimates the reaction at the ignition point well. The energy released by the explosion is dominated by enthalpy and entropy is small in comparison. However, the flammability studies generally take place in a fixed volume reactor such as a spherical reactor. In these situations, it would seem that internal

energy is an appropriate thermodynamic property to study. The reaction may be considered adiabatic because the ignition area is only a very small fraction of the total volume of the vessel. When such a small fraction of the total volume is considered, an adiabatic energy balance is appropriate.

Two adiabatic flame temperatures were chosen to model the upper flammability zone boundary and the lower flammability zone boundary. Several other authors have used a similar approach. Melhem suggested using a constant temperature of 1500 K for the entire flammability envelope (Melhem 1997). The fuel oxygen concentrations are then solved for using a chemical equilibrium algorithm. Mashuga and Crowl use a similar approach with a threshold temperature of 1200 K (Mashuga and Crowl 1999). It is contended that this is a proper temperature due to the fact that CO_2 does not begin to form until approximately 1100 K, so 1200 K would be a good limiting temperature. The reaction that dominates this boundary is the following:

$$CO + OH \rightarrow CO_2 + H \tag{4.37}$$

Mashuga and Crowl have shown a reasonable fit with this assumption for methane and ethylene. Razus, Molnarne, et al. (Razus, Molnarne et al. 2006) use a correlation to fit the adiabatic flame temperature at the LFL to the LOC and then use a chemical equilibrium algorithm to determine the LOC. This method had results within 5-10%. Finally, in three papers, Wierzba, Shrestha, and Karim suggested using a similar energy balance to the one used in this paper to calculate an adiabatic flame temperature at the

41

lower and upper flammability limits. The temperature calculated is then used to calculate a constant based upon the thermodynamic expression used in a relationship to predict the upper and lower flammability limits at other temperatures (Wierzba, Shrestha et al. 1994; Shrestha, Wierzba et al. 1995; Wierzba, Shrestha et al. 1996). This method showed promising results.

The linear method uses an adiabatic flame temperature that is calculated from the upper and lower flammability limit and then relates it to other points along the flammability boundary. This method is preferred since it allows the adiabatic flame temperature to change with the fuel. Two flame temperature values are used for a fuel and this allows the model to account for the differences in the reaction mechanism along the rich and lean limits. So, this model uses some previously established techniques and allows them to be more fuel specific and expand upon flammability limit boundary knowledge.

4.4.2 Analysis of the Results

In the results section, it was shown that the linear model has a 95% confidence interval of $y_{LOC} \pm 0.068$, where y_{LOC} is the limiting oxygen concentration mole fraction, and a R^2 value of 0.151. The results of the linear method are worse than the well-established method of $y_{LOC} = zy_{LFL}$. The 95% confidence interval for the "zy_{LFL}" method is $y_{LOC} \pm$ 0.063 and a R^2 value of 0.415. The results of the two methods can be more clearly seen in Figures 4.4 and 4.5.
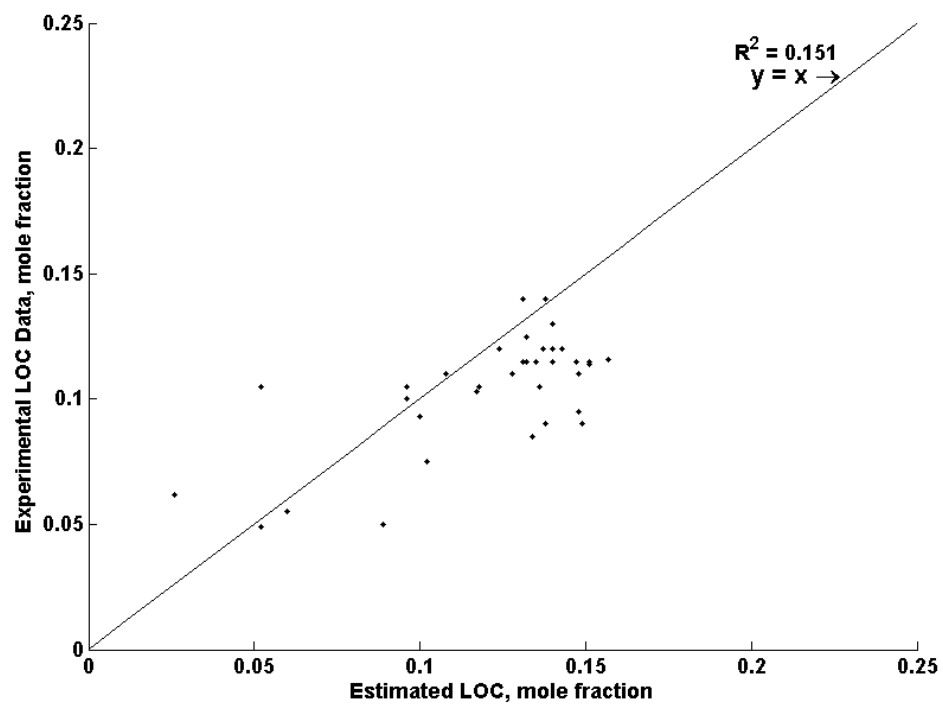
Figure 4.4:   Estimated values of the LOC from the linear method plotted against

experimental data.

Figure 4.4 shows that the fit is not adequate. The data appears to be scattered.

0.25

$R^2 = 0.416$
y = x →

0.2

0.15

0.1

0.05

0

Experimental LOC Data, mole fraction

0   **0.05**   **0.1**   **0.15**   **0.2**   **0.25**

Estimated LOC, mole fraction
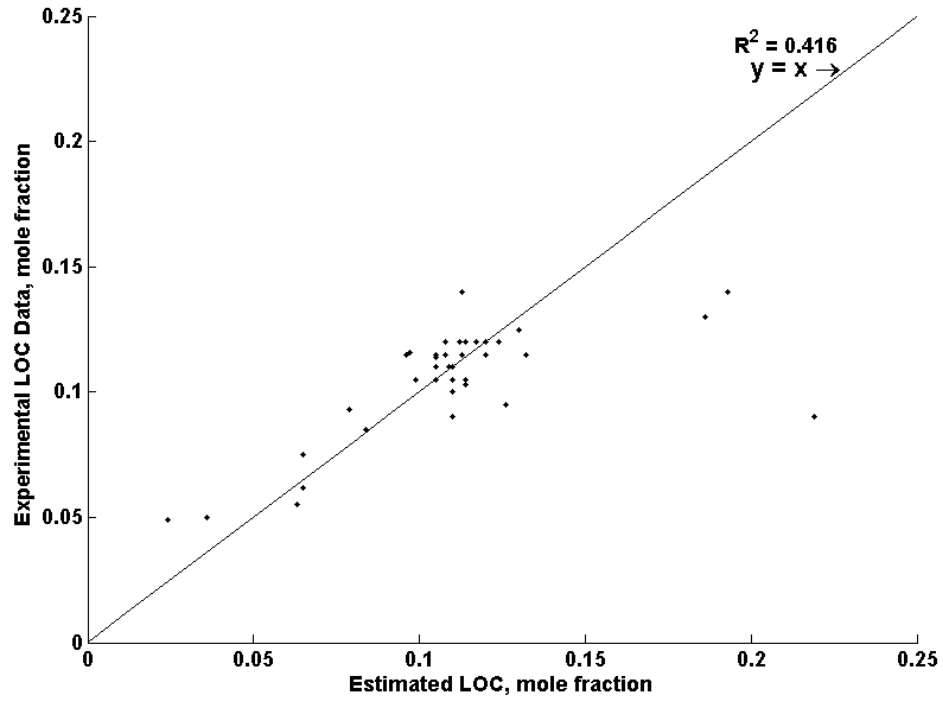
Figure 4.5:   Estimated values of the LOC from the "zy_{LFL}" method are plotted against

experimental LOC data.

The fit is good other than a few outliers present. Figures 4.6 and 4.7 show the residuals

($y_{estimated} - y_{experimental}$) for the estimations of both methods.

44
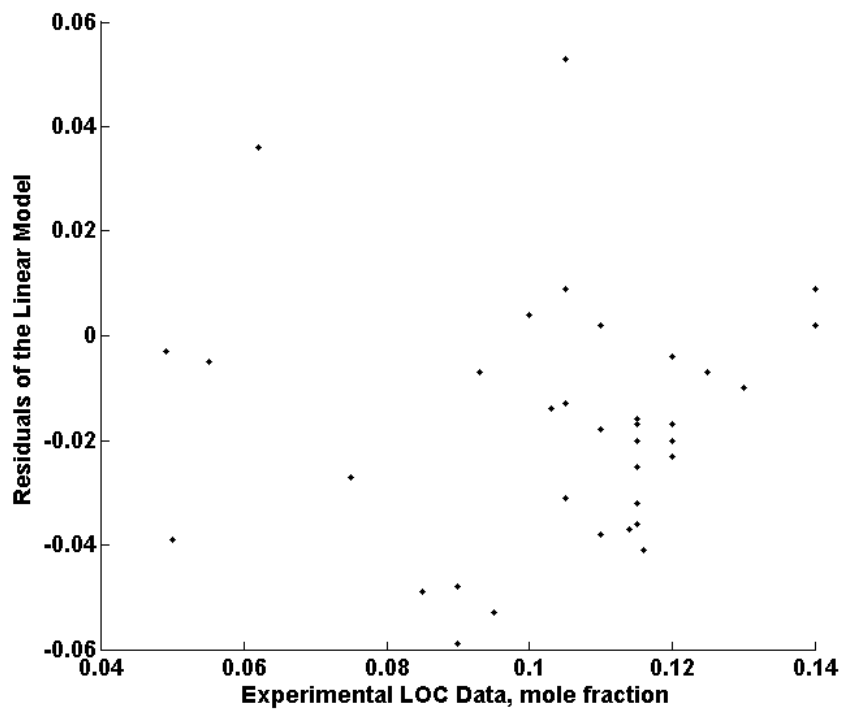
Figure 4.6:   The residuals of the linear model estimates.

Figure 4.6 shows that the linear model under-predicts the LOC. However, there are no outliers. The under-prediction may occur because the model cannot predict the curvature that occurs at the LOC due to the change in reactions.
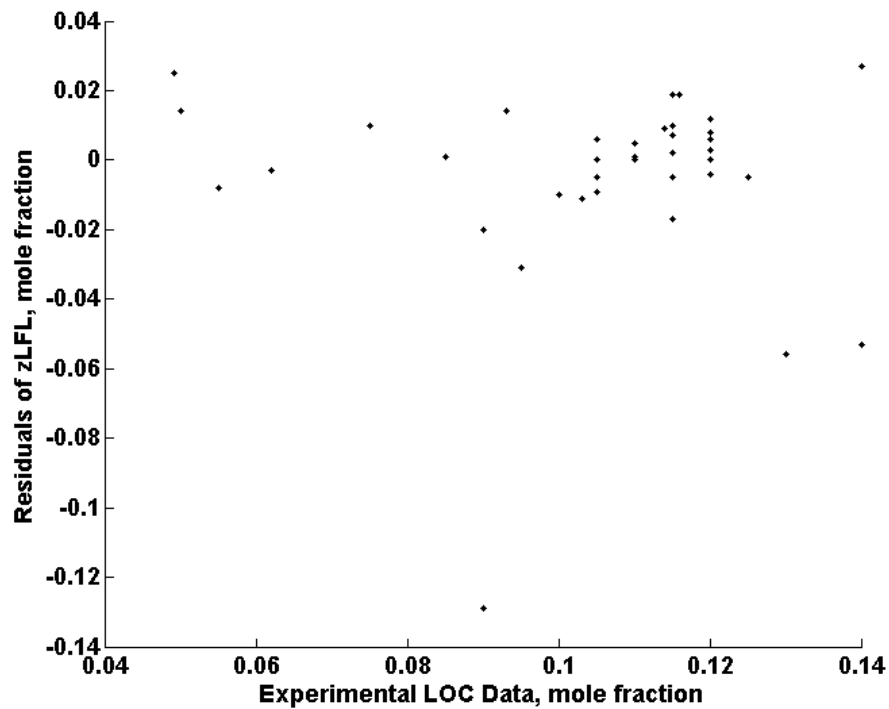
Figure 4.7:   The residuals of the $y_{LOC} = zy_{LFL}$.

Figure 4.7 shows that the fit is even; however, there is an outlier: methylstyrene. The

outliers are defined as points being outside the confidence interval. These graphs show

that the linear model under-predicts the limiting oxygen concentration which is due to the

fact this method requires the LOC to occur along the stoichiometric line. The residuals of

"zy_{LFL}" method are smaller than the linear method for the LOC and thus it has a better fit.

The "zy_{LFL}" method does produce some outliers.

From the results section, the 95% confidence interval on the mean of the upper oxygen limit is $y_{UOL} \pm 0.13$ for the linear method.   Figure 4.8 is plot of the estimated values of the UOL from the linear model vs. the experimental values of the UOL where the regression coefficient is 0.882.
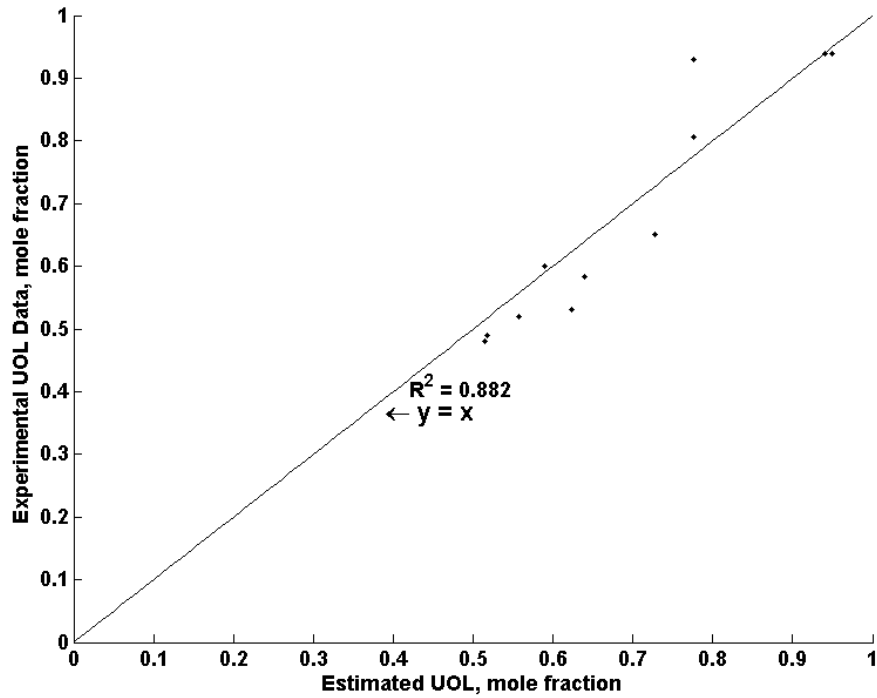
Figure 4.8:   Plot of the estimated values of the UOL from the linear model vs. experimental UOL values.

This shows that the fit is rather good for the upper oxygen limit. Figure 4.9 is the plot of the residuals for the linear model estimate of the UOL.
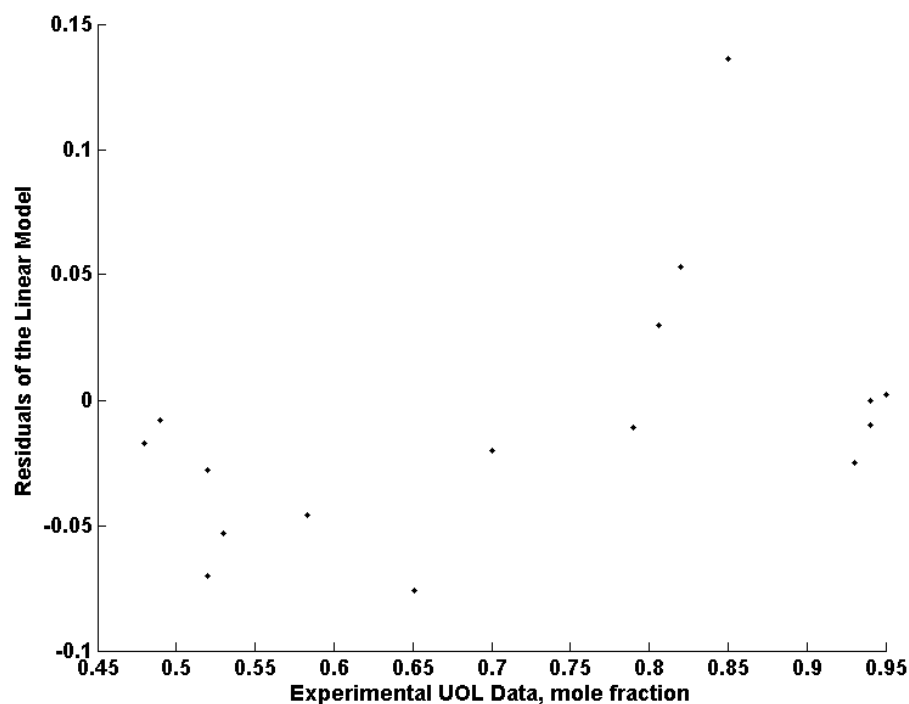
Figure 4.9:   Plot of the residuals of the upper oxygen limit estimated by the linear

                model.

The fit of the linear model for the upper oxygen limit is adequate. The residuals show

that the fit is balanced but the model does have one outlier: divinyl ether. It is not clear

whether this is a result of the experimental data being in error or whether a flaw in the

model is present.

The 95% confidence interval on the mean of the lower oxygen limit was $y_{LOL} \pm 0.020$ as presented in the results section. Figure 4.10 shows the fit of the linear model to the lower oxygen limit with a regression coefficient of 0.954 and figure 4.11 shows the residual of predicting the LOL.
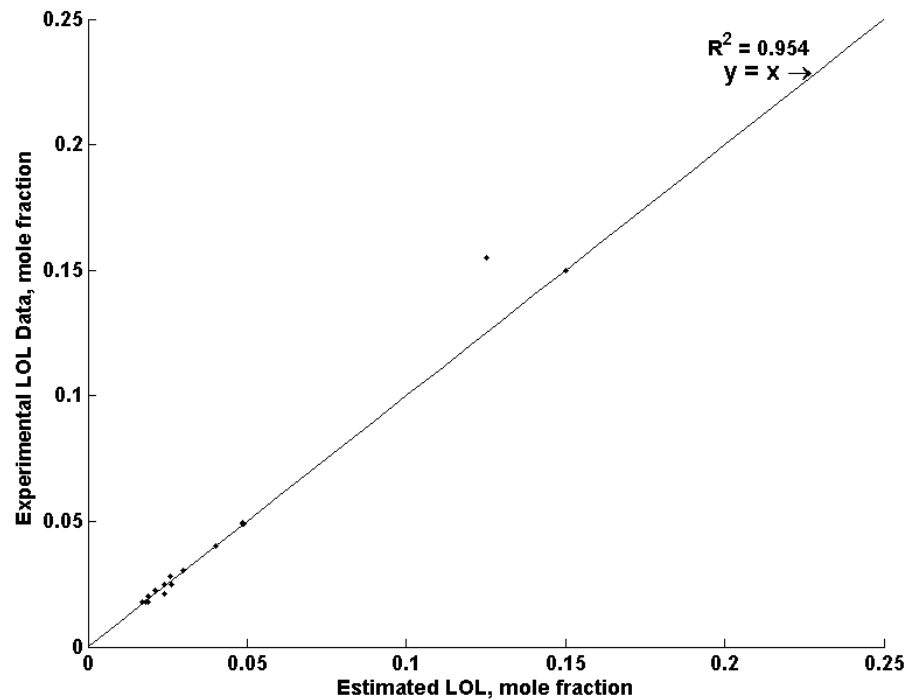
Figure 4.10:   Plot of the estimated lower oxygen limit from the linear model vs.

experimental data.

Figure 4.10 shows that the fit is quite good and there is little scatter to data.
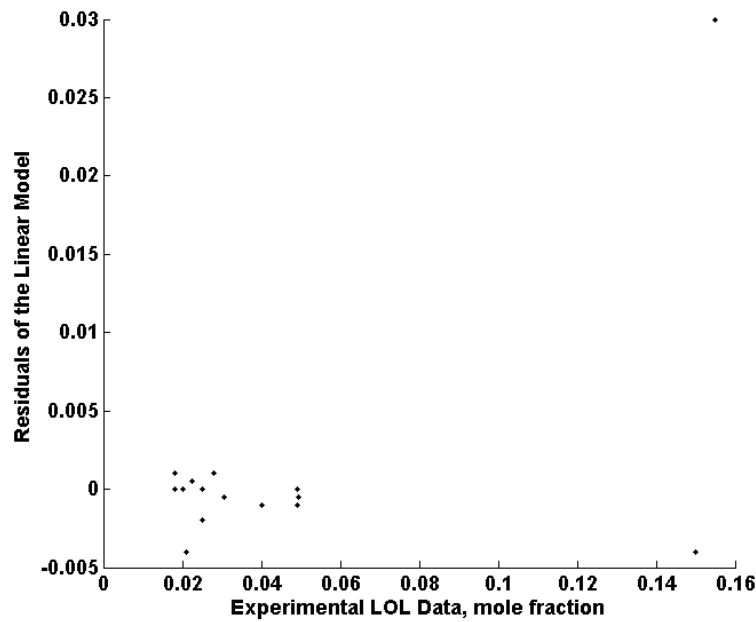
Figure 4.11:   Plot of the lower oxygen limit residuals from the linear model.

Figure 4.11 shows that the fit is good and balanced. However, there is one outlier:

carbon monoxide. The linear model provides a good fit to the lower oxygen limit data.

The residuals are balanced around zero but there is one outlier. Again, it is not clear

whether the outlier is due to an error in the model or the experimental data. The fit is

excellent because the reaction is oxygen-rich and the reaction goes to completion along

this boundary, so it is easy to model.

The linear model does not fit the limiting oxygen concentration adequately. The "zy_{LFL}"

method has been shown to be more reliable than this method. However, the linear model

does fit the upper oxygen limit rather well. This can be explained by the fact that the reaction used to model the flammability limit is fuel-rich and so is the upper oxygen limit. Thus, a fuel-rich reaction predicts the fuel-rich region well. These reactions are dominated by carbon, carbon monoxide, and hydrogen products and, therefore, the linear model estimates well for reactions that are decomposition dominated. These reactions have low heats of reaction so they must be very similar to reaction that only goes to partial completion like the one modeled in the linear model.

Since the limiting oxygen concentration is often a fuel-lean reaction and the products are dominated by carbon monoxide, water, and carbon dioxide, it is not estimated well. However, the limiting oxygen concentration is estimated well for well some compounds. This method works well for compounds such as hydrogen, ethylene, carbon monoxide, methanol, dimethyl ether, etc. These are compounds have oxygen concentrations at the UFL that are less than the UFL. So, the reactions are very fuel-rich at the UFL, and would be dominated by decomposition reactions. It would be reasonable to assume that the LOC is dominated by these reactions too.

Overall, the linear method does not do a satisfactory job in predicting the LOC. It has a low R^2 value and under-predicts the LOC. The "zy_{LFL}" method has been show estimate the LOC with greater accuracy because its R^2 value is larger. However, for fuels that have a fuel concentration at the UFL greater than the oxygen concentration, it does model

the upper flammability limit boundary well. This is because the entire boundary is very fuel-rich and the reaction is dominated by decomposition to carbon and hydrogen. The linear model does predict the lower oxygen limit and the upper oxygen limit with reasonable accuracy.

5 The Extended Linear Model

5.1 Application of the Linear Model on Other Fuels

So far, this model has only been applied graphically to an entire set of hydrogen data in Chapter 4. Now, other fuels will be explored to determine why the fit to the LOC is so poor when compared to a large collection of experimental data. Figure 5.1 is the result of modeling the flammability zone boundaries of ethylene using the methods described above.
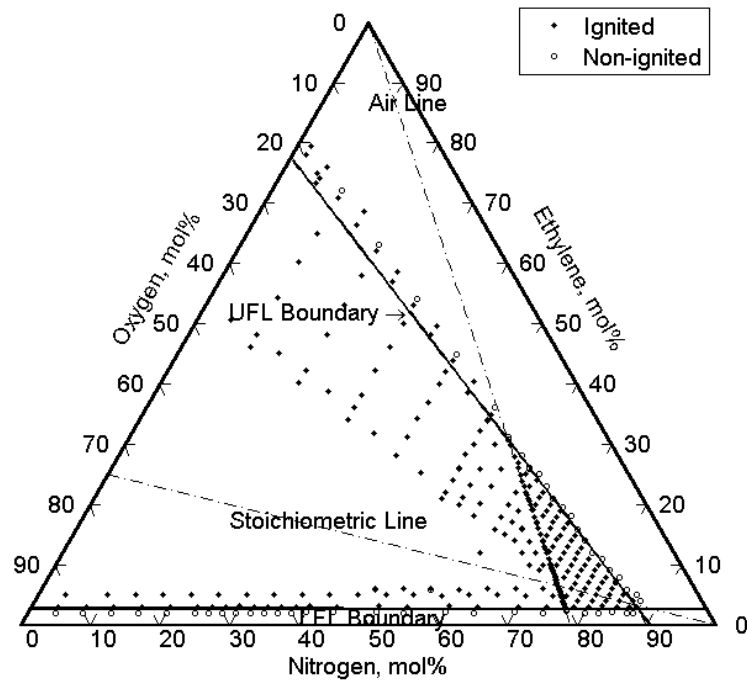
Figure 5.1: The linear model for the flammability zone boundaries applied to ethylene data (Mashuga 1999) with $y_{UFL} = 0.3038$, $y_{LFL} = 0.026$, $T_{ad,U} = 1609$ K, and $T_{ad,L} = 1341$ K.

53

With ethylene data, the fit seems to be rather adequate. The LOC is estimated well and

the UOL is only slightly underestimated. This is hypothesized to estimate the boundary

because at the UFL at the fuel concentration is much greater than the oxygen

concentration (y_{UFL} = 0.3038 and y_{UFL,O_2}= 0.146) and thus the upper flammability limit

boundary is very fuel-rich and decomposition dominated. It seems appropriate to model

fuel with a larger fuel than air concentrations at the UFL in this manner since the reaction

used is a fuel-rich reaction. Table 5.1 shows that equilibrium species (Dandy 2008) at the

upper flammability limit for ethylene.

Table 5.1:   The chemical equilibrium species of ethylene at the upper flammability

limit for constant pressure and enthalpy. The products are dominated by

carbon, carbon monoxide and hydrogen.

	Initial mole fraction	Final mole fraction
C_2H_4	0.304	0.000
O_2	0.146	0.000
N_2	0.550	0.312
C(s)	0.000	0.183
CO	0.000	0.160
CO_2	0.000	0.001
H_2	0.000	0.341
H_2O	0.000	0.003
Total	**1.000**	**1.000**

5.2 Fuels that Require Greater Oxygen Concentrations

However, for fuels that require larger oxygen concentrations than fuel, such as the alkanes, at the UFL the linear model does not correlate well with experimental data. Figure 5.2 is the result of using this method to model the flammability zone boundaries of methane (CH_4) for both the UFL and LFL with actual flammability data:
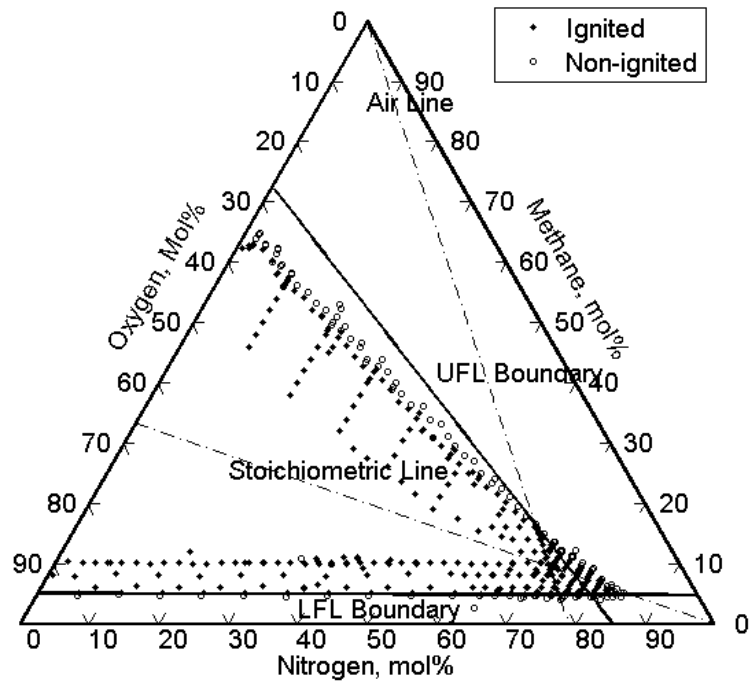
Figure 5.2: The linear model for the flammability zone boundaries applied to methane data (Mashuga 1999) with $y_{UFL} = 0.1614$, $y_{LFL} = 0.0485$, $T_{ad,U} = 2085$ K, and $T_{ad,L} = 1450$ K.

While the lower flammability limit boundary is modeled appropriately, the upper

flammability zone boundary model is not adequate. The upper oxygen limit is

underestimated and the limiting oxygen concentration is overestimated. It appears that

the UFL boundary has a curvature to it and this is believed to be from the change in

reaction stoichiometry. Using a chemical equilibrium program (Dandy 2008), the

products of the reaction change along the upper flammability zone boundary as one tests

the limiting oxygen concentration to the upper flammability limit to the upper oxygen

limit. The products change from carbon dioxide and water to a combination of carbon

monoxide, hydrogen, and water and finally to mixture that mostly contains mostly carbon

monoxide, hydrogen, and solid carbon. Tables 5.2-4 show the initial and final molar

concentrations for the LOC, UFL, and UOL for chemical equilibrium at constant pressure

and enthalpy.

Table 5.2: The chemical equilibrium species of methane at the limiting oxygen
concentration for constant pressure and enthalpy. The products are
dominated by carbon dioxide and water.

	Initial mole fraction	Final mole fraction
CH_4	0.049	0.000
O_2	0.116	0.024
N_2	0.836	0.837
C(s)	0.000	0.000
CO	0.000	0.000
CO_2	0.000	0.077
H_2	0.000	0.000
H_2O	0.000	0.063
Total	**1.000**	**1.000**

Table 5.3:   The chemical equilibrium species of methane at the upper flammability

limit for constant pressure and enthalpy. More carbon monoxide and

water is produced in this reaction.

	Initial mole fraction	Final mole fraction
CH_4	0.161	0.000
O_2	0.176	0.000
N_2	0.662	0.578
C(s)	0.000	0.000
CO	0.000	0.110
CO_2	0.000	0.031
H_2	0.000	0.146
H_2O	0.000	0.135
Total	**1.000**	**1.000**

Table 5.4:   The chemical equilibrium species of methane at the upper oxygen limit for

constant pressure and enthalpy. Mostly carbon monoxide, hydrogen, and

solid carbon are produced in this scenario.

	Initial mole fraction	Final mole fraction
CH_4	0.651	0.000
O_2	0.349	0.000
N_2	0.000	0.000
C(s)	0.000	0.064
CO	0.000	0.248
CO_2	0.000	0.021
H_2	0.000	0.598
H_2O	0.000	0.068
Total	**1.000**	**1.000**

In order to compensate for the change in products, it is suggested that two reaction criteria are used to predict the upper flammability zone boundary. Both reactions should have oxygen stoichiometric coefficients, or z-values, that are near what is the amount of oxygen consumed at the upper flammability limit. One z-value should result in a reaction that is fuel-rich and the other should result in a reaction that is fuel-lean. These z-values will predict the boundary between upper flammability limit and the upper oxygen limit and between the upper flammability and the limiting oxygen concentration, respectively. For example, at methane's UFL, the z-value is equal to approximately 1.09 or the ratio of oxygen to methane is 1.09, so:

$$CH_4 + 1.09\ O_2 \xrightarrow{yields} products \qquad (5.1)$$
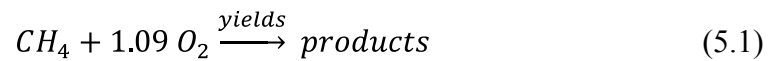
So, the predictor values of z will be 1 for the fuel-lean and 1.5 for the fuel-rich, or:

$$CH_4 + O_2 \xrightarrow{yields} products, \text{ and} \qquad (5.2)$$

$$CH_4 + \frac{3}{2}O_2 \xrightarrow{yields} products \qquad (5.3)$$
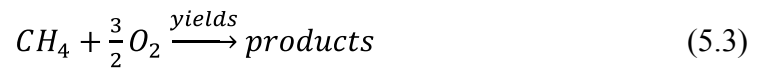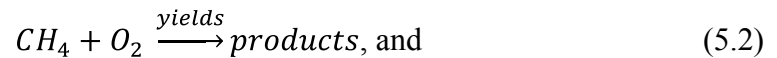
These values were chosen because they are greater or less than the ratio of oxygen to methane at the UFL.

The next step to be taken is to determine the products for each of these reactions. In general, it can be stated that the oxygen involved in the reaction will first react with the outside hydrogen molecules on a hydrocarbon molecule. Once two hydrogen molecules have been removed the OH molecules present will most likely react with the exposed carbon.

For reaction 5.2, it is initially assumed that a hydrogen molecule is separated from the methane molecule with the energy from the ignition source:

$$CH_4 \rightarrow CH_3 + H \tag{5.4}$$

Law and Egolfopoulos (Law and Egolfopoulos 1990) suggest that the following branching reaction is the dominant reaction:

$$H + O_2 \rightarrow OH + O \tag{5.5}$$

If Peter's mechanism (Quiceno, Chejne et al. 2002) is followed, then the free radical oxygen will react with the CH_3:

$$CH_3 + O \rightarrow CH_2O + H \tag{5.6}$$

The OH radical then will react with CH_2O (Glassman 1987):

$$CH_2O + OH \rightarrow CHO + H_2O \tag{5.7}$$

The CHO will then react with the remaining H radical:

$$CHO + H \rightarrow H_2 + CO \tag{5.8}$$

If reactions 5.4-8 are added together, then the following is the result:

$$CH_4 + O_2 \rightarrow CO + H_2 + H_2O \tag{5.9}$$
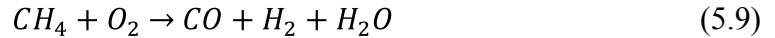
At the UFL, the oxygen concentration is greater than the fuel concentration, so oxygen will be remaining. It is assumed that the oxygen will react with the hydrogen in the system. So, the following equation must be included with the energy balance:

$$2H_2 + O_2 \rightarrow 2H_2O \tag{5.10}$$

59

The same method can be followed to solve for the products of equation 5.3; however, an extra O molecule is present so the following reaction will result:

$$H_2 + O \rightarrow H_2O \tag{5.11}$$

Thus, the final reaction will be:

$$CH_4 + \frac{3}{2}O_2 \rightarrow CO + 2H_2O \tag{5.12}$$
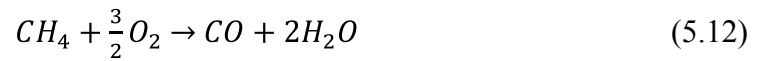
The reaction represented in equation 5.12 will be the fuel-rich equation since the oxygen present at the upper flammability limit will be consumed before the fuel is consumed. It will be assumed that the fuel that remains in the system will be unchanged.

The following reaction may also be present in this system (Glassman 1987):

$$CO + H_2O \Leftrightarrow CO_2 + H_2 \tag{5.13}$$

However, for simplicity's sake, it will be assumed that this reaction is negligible.

Generally, this reaction mechanism uses the oxygen present to first form CO from the carbon present, then H_2O from the hydrogen, and finally would produce CO_2 if there was enough oxygen present. However, there rarely is enough oxygen along the upper flammability zone boundary to produce large amounts of carbon dioxide. This follows the reaction that Wierzba, Shrestha, et al. proposed for predicting the upper flammability limit (Wierzba, Shrestha et al. 1996).

Using the reactions represented in equations 5.9, 5.10, and 5.12; two new linear equations can be derived from the energy balance to describe the upper flammability limit

boundary. The first equation using equations 5.9 and 5.10 will represent the lower

portion of the upper flammability limit boundary predicting towards the limiting oxygen

concentration. It will be used this way because the reaction is fuel-lean so it predicts

toward a fuel-lean region. The second reaction using equation 5.12 will represent the

upper portion of the UFL boundary predicting towards the upper oxygen limit. This

model is used to predict this region since it is a fuel-rich reaction as is the upper part of

the boundary. The lower portion of UFL boundary will be derived first.

For the lower portion of the upper flammability limit boundary, the energy balance for

the lower portion is written as follows:

$$y_f \Delta \bar{H}_{r,a} + \left(y_{O_2} - y_f\right)\Delta \bar{H}_{r,b}$$
$$+ \left(\alpha_{UL} y_f + \beta_{UL} y_{O_2} + \gamma_{UL}\right)(T_{ad} - T_i) = 0 \qquad (5.13)$$

Where:

$\Delta \bar{H}_{r,a}$ = the enthalpy of reaction for equation 5.9

$\Delta \bar{H}_{r,b}$ = the enthalpy of reaction for equation 5.10

And,

$$\alpha_{UL} = \bar{C}_{p,CO} + 3\bar{C}_{p,H_2} - \bar{C}_{p,H_2O} - \bar{C}_{p,N_2} \qquad (5.14)$$

$$\beta_{UL} = 2\bar{C}_{p,H_2O} - 2\bar{C}_{p,H_2} - \bar{C}_{p,N_2} \qquad (5.15)$$

$$\gamma_{UL} = \bar{C}_{p,N_2} \qquad (5.16)$$

Solving equation 5.13 for y_f results in the following:

$$y_f = -\frac{\Delta\bar{H}_{r,b}+\beta_{UL}(T_{ad}-T_i)}{\Delta\bar{H}_{r,a}-\Delta\bar{H}_{r,b}+\alpha_{UL}(T_{ad}-T_i)}y_{O_2} - \frac{\gamma_{UL}(T_{ad}-T_i)}{\Delta\bar{H}_{r,a}-\Delta\bar{H}_{r,b}+\alpha_{UL}(T_{ad}-T_i)} \qquad (5.17)$$

This equation can be used to estimate the upper flammability zone boundary between the upper flammability limit and the LOC. As before, the UFL will be used to determine the adiabatic flame temperature through an iterative solution. The MathCAD® spreadsheet in Appendix III illustrates how this can be done. The limiting oxygen concentration is solved for by setting equation 5.17 equal to equation 4.13, then using equation 4.23, and

$$\frac{\beta_L(T_{ad,L}-T_i)}{-\Delta\bar{H}_r-\alpha_L(T_{ad,L}-T_i)} = 0:$$

$$y_{LOC} = \frac{y_{LFL}\left(\frac{\Delta\bar{H}_{r,a}-\Delta\bar{H}_{r,b}}{T_{ad,UL}-T_i}+\alpha_{UL}\right)+\gamma_{UL}}{-\left(\frac{\Delta\bar{H}_{r,b}}{T_{ad,UL}-T_i}+\beta_{UL}\right)} \qquad (5.18)$$

This equation can be used to estimate the limiting oxygen concentration and is not simplified any further. For use with other fuels, the heat capacity parameters (α_{UL}, β_{UL}, and γ_{UL}) and the value of $\Delta\bar{H}_{r,a}$ must be determined in a similar manner in order to account for those specific reactions.

For the portion of the upper flammability zone boundary between the UFL and UOL, the energy balance is the following:

$$\frac{2}{3}y_{O_2}\Delta\bar{H}_{r,c} + (\alpha_{UU}y_f + \beta_{UU}y_{O_2} + \gamma_{UU})(T_{ad} - T_i) = 0 \qquad (5.19)$$

62

Where:

$\Delta \bar{H}_{r,c}$ = the enthalpy of reaction for equation 5.12

And,

$$\alpha_{UU} = \bar{C}_{p,CH_4} - \bar{C}_{p,N_2} \qquad (5.20)$$

$$\beta_{UU} = \frac{2}{3}\bar{C}_{p,CO} + \frac{4}{3}\bar{C}_{p,H_2O} - \frac{2}{3}\bar{C}_{p,CH_4} - \bar{C}_{p,N_2} \qquad (5.21)$$

$$\gamma_{UU} = \bar{C}_{p,N_2} \qquad (5.22)$$

Solving for y_f yields equation 4.18 where $z = \frac{3}{2}$ and $\Delta \bar{H}_r = \Delta \bar{H}_{r,c}$. This equation is

solved for the upper oxygen limit and equation 4.18 is the result where $z = \frac{3}{2}$ and

$\Delta \bar{H}_r = \Delta \bar{H}_{r,c}$. These equations can be used to solve for the upper flammability zone

boundary above the UFL and for the upper oxygen limit, respectively. For use with other

gases, different heat capacity terms and heats of reactions would have to be determined

based upon the unique reaction stoichiometry of the particular gas. The adiabatic flame

temperature for this reaction should be used and solved for at the UFL. Figure 5.3 shows

lower portions of the upper flammability zone boundary plotted with methane-oxygen-

nitrogen system data. This plot is valid for the boundary between the UFL and LOC.
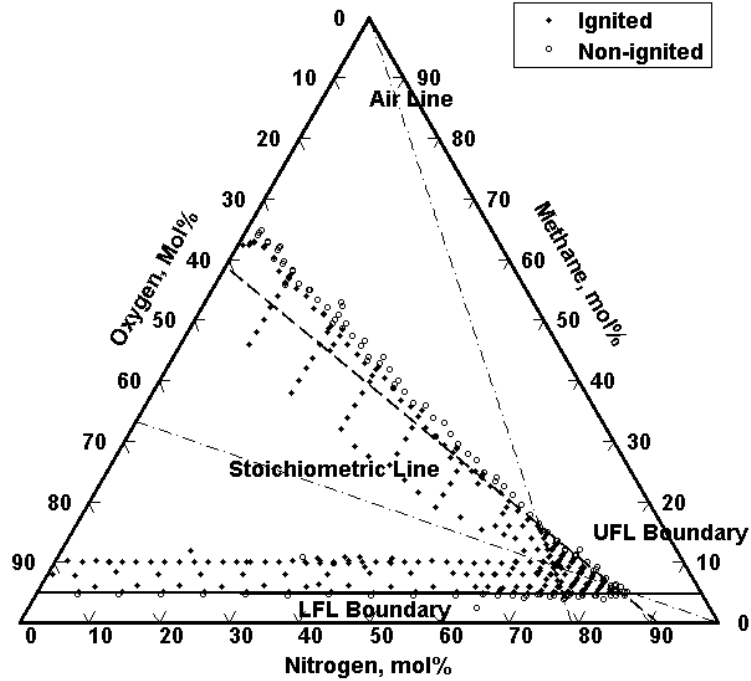
Figure 5.3: The upper flammability zone boundary modeled using the extended model for the boundary between the UFL and LOC with y_{UFL} = 0.1614, y_{LFL} = 0.0485, and $T_{ad,UL}$ = 1646 K for methane data (Mashuga 1999).

Figure 5.4 shows the plot of the portion of the upper flammability zone boundary that is valid for the boundary between the UOL and UFL from the extended linear model.
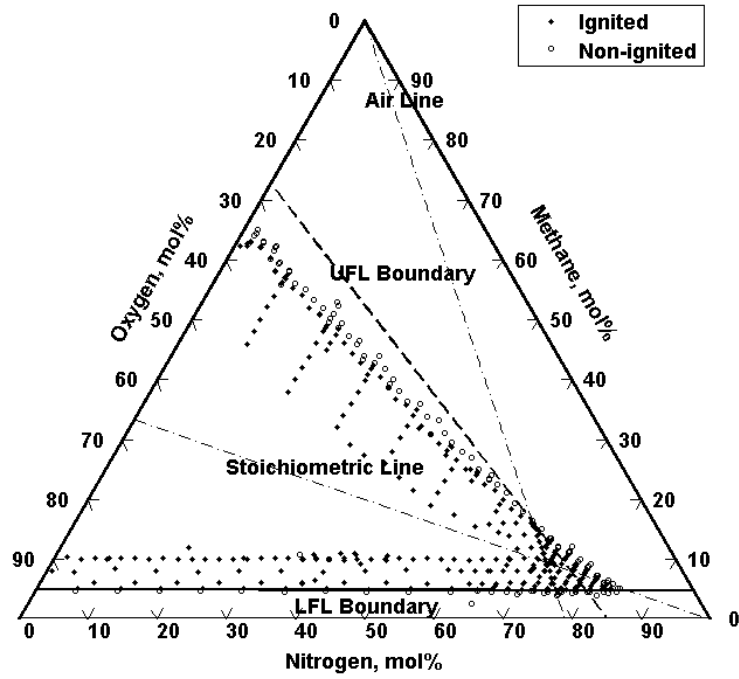
Figure 5.4:   The upper flammability zone boundary modeled using the extended model

for the boundary between the UFL and the UOL with y_{UFL} = 0.1614, y_{LFL}

= 0.0485, and $T_{ad,UU}$ = 1880 K for methane data (Mashuga 1999).

This figures shows that there is better agreement between the estimated LOC than with

equations 4.13 and 4.18. The estimations made with this method will be further analyzed

in the results section. Appendices III and IV show how these solutions were obtained.

5.3   Results for the Extended Linear Model

Obtaining solutions for the extended linear model is more complicated than the original

linear model of the flammability limit boundary. The LFL model is used again; however,

the UFL model is a set of two equations. The first step is to determine the specific

reactions used to solve for the heats of reaction and heat capacity parameters. An

iterative solution is then used to solve for the adiabatic flame temperature at the upper

flammability limit. Tables 5.5 and 5.6 are the results of this procedure for 12 fuels:

Table 5.5:   The reaction stoichiometry, heats of reaction, and adiabatic flame

temperatures for the fuel-lean reactions computed to estimate the upper

flammability zone boundary.

Compound	Reaction	ΔH_r kJ/mole	Adiabatic Flame Temperature (K)
Hydrogen	$H_2 + \frac{1}{2}O_2 \rightarrow H_2O$	-237	1123
Methane	$CH_4 + O_2 \rightarrow CO + H_2 + H_2O$	-278	1646
Carbon Monoxide	$CO + \frac{1}{2}O_2 \rightarrow CO_2$	-283	1349
Ethylene	$C_2H_4 + 3O_2 \rightarrow 2CO_2 + 2H_2O$	-1332	1341
Ethane	$C_2H_6 + O_2 \rightarrow 2CO + 3H_2$	-137	1363
Cyclopropane	$C_3H_6 + 1.5O_2 \rightarrow 3CO + 3H_2$	-385	1506
Propene	$C_3H_6 + 1.5O_2 \rightarrow 3CO + 3H_2$	-351	1180
Propane	$C_3H_8 + 2O_2 \rightarrow 3CO + 3H_2 + H_2O$	-469	1541
Isobutane	$C_4H_{10} + 2O_2 \rightarrow 4CO + 5H_2$	-316	1382
n-Butane	$C_4H_{10} + 2O_2 \rightarrow 4CO + 5H_2$	-316	1382
Acetylene	$C_2H_2 + \frac{5}{2}O_2 \rightarrow 2CO_2 + H_2O$	-1236	729

Table 5.6: The reaction stoichiometry, heats of reaction, and adiabatic flame temperatures for the fuel-rich reactions computed to estimate the upper flammability zone boundary.

Compound	Reaction	ΔH_r kJ/mole	Adiabatic Flame Temperature (K)
Hydrogen	$H_2 + \frac{1}{2}O_2 \rightarrow H_2O$	-237	1123
Methane	$CH_4 + \frac{3}{2}O_2 \rightarrow CO + 2H_2O$	-520	1880
Carbon Monoxide	$CO + \frac{1}{2}O_2 \rightarrow CO_2$	-283	1349
Ethylene	$C_2H_4 + 3O_2 \rightarrow 2CO_2 + 2H_2O$	-1332	1341
Ethane	$C_2H_6 + \frac{3}{2}O_2 \rightarrow 2CO + H_2O + 2H_2$	-379	1491
Cyclopropane	$C_3H_6 + 2O_2 \rightarrow 3CO + H_2O + 2H_2$	-627	1587
Propene	$C_3H_6 + 2O_2 \rightarrow 3CO + H_2O + 2H_2$	-593	865
Propane	$C_3H_8 + \frac{5}{2}O_2 \rightarrow 3CO + 2H_2O + 2H_2$	-710	1524
Isobutane	$C_4H_{10} + \frac{5}{2}O_2 \rightarrow 4CO + H_2O + 4H_2$	-558	1227
n-Butane	$C_4H_{10} + \frac{5}{2}O_2 \rightarrow 4CO + H_2O + 4H_2$	-558	1227
Acetylene	$C_2H_2 + \frac{5}{2}O_2 \rightarrow 2CO_2 + H_2O$	-1236	729

The LOC and UOL were then solved for using equations 4.13, 4.18, and 5.17. Table 5.7 shows the results of the extended linear model for 11 species in which the most appropriate model was used to determine the solution. If the fuel had a larger concentration of fuel than oxygen at the UFL, the linear model was used. If the fuel had a greater oxygen concentration than fuel at the UFL then the extended model was used.

Table 5.7:   Estimates of the limiting oxygen concentration and the upper oxygen limit

using the extended linear model compared to experimental data located in

Appendix I.

Compound	LOC	|Experimental - Estimated|	UOL	|Experimental - Estimated|
Hydrogen	0.052	0.003	0.950	0.010
Methane	0.114	0.002	0.727	0.076
Carbon Monoxide	0.060	0.005	0.940	0.000
Ethylene	0.100	0.007	0.776	0.030
Ethane	0.098	0.012	0.640	0.057
Cyclopropane	0.103	0.012	0.590	0.010
Propene	0.102	0.013	0.624	0.094
Propane	0.099	0.016	0.558	0.038
Isobutane	0.097	0.023	0.515	0.035
n-Butane	0.096	0.024	0.517	0.027
Acetylene	0.026	0.036	0.955	0.025
Average Difference		0.014		0.037
95% Confidence Interval		0.047		0.119
R^2		0.572		0.904

The extended linear model estimates 95% confidence interval on the mean for the LOC at

$y_{LOC} \pm 0.047$ and the estimates the 95% confidence interval on the mean for the UOL at

$y_{UOL} \pm 0.119$. The R^2 values are 0.572 and 0.904 for the LOC and UOL, respectively.

5.4   Discussion of the Extended Linear Model

The extended linear model was presented as an extension to the linear model in order to better predict the limiting oxygen concentration. It was hypothesized that the linear model was not predicting the limiting oxygen concentration well because it was using a fuel-rich reaction to predict a fuel-lean point. The extended model works best for fuels that have a greater oxygen concentration than fuel concentration at the upper flammability limit.

From Tables 5.2-4, it can be seen that the products for methane combustion change along the upper flammability zone boundary. This is what accounts for the change in slope along the UFL boundary. It seems appropriate to estimate the slope with another reaction than the fuel-rich reaction in equation 4.6. So, a reaction where the fuel was the limiting factor was chosen which also produces hydrogen and some of this hydrogen will be consumed by the remaining oxygen in the system. Since this reaction is fuel-limited, it predicts a fuel limited slope and fuel-limited points such as the LOC better than reaction 4.6.

In order to properly represent the extended linear model, both models were used to best represent fuels with both limiting oxygen concentration and upper oxygen limit data available. For fuels with a fuel concentration greater than the oxygen concentration at the

UFL, the linear model was used. For fuels with a greater oxygen concentration than fuel at the UFL, the extended model was used.

Results of the extended linear model were presented for a small data set. This was because of a lack of data for the upper oxygen limit and that the extended linear model is only valid for compounds with a greater concentration of oxygen than fuel at the upper flammability limit. The 95% confidence interval on the mean of the limiting oxygen concentration is $y_{LOC} \pm 0.047$. The 95% confidence on the mean of the upper oxygen limit is $y_{UOL} \pm 0.119$.

Figure 5.5 is a plot of the estimates of the LOC with the extended linear model vs. experimental data showing a R^2 value of 0.573.
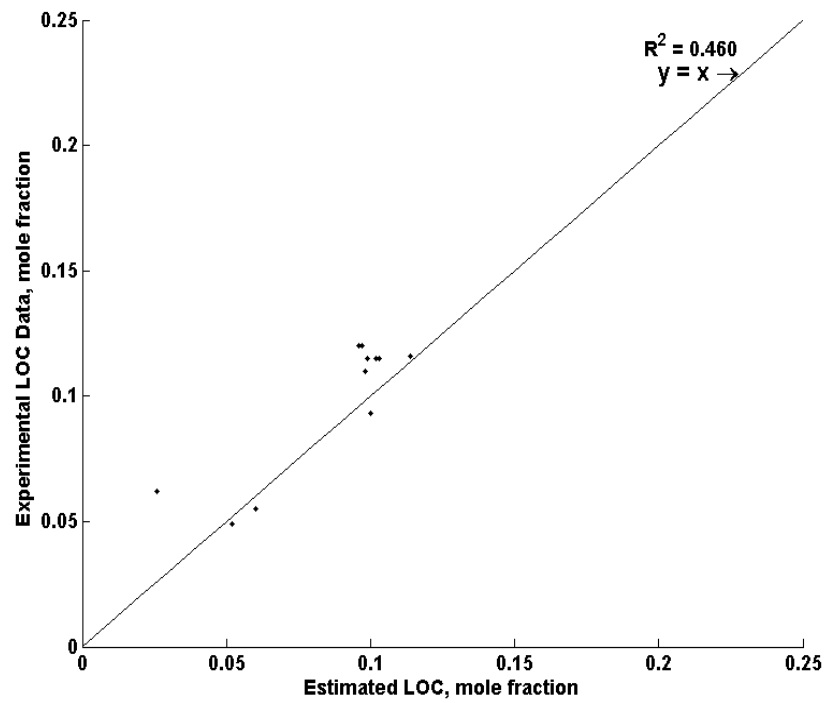
Figure 5.5: Plot of the LOC estimations from the extended linear model vs. experimental LOC data.

This shows a better correlation with the experimental data than that of the "zy_{LFL}" method. Figure 5.6 is a plot of the estimates of the UOL with the extended linear model vs. experimental data showing a R^2 value of 0.904.
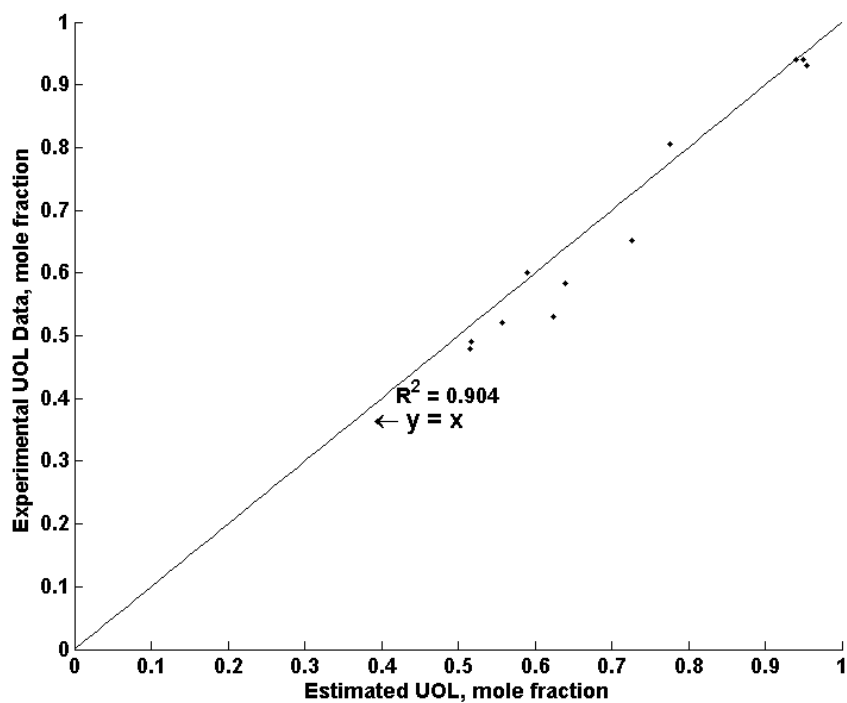
Figure 5.6:   Plot of the UOL estimations from the extended linear model vs. the

experimental data.

These estimations are very close to the linear model's estimations. The plot of the LOC

data shows a better fit to the experimental data than the linear method and the "zy_{LFL}"

method. The fit is still not that good though. The estimates of the UOL fit as well as the

linear model.

Figure 5.7 is the residuals of estimates of the LOC from the extended linear model.
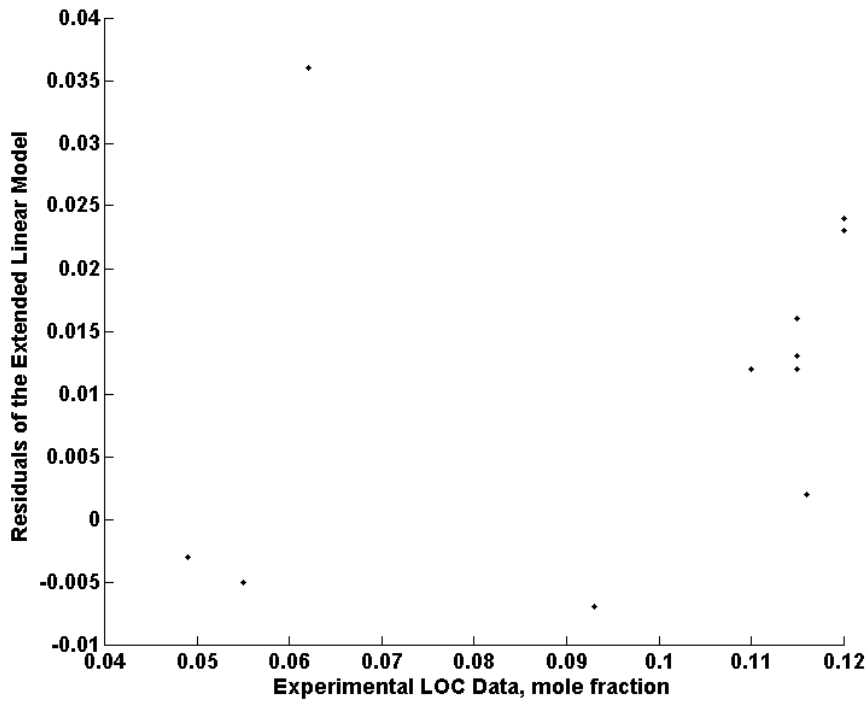
Figure 5.7:   Plot of the residuals of the LOC estimations from the extended linear model.

Figure 5.7 shows that the fit is over-estimated but all of the residuals are within the confidence interval. However, all the residuals are within the confidence interval. The overestimation may show that the intersection of the two models is not necessarily the proper point for the LOC. Figure 5.8 is the residuals of estimates of the UOL from the extended linear model.
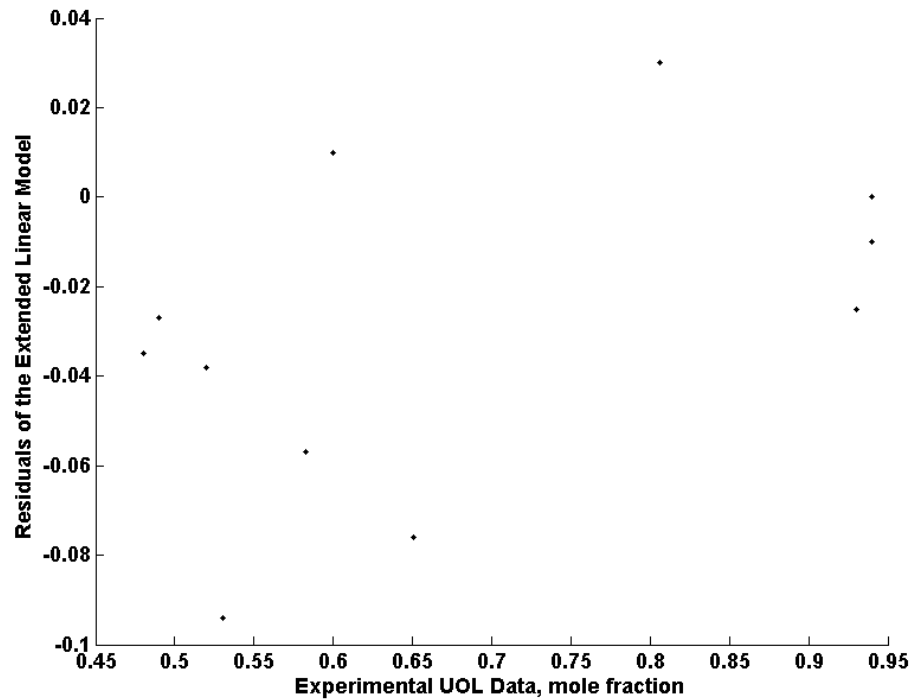
Figure 5.8:   Plot of the residuals of the UOL estimations from the extended linear

model.

Figure 5.8 shows that the UOL is modeled rather well but it seems to favor

underestimates. This still could show that a linear model does not account well enough

for the change in reaction along the upper boundary.

A limit to accuracy of this model is the limited amount of experimental data. With a

limited amount of data available it is hard to determine its accuracy. Also, the model is

difficult to use since it requires some complicated steps in order to determine the reaction

that characterizes the energy balance. The equations seem to not be affected by changes in the values of the heat capacity parameters. This method is more sensitive to the heat of reaction.

This method shows that changing the reaction mechanism can improve the accuracy of this thermodynamic model.   The method that should be used is dependent on what reactions dominate the system. As a general rule, if the oxygen concentration at the UFL is greater than the fuel concentration, the extended model should be used. Otherwise, the linear model will work best. The analysis of the results of the extended linear model is limited by the lack of data and difficulty in determining the reactions that characterize the energy balance.

6 The Empirical Model

6.1 An Empirical Method for Estimating the Flammability Zone Boundaries

In this thesis, a thermodynamic-based method for estimating the flammability zone boundaries has been presented. The linear method was initially presented because it is has a clear theoretical basis. However, the results for this method are not always satisfactory with this method and retrieving results can be tedious and complex. So, accordingly, a simple empirical method was developed for use with flammable gases.

It was observed that if the flammable boundary for the UFL was extended beyond the flammable area, it would extend down in the negative portion of the graph and cross the fuel axis at approximately the negative of the upper flammability limit. The initial purpose of this exercise was to determine if a linear relationship exists between the UFL and LOC. In order to determine, a line was draw between the UFL and LOC. Figures 6.1 and 6.2 shows an example of this observation for methane data:
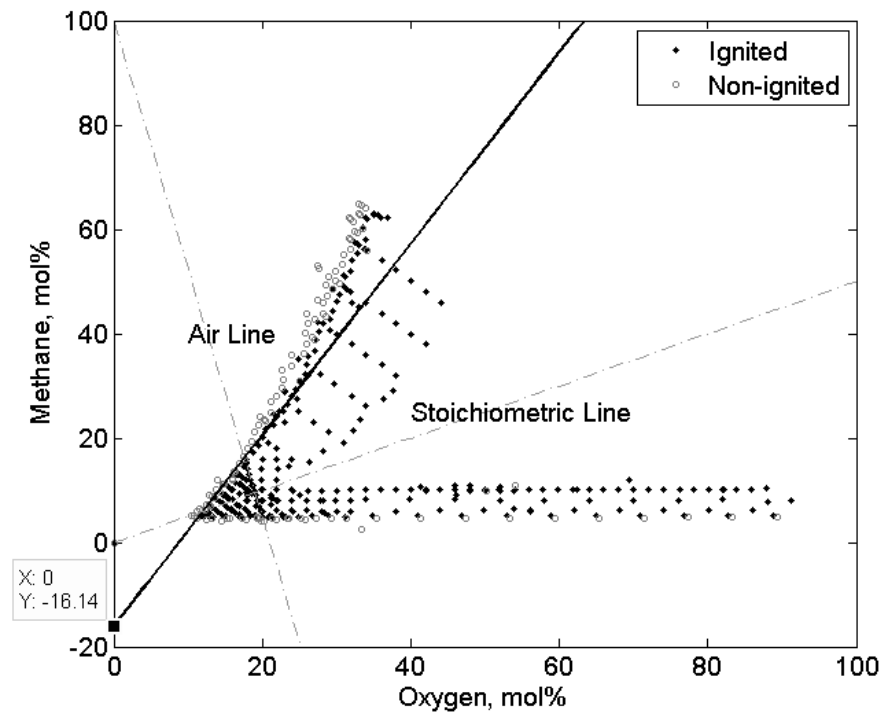
Figure 6.1: A line approximating the slope the upper flammability zone boundary drawn against methane data (Mashuga 1999).

From Figure 6.1, it appears that the line intercepts the y-axis at $(0,-y_{UFL})$. In order to determine this even better, a closer look is taken in Figure 6.2.
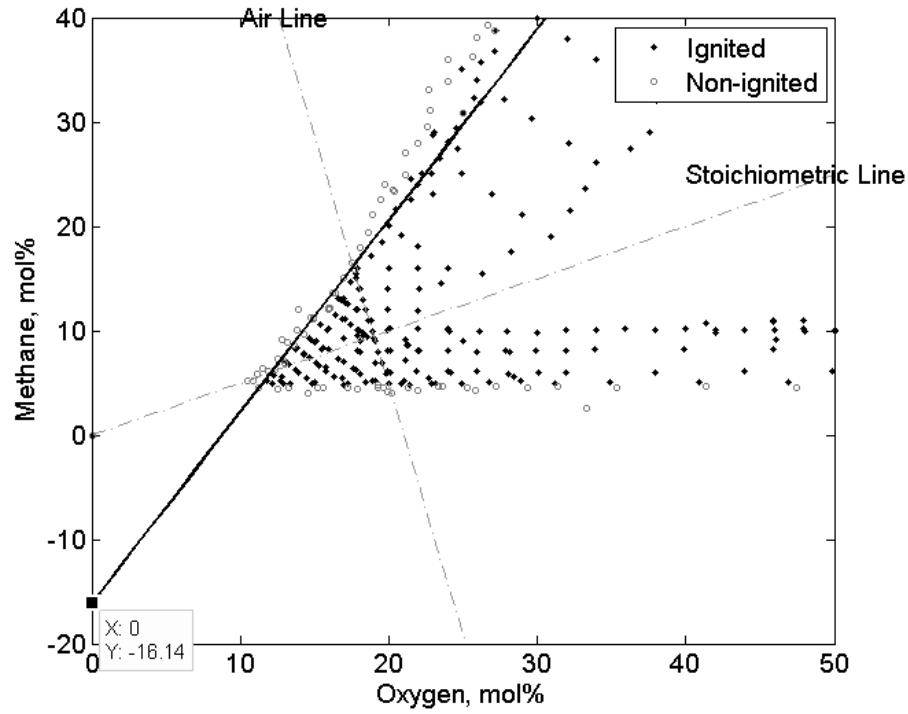
Figure 6.2:   A close-up the limiting oxygen concentration area for the line drawn to

match the slope of the UFL boundary of methane data (Mashuga 1999).

Figure 6.2 shows that the y-intercept is $(0,-y_{UFL})$. If it is assumed that the UFL boundary

is linear, the equation to represent this line can be made by forcing it to pass through the

UFL and equation 6.1:

$$y_f = \frac{y_{UFL}-y_{UFBI}}{y_{UFL,O_2}} y_{O_2} + y_{UFBI}$$ (6.1)

Equation 6.1 will only be used to model the area between the limiting oxygen

concentration and the upper flammability limit. The result is generalized by multiplying

the UFL by a constant:

$$y_{UFBI} = C_{LOC}y_{UFL} \tag{6.2}$$

where C_{LOC} is the constant used for determining the lower section of the line. Equation

6.1 is now stated as the following:

$$y_f = \frac{y_{UFL} - C_{LOC}y_{UFL}}{y_{UFL,O_2}} y_{O_2} + C_{LOC}y_{UFL} \tag{6.3}$$

Equation 6.3 is then solved for the limiting oxygen concentration. The lower

flammability zone boundary is assumed to be a line with a slope of zero:

$$y_f = y_{LFL} \tag{6.4}$$

Using equation 6.4, an empirical equation for the LOC is:

$$y_{LOC} = \left(\frac{y_{LFL} - C_{LOC}y_{UFL}}{y_{UFL} - C_{LOC}y_{UFL}}\right) y_{UFL,O_2} \tag{6.5}$$

If the upper flammability zone boundary between the upper flammability limit and the

upper oxygen limit is estimated using the same method, it results in the following

equation:

$$y_f = \frac{y_{UFL} - y_{UOLI}}{y_{UFL,O_2}} y_{O_2} + y_{UOLI} \tag{6.6}$$

Where the y-intercept of this equation is:

$$y_{UOLI} = C_{UOL}y_{UFL} \tag{6.7}$$

Substituting equation 6.7 into 6.6 results in equation 6.8:

$$y_f = \frac{y_{UFL} - C_{UOL} y_{UFL}}{y_{UFL,O_2}} y_{O_2} + C_{UOL} y_{UFL} \qquad (6.8)$$

In order to solve equation 6.8 for the upper oxygen limit, $y_{O_2} = 1 - y_{UOL}$ and $y_f = y_{UOL}$:

$$y_{UOL} = \frac{y_{UFL}(1 - C_{UOL}(1 - y_{UFL,O_2}))}{y_{UFL,O_2} + y_{UFL}(1 - C_{UOL})} \qquad (6.9)$$

In order to solve for the UFL boundary using these empirical equations, C_{LOC} and C_{UOL}

must be solved for. The best approach for solving for these constants is to use a large

collection of LOC and UOL data and maximize the R^2 value of the fitted line. This

approach is taken in this thesis where C_{LOC} is determined to be -1.11 and C_{UOL} is

determined to be -1.87. When modeled against methane-oxygen-nitrogen data, the

following are the results for the boundary between the UFL and LOC in Figure 6.3:
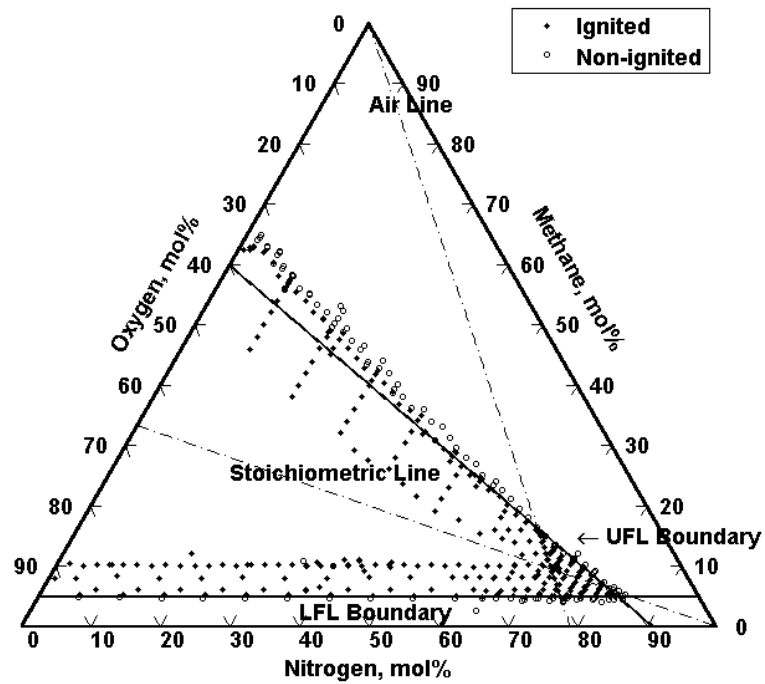
Figure 6.3:   The upper flammability zone boundary from the empirical model for the boundary between the LOC and UFL with C_{LOC} = -1.11 compared to methane data (Mashuga 1999).

The results for the empirical model to estimate the boundary between the UFL and UOL are plotted in Figure 6.4:
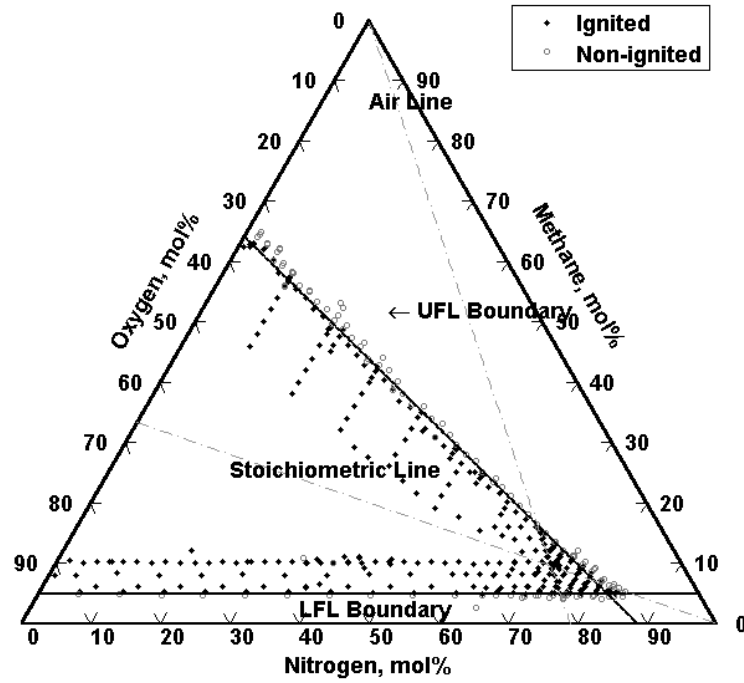
Figure 6.4:   The upper flammability zone boundary from the empirical model for the boundary between the UFL and UOL with C_{UOL} = -1.87 compared to methane data (Mashuga 1999).

The results and the method determining the constant values are further discussed in the results section.

6.2   Results for the Empirical Method

The empirical method for estimating the flammability zone boundaries contains a constant, C_{UOL} or C_{LOC}, which must be solved for. In this thesis, the procedure for solving the flammability zone boundary is to maximize the R^2 value by changing the

constant value. Figures 6.5-6 show the maximization of the R^2 values when the constant

values are changed for 38 compounds:
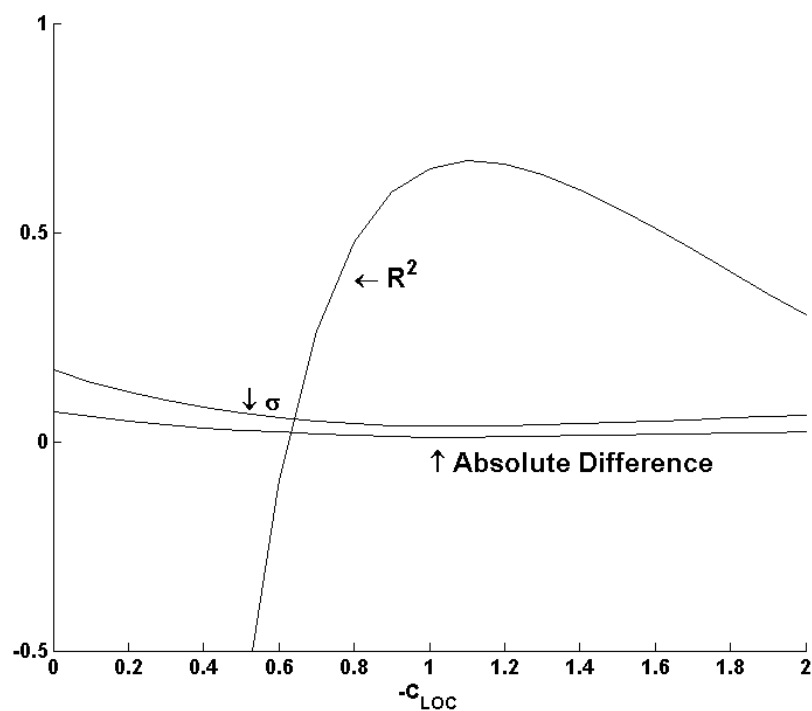
Figure 6.5:   Maximization of the R^2 value and minimization of the standard deviation

(σ) and absolute difference for the LOC constant for the empirical model.

The R^2 value is maximized at $C_{LOC} = -1.11$.
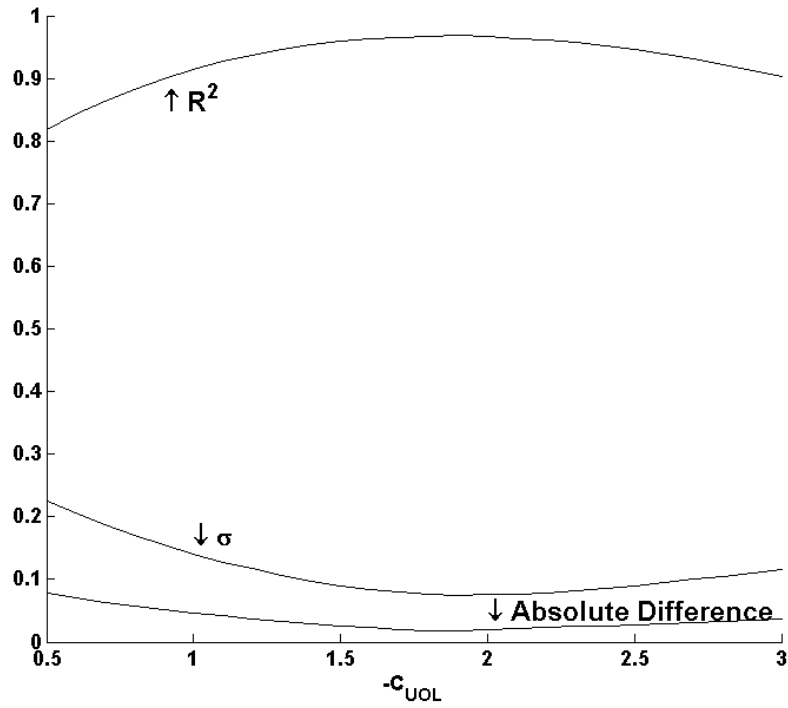
Figure 6.6: Maximization of the R^2 value and minimization of the standard deviation (σ) and absolute difference for the UOL constant for the empirical model. The R^2 value is maximized at $C_{UOL} = -1.87$.

Using $C_{LOC} = -1.11$ and $C_{UOL} = -1.87$, the limiting oxygen concentration and upper oxygen limit were estimated. For this method, the lower oxygen limit is estimated as the lower flammability limit. Tables 6.1 and 6.2 are the results of the empirical method:

Table 6.1: The results of the empirical method for the limiting oxygen concentration compared to the "zy_{LFL}" method and experimental data in Appendix I.

Compound	zy_{LFL}	|Experimental - Estimated|	Empirical	|Experimental - Estimated|
Hydrogen	0.024	0.025	0.028	0.021
Hydrogen Sulfide	0.065	0.011	0.066	0.009
Methane	0.097	0.019	0.118	0.002
Carbon Monoxide	0.063	0.008	0.033	0.022
Methanol	0.110	0.009	0.084	0.016
Carbon Disulfide	0.036	0.014	0.063	0.013
Acetylene	0.065	0.003	0.023	0.039
Ethylene	0.079	0.014	0.083	0.010
Ethane	0.105	0.005	0.118	0.008
Dimethyl Ether	0.099	0.006	0.091	0.014
Ethanol	0.105	0.000	0.105	0.000
Methyl Formate	0.114	0.011	0.107	0.004
1,2-Dichloroethane	0.186	0.056	0.125	0.005
1,1,1-trichloroethane	0.193	0.053	0.129	0.011
Cyclopropane	0.108	0.007	0.120	0.005
Propene	0.108	0.007	0.120	0.005
Propane	0.105	0.010	0.120	0.005
Acetone	0.120	0.005	0.116	0.001
Methyl Acetate	0.109	0.002	0.109	0.001
1,3-Butadiene	0.110	0.005	0.113	0.008
1-Butene	0.096	0.019	0.116	0.001
Isobutene	0.108	0.012	0.117	0.003
Isobutane	0.117	0.003	0.121	0.001
n-Butane	0.124	0.004	0.122	0.002
Butanone (MEK)	0.110	0.000	0.114	0.004
Diethyl Ether	0.114	0.009	0.074	0.031
1-chlorobutane	0.113	0.028	0.115	0.025
Isobutyl formate	0.130	0.005	0.121	0.004
3-methyl-1-Butene	0.113	0.003	0.115	0.000
Isopentane	0.112	0.008	0.119	0.001
n-Pentane	0.120	0.000	0.120	0.000
Benzene	0.105	0.009	0.121	0.007
n-Hexane	0.114	0.006	0.117	0.003
Toluene	0.126	0.031	0.123	0.028
n-Heptane	0.132	0.017	0.120	0.005

Table 6.1 (continued): The results of the empirical method for the limiting oxygen concentration compared to the "zy_{LFL}" method and experimental data in Appendix I.

Styrene	0.110	0.020	0.117	0.027
Ethylbenzene	0.084	0.001	0.114	0.029
Methylstyrene	0.219	0.129	0.133	0.043
Averages		0.015		0.011
95% Confidence Interval		0.063		0.037
R^2		0.416		0.672

Table 6.2: Estimates of the upper oxygen limit and the lower oxygen limit using the empirical method presented compared to experimental data in Appendix I.

Compound	UOL	|Experimental - Estimated|	LOL	|Experimental - Estimated|
Hydrogen	0.946	0.006	0.048	0.001
Deuterium	0.943	0.007	0.049	0.000
Ammonia	0.759	0.031	0.150	0.000
Methane	0.641	0.010	0.049	0.001
Carbon Monoxide	0.940	0.000	0.125	0.030
Acetylene	0.955	0.025	0.026	0.002
Ethylene	0.775	0.031	0.026	0.001
Ethane	0.582	0.001	0.030	0.001
Chloroethane	0.706	0.006	0.040	0.000
Cyclopropane	0.562	0.042	0.024	0.001
Propene	0.536	0.006	0.024	0.003
Propane	0.516	0.004	0.021	0.002
Isobutane	0.486	0.006	0.018	0.000
n-Butane	0.489	0.001	0.019	0.001
Divinyl Ether	0.751	0.099	0.017	0.001
Diethyl Ether	0.807	0.013	0.019	0.001
Averages		0.018		0.004
95% Confidence Interval		0.076		0.019
R^2		0.968		0.959

The R^2 value for the estimated LOC from the empirical method shows a better agreement with experimental data than the "zy_{LFL}" method. The 95% confidence interval on the mean of the LOC obtained is $y_{LOC} \pm 0.037$. The R^2 values obtained for the UOL and LOL empirical methods shows a good fit. The 95% confidence intervals on the means of the UOL and LOL are $y_{UOL} \pm 0.076$ and $y_{LOL} \pm 0.019$.

6.3   Discussion of the Empirical Model

An empirical model of the flammability boundaries was presented. This model is a graphical method that plots a line between the UFL and the intersection with the y axis. It is assumed that the intersection is the UFL multiplied by a constant. By maximizing the R^2 value, the following values for the constants were determined for 38 compounds:

C_{LOC} = -1.11 and

C_{UOL} = -1.87.

6.3.1 Statistical Significance of the Model Parameters

It can be shown that this method is statistically significant and thus appropriate to the model in this manner. A least squares linear regression is used to determine this (Montgomery 2004). The least squares linear regression equation is:

$$\hat{\beta}_{n+1\times1} = (X_{n+1\times m}^T X_{n+1\times m})^{-1} X_{n+1\times m}^T y_{n+1\times1} \qquad (6.10)$$

The first parameter to be analyzed is the limiting oxygen concentration. The independent variables to be considered are the lower flammability limit and the upper flammability limit. The results of the linear regression are the following:

$$\hat{y}_{LOC} = 0.118 + 0.264 y_{LFL} - 0.105 y_{UFL} \qquad (6.11)$$

This model has a regression coefficient of 0.986 and the results of the ANOVA are reported in Table 6.3:

Table 6.3:   Analysis of variance (ANOVA) for the linear regression of the limiting oxygen concentration.

ANOVA

Source	*SS*	*dof*	*MS*	F_o	$F_{0.05,v_1,v_2}$
Regression	0.4304	2	0.2152	1220	3.26
Error	0.0062	35	0.0002		
Total	0.4367	37			

This shows that the fit is significant because $F_o \gg F_{0.05,v_1,v_2}$ and the independent variables can be tested individually. The t-values for the LFL and UFL are 2.32 and -7.82. When compared to $t_{0.05,\ 35} = 2.03$, it shows that the absolute values of the t-values for the LFL and UFL are greater than this value so these independent variables are both significant to the regression.

The next parameter to be analyzed is the upper oxygen limit and the independent variables considered are the upper flammability limit and the lower flammability limit. The results of the regression are:

$$\hat{y}_{UOL} = 0.534 + 0.324y_{LFL} + 0.526y_{UFL} \qquad (6.12)$$

The R^2 value is 0.991 for this regression and the Table 5.2 is the results of the ANOVA.

Table 6.4:   Analysis of variance for the linear regression of the upper oxygen limit.

ANOVA

Source	SS	dof	MS	F_o	$F_{0.05,v_1,v_2}$
Regression	9.196	2	4.598	766	3.81
Error	0.084	14	0.006		
Total	9.280	16			

The fit is shown to be significant because $F_o \gg F_{0.05, v_1, v_2}$. The independent variables

are tested individually next. The t-values for the LFL and UFL are 0.698 and 7.47,

respectively. When compared to $t_{0.05, 14} = 2.16$, it shows that the UFL is significant ($t_o >$

$t_{0.05, 14}$) in the regression but the LFL is not significant ($t_o < t_{0.05, 14}$).

Finally, the regression for the lower oxygen limit is tested where the independent

variables are the upper flammability limit and the lower flammability limit. The results

of the regression are the following equation:

$$\hat{y}_{LOL} = 0.011 + 0.941 y_{LFL} + 0.019 y_{UFL} \qquad (6.13)$$

The regression coefficient is 0.754. The results for the analysis of variance are in Table

6.5:

Table 6.5:   Analysis of variance for the linear regression of the lower oxygen limit.

ANOVA

Source	*SS*	*dof*	*MS*	*F_o*	*$F_{0.05, v_1, v_2}$*
Regression	0.094	2	0.047	21.5	3.81
Error	0.030	14	0.002		
Total	0.124	16			

The fit is shown to be significant because F_o is larger than $F_{0.05,v_1,v_2}$. The independent variables are tested individually. The t-values for the LFL and UFL are 3.37 and 0.413 and when compared to $t_{0.05,14} = 2.16$, it shows that the LFL is significant ($t_o > t_{0.05,14}$) and the UFL is not significant ($t_o < t_{0.05,14}$). In fact for this case, the constant is not significant because the t-value for it is 0.526 ($t_o < t_{0.05,14}$).

Fitting linear regression models to flammability data showed that the UFL and LFL have a significant relationship to the LOC and the LFL has a significant relationship with the LOL. Since equation 6.5 is derived with only the LFL and UFL as variables, it shows that this relationship is appropriate. With this equation only being derived from equations 6.3 and 6.4, these models for the upper flammability limit boundary between the upper flammability limit and the limiting oxygen concentration and lower flammability limit boundary must be appropriate, too. It also showed that the UFL has a significant relationship with the UOL. Since equation 6.9 only contains this variable, it must be appropriate and so is the model for the upper flammability zone boundary between the upper flammability limit and the upper oxygen limit.

The major reason for developing the empirical equation for calculating the flammability zone boundary was to develop an easy-to-use equation. This model is very simple since it requires only two inputs, the UFL and LFL, and solving three equations to model the entire flammability boundary. This is in contrast with the linear model that requires heat

capacities, heats of combustion, knowledge of how the reaction will proceed, and the values of the LFL and the UFL. The empirical equation for determining the LOC is only slightly more complicated than the "zy_{LFL}" equation. However, it appears that it estimates the LOC better and this will be discussed in the next section. Another advantage of this model is that it also has the ability to be updated if more data becomes available. So, this model is simple, rather accurate, and flexible.

6.3.2 Analysis of the Results

The empirical model has a 95% confidence interval on the mean of $y_{LOC} \pm 0.037$ and an R^2 value of 0.672. The R^2 value indicates a better fit than the $y_{LOC} = z \cdot y_{LFL}$ method and the linear and extended linear models presented in this paper. The 95% confidence interval on the mean from the empirical model of the UOL is $y_{UOL} \pm 0.076$ and an R^2 of 0.968. Again, this model outperforms any of the other models discussed. The 95% confidence interval on the mean of the LOL from the empirical model is $y_{LOL} \pm 0.019$ and has an R^2 value of 0.959. The fit slightly worse than the linear model; however, this model is much easier to use than the linear model. All of the models have 95% confidence intervals that are smaller than or the same size as the previously described models.

Figure 6.7 is the estimates of the LOC plotted against the experimental data.
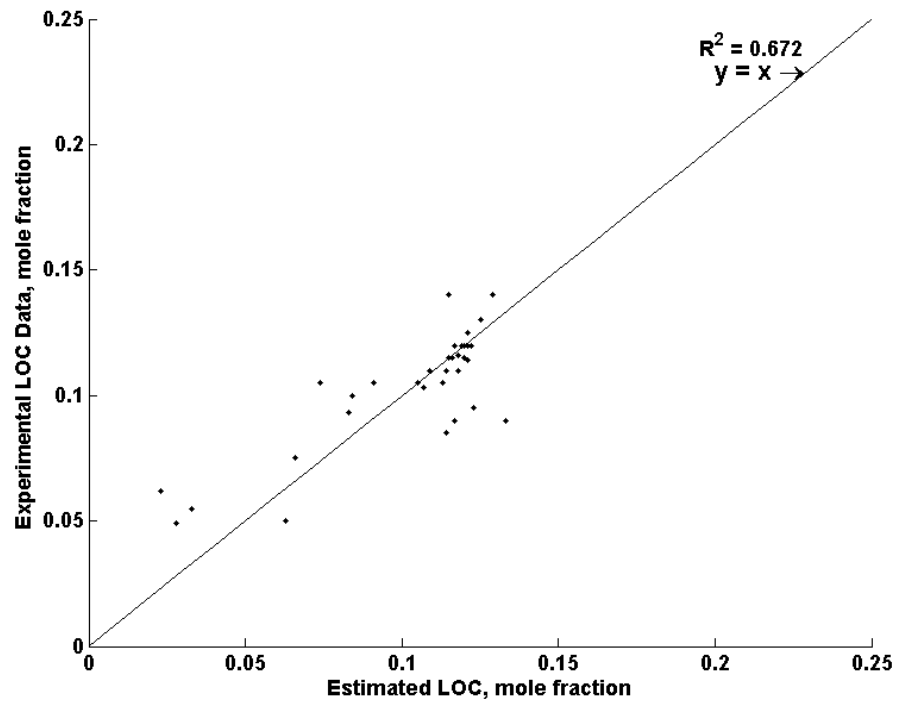
Figure 6.7:   Plot of the LOC estimations from the empirical model vs. experimental
               data.

Figure 6.7 shows the best fit of all models discussed in this paper for the LOC. Figure

6.8 is the estimates of the UOL plotted against the experimental data.
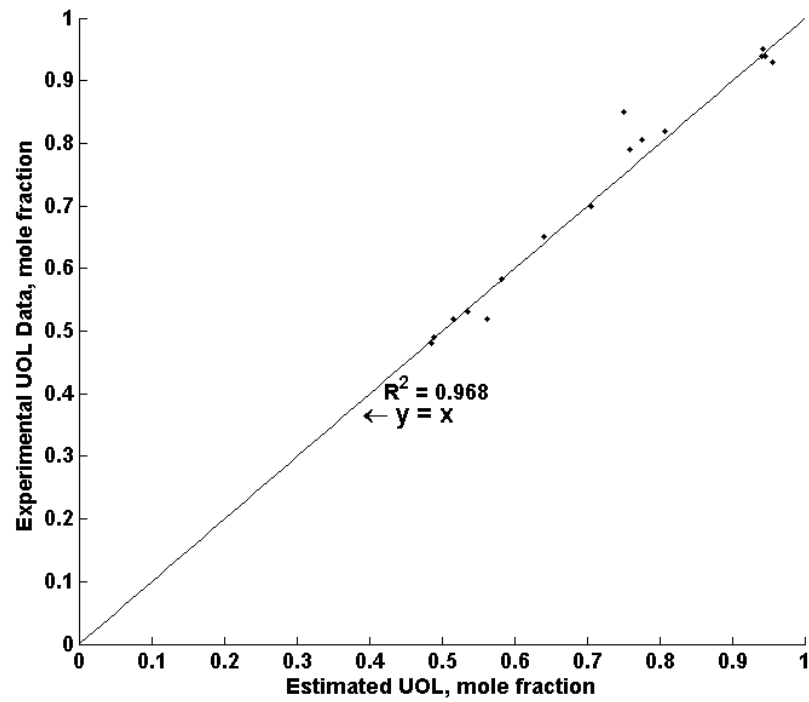
Figure 6.8:   Plot of the UOL estimations from empirical model vs. experimental data.

Figure 6.8 shows a good fit for the UOL. Figure 6.9 is the estimates of the LOL plotted

against the experimental data.
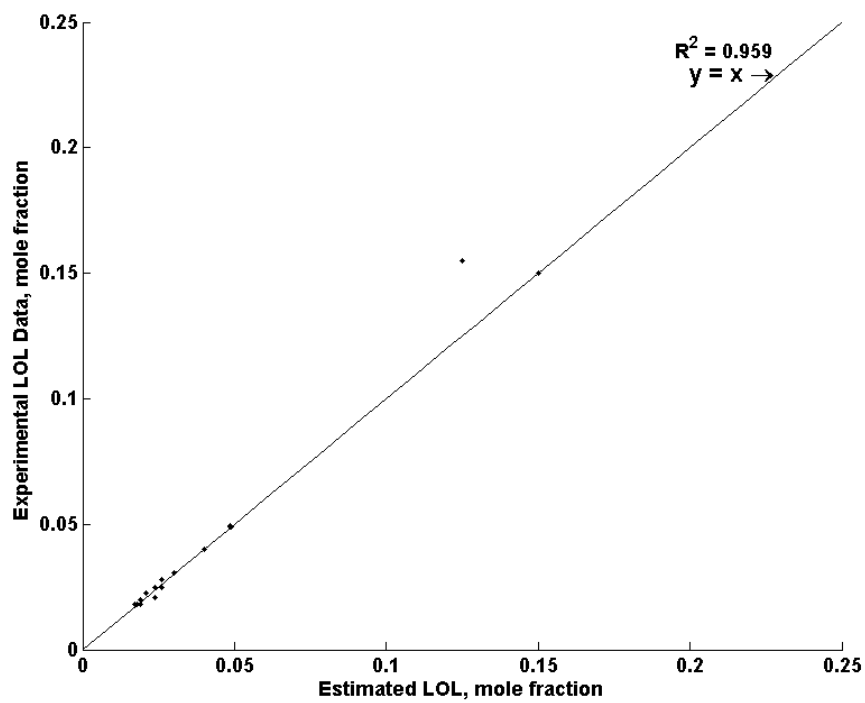
Figure 6.9:   Plot of LOL estimations from the empirical model vs. experimental data.

Figure 6.9 shows the fit is not as good as the linear model but is still adequate. Figure

6.10 is a plot of the residuals of the empirical method for the LOC:
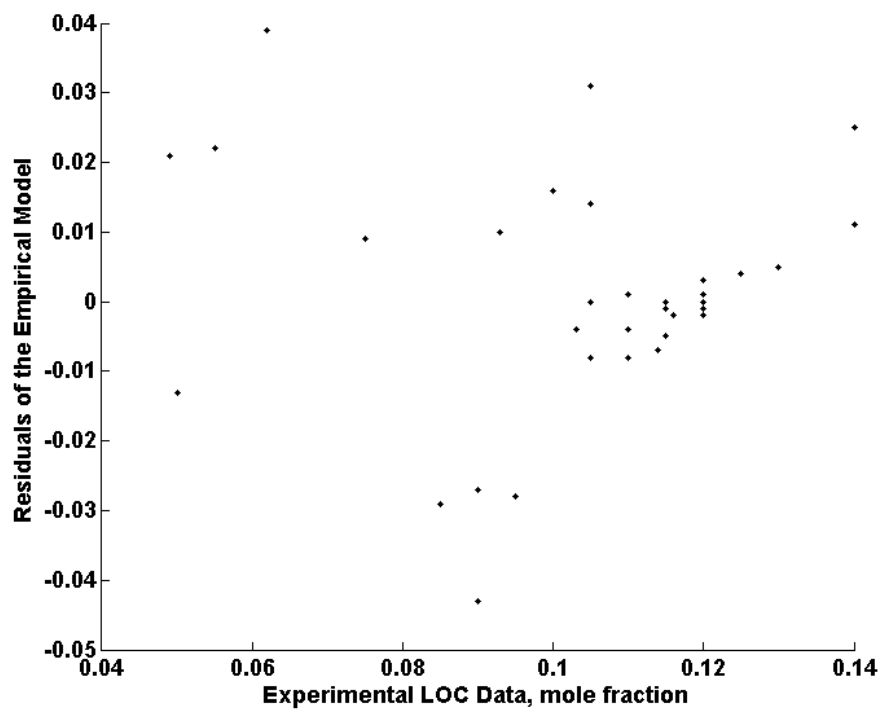
Figure 6.10:   Plot of residuals of the LOC estimations from the empirical method.

Figure 6.10 shows an adequate fit that is well balanced. There are two outliers, methyl styrene and acetylene, and the data is slightly scattered. Figure 6.11 shows the residuals of the UOL from the empirical method.
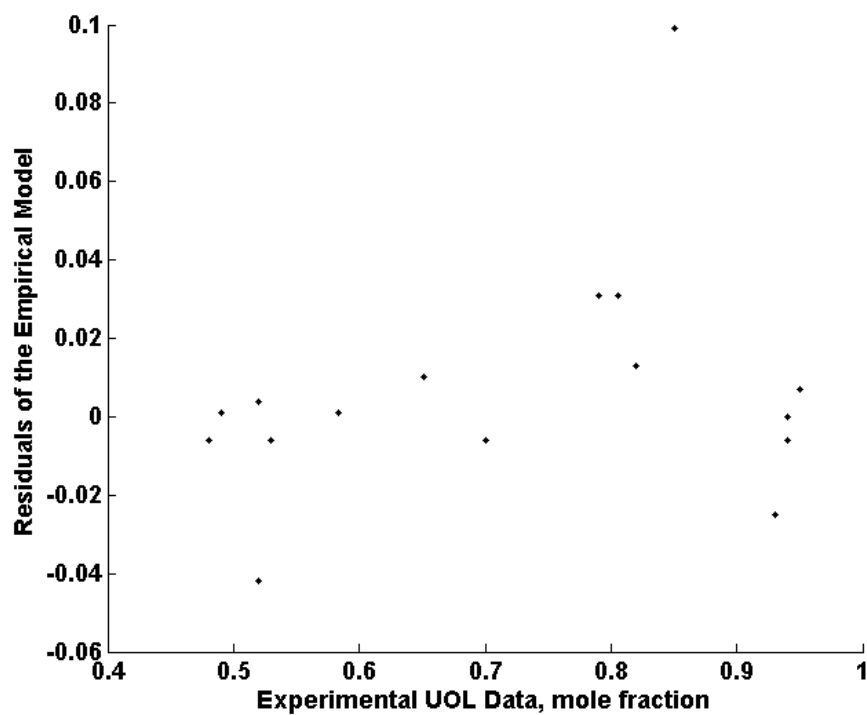
Figure 6.11   Plot of the residuals of the UOL estimations from the empirical method.

Figure 6.11 shows the fit is balanced; however, there is one outlier: divinyl ether. Figure

6.12 is a plot of the residuals for the LOL from the empirical method.
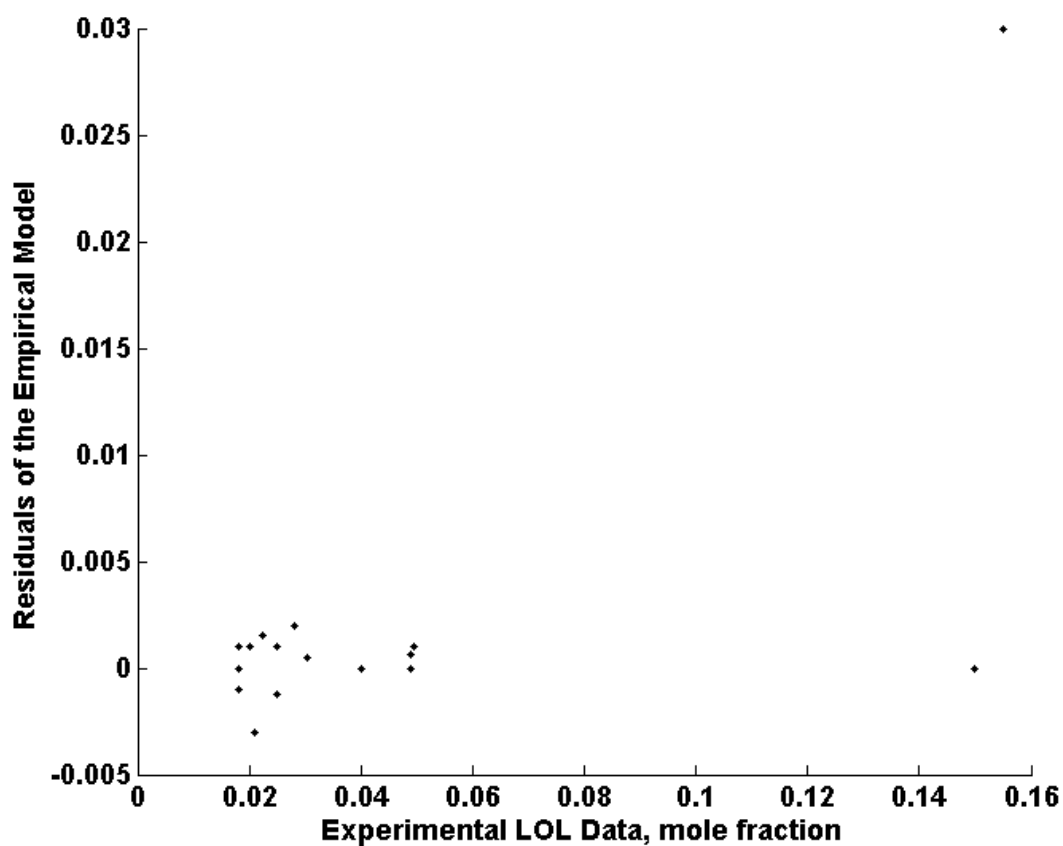
Figure 6.12:   Plot of the residuals of the LOL estimations from the empirical method.

Figure 6.12 shows the fit is balanced for the LOL; however, there is one outlier: carbon

monoxide. It cannot be determined whether this is due to error in the model or an error in

the data.

It has been shown that the empirical model of the flammability limit boundaries is a

rather good model of the flammability limit. When compared to the linear model,

extended linear model, and the "zy_{LFL}" method, the empirical model has a better fit with the LOC and a smaller confidence interval. This model also has a better fit when compared to the linear and extended linear models with the UOL and LOL. The empirical method presented is a relatively accurate, simple, and flexible method to model the flammability zone boundaries.

7   Using the Models as a Guide for Explosion Prevention

The models of the flammability zone have two practical applications that will be

discussed: explosion prevention and a guide for flammability experimentation. The

models can help determine safe levels of oxygen for vessels that operate with flammable

gases. For flammability experimentation, a model of the flammability zone is useful as a

starting point to begin the determination of the flammability zone boundary. A

recommended use of the models will be described for both of these uses.

In order to estimate the flammability limit boundary, the lower flammability limit and

upper flammability limit must be known. If this data is not available, it is possible to use

a correlation such as the one presented by Jones (Jones 1938):

$$y_{LFL} = \frac{0.55 C_{st}}{100} \qquad\qquad (1.2)$$

$$y_{UFL} = \frac{3.50 C_{st}}{100} \qquad\qquad (1.3)$$

Or the correlations presented by Suzuki and Koide (Suzuki 1994; Suzuki and Koide 1994) that depend on the heat of combustion in kJ/mol may be used:

$$y_{LFL} = \left(\frac{-3.42}{\Delta H_c} + 0.569\Delta H_c + 0.0538\Delta H_c^2 + 1.80\right)\frac{1}{100} \tag{1.5}$$

$$y_{UFL} = (6.30\Delta H_c + 0.567\Delta H_c^2 + 23.5)\frac{1}{100} \tag{1.6}$$

Once the flammability limits are known, the flammability zone boundary can be plotted using the empirical model. If the linear or extended linear model is to be used, heat capacity data and heats of combustion must be collected. Once the flammability zone boundaries are plotted, a reasonable error must be established. Since the empirical method was found to have a 95% confidence interval in mole fractions of 0.076 near the UOL, 0.037 near the LOC, and 0.019 near the LOL, these will be used for the models of the UFL boundary between the UFL and the UOL, the UFL boundary between the UFL and LOC, and the LFL boundary, respectively. For an explosion prevention application, this will determine an outside boundary. Figure 7.1 is the results of the modeling the flammability zone for methane with the empirical method:
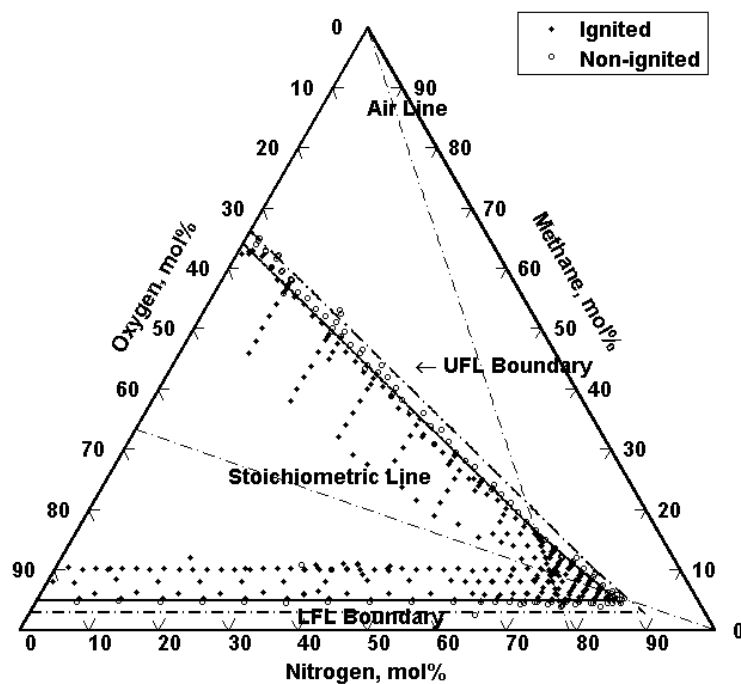
Figure 7.1:   The estimated flammability zone boundaries from the empirical equation

are used to represent the "safe zone" with flammability data (Mashuga

1999) where the confidence interval on the boundary is the outside dotted

line.

The outside dashed line shows the 95% confidence interval of the model. In order to

operate a vessel safely with a methane-oxygen-nitrogen mixture, the mixture within it

would have to be outside of the dashed line.

A similar method is applied for guiding flammability experiments. Instead, for this application, the inside confidence interval is used as a starting point to being determining the flammability boundary. Again, it is necessary to have the upper flammability limit and the lower flammability limit. If this data are not available, it would have to be determined with experimentation. The researcher would then being working towards the flammability limit with increasing fuel along constant nitrogen lines. Figure 7.2 is an example of the inside confidence interval plotted for methane.
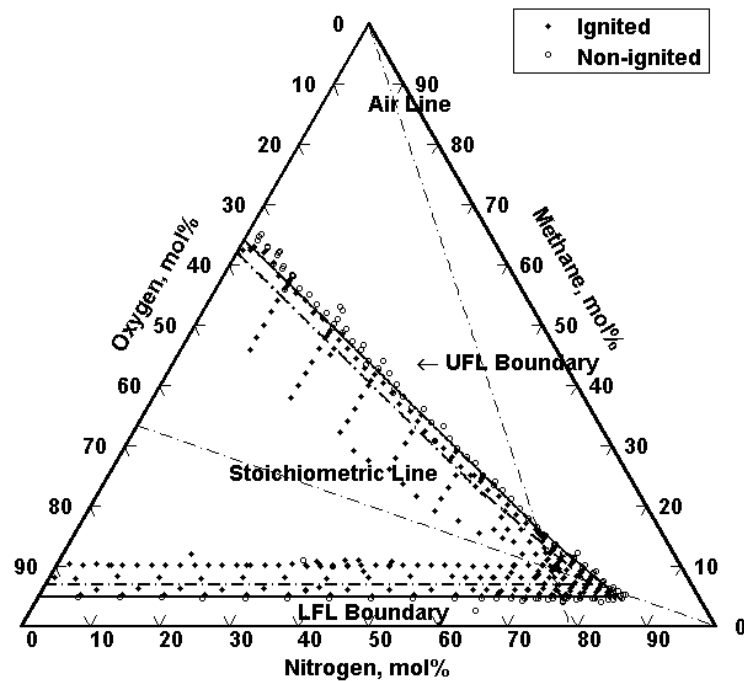
Figure 7.2:   Plot of the flammability zone boundaries of methane with the inner confidence interval (the dashed line) and flammability data (Mashuga 1999).

Since experimental data is always preferred over correlations and theoretical models, this technique can be very valuable. This modeling can help reduce the number of experimental points taken. It can be seen in Figure 7.2 that the confidence interval is closer to the flammability zone boundary than the points where the researcher began testing for flammability.

Modeling the flammability limits is a useful practice in determining the entire boundary. It can help a safety engineer determine the "safe" zone for a vessel to operate or it can help a researcher determine the flammability boundary. In either case, this will lead to safer operations and lower costs.

8   Summary and Conclusions

Three models have been presented to model the flammability zone boundaries. The first

model was a thermodynamic based model that assumed a complete combustion reaction

and an adiabatic energy balance referred to as the linear model:

Lower flammability zone boundary:

$$y_f = \frac{\beta_L(T_{ad,L}-T_i)}{-\Delta\bar{H}_r-\alpha_L(T_{ad,L}-T_i)}y_{O_2} + \frac{\gamma_L(T_{ad,L}-T_i)}{-\Delta\bar{H}_r-\alpha_L(T_{ad,L}-T_i)} \tag{3.13}$$

Upper flammability zone boundary:

$$y_f = \frac{-\frac{1}{z}\Delta\bar{H}_r-\beta_U(T_{ad,U}-T_i)}{\alpha_U(T_{ad,U}-T_i)}y_{O_2} - \frac{\gamma_U}{\alpha_U} \tag{3.18}$$

The second model used the same adiabatic energy balance but attempted to account for a

change in reaction stoichiometry along the upper flammability zone boundary. This

model is referred to as the extended linear model:

Between the LOC and the UFL:

$$y_f = -\frac{\Delta \bar{H}_{r,b} + \beta_{UL}(T_{ad,UL} - T_i)}{\Delta \bar{H}_{r,a} - \Delta \bar{H}_{r,b} + \alpha_{UL}(T_{ad,UL} - T_i)} y_{O_2} - \frac{\gamma_{UL}(T_{ad,UL} - T_i)}{\Delta \bar{H}_{r,a} - \Delta \bar{H}_{r,b} + \alpha_{UL}(T_{ad,UL} - T_i)} \quad (5.17)$$

Between the UFL and the UOL:

$$y_f = \frac{-\frac{1}{z_U}\Delta \bar{H}_r - \beta_{UU}(T_{ad,UU} - T_i)}{\alpha_{UU}(T_{ad,UU} - T_i)} y_o - \frac{\gamma_{UU}}{\alpha_{UU}} \quad (3.18)$$

The third model is an empirical model that uses the LFL and UFL to model the upper and lower flammability zone boundaries:

Lower flammability zone boundary:

$$y_f = y_{LFL} \quad (6.4)$$

Upper flammability zone boundary between the LOC and the UFL:

$$y_f = \frac{y_{UFL} - C_{LOC}y_{UFL}}{y_{UFL,O_2}} y_{O_2} + C_{LOC}y_{UFL} \quad (6.3)$$

Upper flammability zone boundary between the UFL and the UOL:

$$y_f = \frac{y_{UFL} - C_{UOL}y_{UFL}}{y_{UFL,O_2}} y_{O_2} + C_{UOL}y_{UFL} \quad (6.8)$$

Where:

$$C_{UOL} = -1.87$$

$$C_{LOC} = -1.11$$

The constant (C) values were determined by maximizing the R^2 values when fit to the data set.

Table 8.1 is a summary of the results of the three models when compared to experimental data:

Table 8.1: Summary of the results of the models presented.

Model	Parameter	Average Absolute Difference	95% Confidence Interval	R^2
zy_{LFL}				
	LOC	0.028	0.063	0.416
Linear				
	LOC	0.031	0.068	0.151
	UOL	0.040	0.130	0.882
	LOL	0.015	0.020	0.954
Extended Linear				
	LOC	0.014	0.047	0.572
	UOL	0.037	0.119	0.904
	LOL	0.015	0.020	0.954
Empirical				
	LOC	0.011	0.037	0.672
	UOL	0.018	0.078	0.968
	LOL	0.004	0.019	0.959

The linear model was shown to predict the flammability zone boundaries for hydrogen well. The linear model also predicts the upper flammability zone boundary well for fuels that have a fuel concentration greater than oxygen concentration at the UFL. It also was shown that if several assumptions were made the well-known LOC correlation is derived:

$$y_{LOC} = z y_{LFL} \qquad (1.9)$$

However, the linear model only has a regression coefficient of 0.151 for estimation of the LOC. This is much worse than what the "$z y_{LFL}$" predicts. The linear method has R^2 values for the UOL and LOL of 0.897 and 0.967, respectively. This shows a good fit for the linear method in respect to the UOL and LOL.

The extended linear model is an attempt to predict the upper flammability zone boundary in two parts and modifying the reaction mechanism for fuels with a greater oxygen concentration than fuel at the UFL. When this model is used, the LOC R^2 value is increased to 0.572 and the UOL R^2 is slightly better at 0.904. However, this model is harder to use than the linear model and the "$z y_{LFL}$" method.

The final empirical model was shown to the most accurate at predicting the LOC. Its R^2 value is 0.672. The R^2 values for the UOL and LOL are 0.968 and 0.959, respectively. For predicting the UOL and LOL, it is also quite accurate. The model was shown to be appropriate because the UFL and LFL were shown to be statistically significant. This

equation is simple and easy-to-use. It is also adaptable because when more LOC and

UOL data becomes the constants can be changed to maximize the R^2 value.

Three models have been presented to estimate the upper and lower flammability zone

boundaries. These models were the linear model, extended linear model, and empirical

model. The empirical model was found to be the most accurate for the LOC and UOL.

The linear model was slightly more accurate for the LOL. These models have been

shown to be useful in explosion prevention and flammability zone experimentation.

Referenced Literature

ASTM (1992). Standard Practice for Determining Limits of Flammability of Chemicals at Elevated Temperatures and Pressures. ASTM E 918-83. Philadelphia, PA.

Britton, L. G. (2002). "Using Heats of Oxidation to Evaluate Flammability Hazards." Process Safety Progress **21**(1): 31-54.

Brooks, M. R. (2001). Vapor Flammability Above Flammable Liquids and Aqueous Solutions of Flammable Liquids. Department of Chemical Engineering. Houghton, MI, Michigan Technological University. **Master of Science:** 114.

Burgess, D. S., A. L. Furno, et al. (1982). Flammability of Mixed Gases. B. o. Mines. Washington, D.C., United States Department of the Interior.

Burgess, J. and R. V. Wheeler (1911). "The Lower Limits of Inflammation of Mixtures of the Paraffin Hydrocarbons in Air." Trans. Chem. Society **99**: 2013-2030.

Cashdollar, K. L., I. A. Zlochower, et al. (2000). "Flammability of methane, propane, and hydrogen gases." Journal of Loss Prevention in the Process Industries **13**: 327-340.

Coward, H. F. and C. W. Jones (1952). Limits of Flammability of Gases and Vapors. U. S. D. o. t. Interior. Pittsburgh, Pennsylvania, Bureau of Mines.

Crowl, D. A. (2003). Understanding Explosions. New York, NY, Wiley-AIChE.

Crowl, D. A. and J. A. Louvar (2001). Chemical Process Safety: Fundamentals with Applications. Upper Saddle River, NJ, Prentice Hall, Inc.

Dandy, D. S. (2008). "Chemical Equilibrium." Retrieved January 20, 2009, from http://navier.engr.colostate.edu/tools/equil.html.

Glassman, I. (1987). Combustion. New York, NY, Academic Press Inc.

Goldmann, F. (1929). "Diffusion Phenomena at the Lower Explosion Limits of Hydrogen-Oxygen Mixtures." Ztschr. physikal. Chem. **B5**: 307-315.

High, M. S. and R. P. Danner (1987). "Prediction of Upper Flammability Limit by a Group Contribution Method." Ind. Eng. Chem. Res. **26**: 1395-1399.

Jo, Y.-D. and D. A. Crowl (2006). Hydrogen Flammability Data. Houghton, MI, Hazards Laboratory, Department of Chemical Engineering, Michigan Technological University.

Jones, G. W. (1938). "Inflammation Limits and Their Practical Application in Hazardous Industrial Operations." Chem. Rev. **22**(1): 1-26.

Kutcha, J. M. (1985). Investigation of Fire and Explosion Accidents in the Chemical, Mining, and Fuel-Related Industries - A Manual. U. S. D. o. t. Interior. Washington, D.C., Bureau of Mines**:** 84.

Law, C. K. and F. N. Egolfopoulos (1990). A Kinetic Criterion of Flammabiliity Limits: The C-H-O-Inert System. Twenty-Third Symposium (International) on Combustion. University of Orleans, Orleans, France, The Combustion Institute**:** 413-421.

Le Chatelier, H. (1891). "Estimation of Firedamp by Flammability Limits." Ann. Mines **19**(8): 388-395.

Lewis, B. and G. von Elbe (1934). "On the Theory of Flame Propagation." Journal of Chemical Physics **2**: 537.

Lewis, B. and G. von Elbe (1987). Combustion, Flames, and Explosions of Gases. New York, NY, Academic Press Inc.

Lide, D. R., Ed. (2006). CRC Handbook of Chemistry and Physics. London, Taylor and Francis/CRC Press.

Mashuga, C. V. (1999). Determination of the Combustion Behavior of Pure Components and Mixtures Using a 20-Liter Sphere. Department of Chemical Engineering. Houghton, MI, Michigan Technological University. **Phd Dissertation**.

Mashuga, C. V. and D. A. Crowl (1999). "Flammability Zone Prediction Using Calculated Adiabatic Flame Temperatures." Process Safety Progress **18**(3): 127-134.

Mashuga, C. V. and D. A. Crowl (2000). "Derivation of Le Chatelier's Mixing Rule for Flammable Limits." Process Safety Progress **19**(2): 112-117.

Melhem, G. A. (1997). "A Detailed Method for Estimating Mixture Flammability Limits Using Chemical Equilibrium." Process Safety Progress **16**(4): 203-218.

Montgomery, D. C. (2004). Design and Analysis of Experiments. New York, NY, J. Wiley & Sons.

NFPA (1994). Venting of Deflagrations. Quincy, MA. **68**.

Perman, E. P. (1911). "Limits of Explosibility in Gaseous Mixtures." Nature **87**(2187): 416.

Quiceno, R., F. Chejne, et al. (2002). "Proposal of a Methodology for Determining the Main Chemical Reactions Involved in Methane Combustion." Energy and Fuels **16**: 536-542.

Razus, D., M. Molnarne, et al. (2004). "Limiting Oxygen Concentration Evaluation in Flammable Gaseous Mixtures by Means of Calculated Adiabatic Flame Temperatures." Chemical Engineering and Processing **43**: 775-784.

Razus, D., M. Molnarne, et al. (2006). "Estimation of LOC (limiting oxygen concentration) of fuel-air-inert mixtures at elevated temperatures by means of adibatic flame temperatures." Chemical Engineering and Processing **45**: 193-197.

Sandler, S. I. (2006). Chemical, Biochemical, and Engineering Thermodynamics. New York, NY, J. Wiley & Sons.

Shimy, A. A. (1970). "Calculating Flammability Characteristics of Hydrocarbons and Alcohols." Fire Technology: 135-139.

Shrestha, S. O. B., I. Wierzba, et al. (1995). "A Thermodynamic Analysis of the Rich Flammability Limits of Fuel-Diluent Mixtures in Air." Journal of Energy Resources Technology **117**: 238-242.

Suzuki, T. (1994). "Empirical Relationship Between Lower Flammability Limits and Standard Enthalpies of Combustion of Organic Compounds." Fire and Materials **18**: 333-336.

Suzuki, T. and K. Koide (1994). "Correlation between Upper Flammability Limits and Thermochemical Properties of Organic Compounds." Fire and Materials **18**: 393-397.

Van der Schoor, F., R. T. E. Hermanns, et al. (2007). "Comparison and evaluation of methods for the determination of flammability limits, applied to methane/hydrogen/air mixtures." Journal of Hazardous Materials **150**(3): 573-581.

Vidal, M., W. Wong, et al. (2006). "Evaluation of Lower Flammability Limits of Fuel-Air-Diluent Mixtures Using Calculated Adiabatic Flame Temperatures." Journal of Hazardous Materials **130**: 21-27.

Wierzba, I. and B. B. Ale (1999). "The time effect of exposure to elevated temperatures on the flammability limits of some common fuels in air." Journal of Engineering for Gas Turbines and Power **121**: 74-79.

Wierzba, I., S. O. B. Shrestha, et al. (1994). "A Thermodynamics Analysis of the Lean Flammability Limts of Fuel-Diluent Mixtures in Air." Journal of Energy Resources Technology **116**: 181-185.

Wierzba, I., S. O. B. Shrestha, et al. (1996). "An Approach for Predicting the Flammability Limits of Fuel/Diluent Mixtures in Air." <u>Journal of the Institute of Energy</u> **69**: 122-130.

Yaws, C. L. (2003). Yaws' Handbook of Thermodynamic and Physical Properties of Chemical Compounds, Knovel.com.

Zabetakis, M. G. (1965). Flammability Characteristics of Combustible Gases and Vapors. U. S. D. o. t. Interior. Washington, D.C.

Appendix I: Experimental Flammability Data

The models presented in this paper are evaluated by comparing the upper oxygen limits, lower oxygen limits (LOL), and limiting oxygen concentrations predicted to actual data. This differs from the theory section in which the validity of the results was judged by how well the models were plotted next to a full flammability data set. The following flammability data will be used to compare the estimates to:

Table A1.1: Experimental flammability data used to evaluate estimates of the limiting oxygen concentration for the linear method and the empirical method.

Compound	Formula	z	LOC	LFL	UFL
Hydrogen[1]	H_2	0.5	0.049	0.0484	0.761
Hydrogen Sulfide[2]	H_2S	1.5	0.075	0.043	0.45
Methane[3]	CH_4	2	0.116	0.0485	0.1614
Carbon Monoxide[2]	CO	0.5	0.055	0.125	0.74
Methanol[2]	CH_3OH	1.5	0.1	0.073	0.36
Carbon Disulfide[2]	CS_2	3	0.05	0.012	0.44
Acetylene[4]	C_2H_2	2.5	0.062	0.026	0.8
Ethylene[3]	C_2H_4	3	0.093	0.0262	0.3038
Ethane[2]	C_2H_6	3.5	0.11	0.03	0.125
Dimethyl Ether[4]	C_2H_6O	3	0.105	0.033	0.26
Ethanol	C_2H_5OH	3	0.105	0.035	0.187
Methyl Formate	$C_2H_4O_2$	2	0.103[4]	0.057[2]	0.217[2]
1,2-Dichloroethane	$C_2H_4Cl_2$	3	0.13[2]	0.062[5]	0.16[5]
1,1,1-trichloroethane	$C_2H_3Cl_3$	2.75	0.14[2]	0.07[5]	0.16[5]
Cyclopropane[2]	C_3H_6	4.5	0.115	0.024	0.104
Propene[2]	C_3H_6	4.5	0.115	0.024	0.103
Propane[2]	C_3H_8	5	0.115	0.021	0.095

Table A1.1 (continued): Experimental flammability data used to evaluate estimates of the

limiting oxygen concentration for the linear method and the empirical

method.

Acetone[2]	C_3H_6O	4	0.115	0.03	0.13
Methyl Acetate[2]	$C_3H_6O_2$	3.5	0.11	0.031	0.16
1,3-Butadiene	C_4H_6	5.5	0.105[2]	0.02[4]	0.116[4]
1-Butene[2]	C_4H_8	6	0.115	0.016	0.093
Isobutene[2]	C_4H_8	6	0.12	0.018	0.097
Isobutane[2]	C_4H_{10}	6.5	0.12	0.018	0.084
n-Butane[2]	C_4H_{10}	6.5	0.12	0.019	0.085
Butanone (MEK)[4]	C_4H_8O	5.5	0.11	0.02	0.112
Diethyl Ether[2]	$C_4H_{10}O$	6	0.105	0.019	0.36
1-chlorobutane[2]	C_4H_9Cl	6.25	0.14	0.018	0.101
Isobutyl Formate	$C_5H_{10}O2$	6.5	0.125[2]	0.02[4]	0.089[4]
3-methyl-1-Butene	C_5H_{10}	7.5	0.115[2]	0.015[4]	0.091[4]
Isopentane[2]	C_5H_{12}	8	0.12	0.014	0.076
n-Pentane[2]	C_5H_{12}	8	0.12	0.015	0.078
Benzene[2]	C_6H_6	7.5	0.114	0.014	0.071
n-Hexane[2]	C_6H_{14}	9.5	0.12	0.012	0.075
Toluene[2]	C_7H_8	9	0.095	0.014	0.067
n-Heptane[2]	C_7H_{16}	11	0.115	0.012	0.067
Styrene[2]	C_8H_8	10	0.09	0.011	0.07
Ethylbenzene	C_8H_{10}	10.5	0.085[2]	0.008[5]	0.067[5]
Methylstyrene	C_9H_{10}	11.5	0.09[2]	0.019[5]	0.061[5]

Data from [1](Jo and Crowl 2006), [2](Lewis and von Elbe 1987), [3](Mashuga 1999), [4](Zabetakis 1965), and [5](Lide 2006).

Table A1.2: Experimental flammability data used to evaluate estimates of the upper

oxygen limit for the linear model and empirical model.

Compound	Formula	z	LFL	UFL	LOL	UOL
Hydrogen[1]	H_2	0.5	0.0484	0.761	0.049	0.94
Deuterium[2]	H_2	0.5	0.049	0.75	0.049	0.95
Ammonia[3]	NH_3	0.75	0.15	0.28	0.15	0.79

Table A1.2 (continued): Experimental flammability data used to evaluate estimates of the

upper oxygen limit for the linear model and the empirical model.

Methane[4]	CH$_4$	2	0.0485	0.1614	0.0495	0.651
Carbon Monoxide[3]	CO	0.5	0.125	0.74	0.155	0.94
Acetylene[5]	C$_2$H$_2$	2.5	0.026	0.8	0.028	0.93
Ethylene[4]	C$_2$H$_4$	3	0.0262	0.3038	0.025	0.806
Ethane[3]	C$_2$H$_6$	3.5	0.03	0.125	0.0305	0.583
Chloroethane[2]	C$_2$H$_5$Cl	3.25	0.04	0.217	0.04	0.7
Cyclopropane[3]	C$_3$H$_6$	4.5	0.024	0.104	0.025	0.6
Propene[3]	C$_3$H$_6$	4.5	0.024	0.103	0.021	0.53
Propane[3]	C$_3$H$_8$	5	0.021	0.095	0.0225	0.52
Isobutane[2]	C$_4$H$_{10}$	6.5	0.018	0.084	0.018	0.48
n-Butane[3]	C$_4$H$_{10}$	6.5	0.019	0.085	0.018	0.49
Divinyl Ether[3]	C$_4$H$_6$O	5	0.017	0.27	0.018	0.85
Diethyl Ether[3]	C$_4$H$_{10}$O	6	0.019	0.36	0.2	0.82

Data from [1](Jo and Crowl 2006), [2](Coward and Jones 1952), [3](Lewis and von Elbe 1987), [4](Mashuga 1999), and [5](Zabetakis 1965).

Table A1.3:   Experimental flammability data used to evaluate estimates of the extended

linear model.

| Compound	Formula	z	LOC	LFL	UFL	LOL	UOL
Hydrogen[1]	H$_2$	0.5	0.049	0.048	0.761	0.049	0.940
Methane[2]	CH$_4$	2	0.116	0.049	0.161	0.050	0.651
Carbon Monoxide[3]	CO	0.5	0.055	0.125	0.74	0.155	0.94
Ethylene[2]	C$_2$H$_4$	3	0.093	0.0262	0.304	0.025	0.806
Ethane[3]	C$_2$H$_6$	3.5	0.11	0.030	0.125	0.031	0.583
Cyclopropane[3]	C$_3$H$_6$	4.5	0.115	0.024	0.104	0.025	0.6
Propene[3]	C$_3$H$_6$	4.5	0.115	0.024	0.103	0.021	0.53
Propane[3]	C$_3$H$_8$	5	0.115	0.021	0.095	0.023	0.520
Isobutane	C$_4$H$_{10}$	6.5	0.12[3]	0.018[3]	0.084[3]	0.018[4]	0.480[4]
n-Butane	C$_4$H$_{10}$	6.5	0.12[3]	0.019[3]	0.085[3]	0.018[3]	0.490[3]
Acetylene[5]	C$_2$H$_2$	2.5	0.062	0.026	0.8	0.028	0.93

Data from [1](Jo and Crowl 2006), [2(Mashuga 1999), [3](Lewis and von Elbe 1987), [4](Coward and Jones 1952), and [5](Zabetakis 1965).

Appendix II: Linear Model MathCAD® Spreadsheet for Methane

This spreadsheet is calculating the estimates of the linear model for methane. Please refer to Chapter 4 for the equations and theory behind the spreadsheet. MathCAD® was used to easily calculate the adiabatic flame temperatures through an iterative solution.

Initial Conditions (ideal gas):

$$T_1 := 298 \qquad T_2 := 1498$$

Reaction:

$C_xH_y + z\ O_2 \longrightarrow x\ CO_2 + (y/2)\ H_2O$ Source: C.V. Mashuga 1999
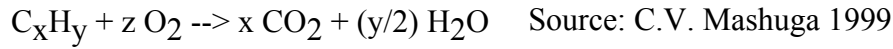
$$x := 1 \qquad y := 4$$

$$z := \left(x + \frac{y}{4}\right)$$

$$y_{ufl} := 0.1614 \qquad\qquad y_{oufl} := 0.651$$

$$y_{lfl} := 0.0485 \qquad\qquad y_{olfl} := 0.0495$$

System Data

Source: Chemical Biological and Engineering Thermodynamics, Sandler 2006

$$\Delta H_r := \left(x \cdot -393.5 + \frac{y}{2}\cdot -241.8 - -74.5\right)\cdot 10^3$$

$$\Delta H_r = -8.026\times 10^5$$

For Methane:

$$a1 := 19.25$$

$$b1 := 5.213\cdot 10^{-2}$$

$$c1 := 1.197\cdot 10^{-5}$$

$$d1 := -1.132 \times 10^{-8}$$

For Oxygen:

$$a2 := 28.167$$

$$b2 := 0.630\cdot 10^{-2}$$

$$c2 := -0.075\cdot 10^{-5}$$

$$d2 := 0$$

$$Cp_1(T) := \frac{\displaystyle\int_{T_1}^{T} a1 + b1\cdot T + c1\cdot T^2 + d1\cdot T^3\ dT}{T - T_1}$$

$$Cp_2(T) := \frac{\displaystyle\int_{T_1}^{T} a2 + b2\cdot T + c2\cdot T^2 + d2\cdot T^3\ dT}{T - T_1}$$

For Nitrogen:

$a3 := 27.318$

$b3 := 0.623 \cdot 10^{-2}$

$c3 := -0.095 \cdot 10^{-5}$

$d3 := 0$

$$Cp_3(T) := \frac{\int_{T_1}^{T} a3 + b3 \cdot T + c3 \cdot T^2 + d3 \cdot T^3 \, dT}{T - T_1}$$

For Carbon Dioxide:

$a4 := 75.464$

$b4 := -1.872 \cdot 10^{-4}$

$c4 := -661.42$

$d4 := 0$

$$Cp_4(T) := \frac{\int_{T_1}^{T} a4 + b4 \cdot T + c4 \cdot T^{-\frac{1}{2}} + d4 \cdot T^3 \, dT}{T - T_1}$$

For Steam:

$a5 := 29.163$

$b5 := 1.449 \cdot 10^{-2}$

$c5 := -0.202 \cdot 10^{-5}$

$d5 := 0$

$$Cp_5(T) := \frac{\int_{T_1}^{T} a5 + b5 \cdot T + c5 \cdot T^2 + d5 \cdot T^3 \, dT}{T - T_1}$$

$y_{uflo} := (1 - y_{ufl}) \cdot 0.21$ $y_{lflo} := (1 - y_{lfl}) \cdot 0.21$

$y_{uflo} = 0.176$ $y_{lflo} = 0.2$

Linear equation theory:

Lower Flammability Limit Boundary:

$$\alpha_L(T) := x \cdot Cp_4(T) + \frac{y}{2} \cdot Cp_5(T) - z \cdot Cp_2(T) - Cp_3(T)$$

$$\beta_L(T) := Cp_2(T) - Cp_3(T)$$

$$\gamma_L(T) := Cp_3(T)$$

$$y_{fL}(T, y_2) := \frac{\beta_L(T)}{\dfrac{-\Delta H_r}{T - T_1} - \alpha_L(T)} \cdot y_2 + \frac{\gamma_L(T)}{\dfrac{-\Delta H_r}{T - T_1} - \alpha_L(T)}$$

$$Cp_L(T) := \alpha_L(T) \cdot y_{lfl} + \beta_L(T) \cdot y_{lflo} + \gamma_L(T)$$

Upper Flammability Limit Boundary:

$$\alpha_U(T) := Cp_1(T) - Cp_3(T)$$

$$\beta_U(T) := \frac{x}{z} \cdot Cp_4(T) + \frac{y}{2 \cdot z} \cdot Cp_5(T) - \frac{1}{z} \cdot Cp_1(T) - Cp_3(T)$$

$$\gamma_U(T) := Cp_3(T)$$

$$y_{fU}(T, y_2) := \left(\frac{1}{\alpha_U(T) \cdot z} \cdot \frac{-\Delta H_r}{T - T_1} - \frac{\beta_U(T)}{\alpha_U(T)} \right) \cdot y_2 - \frac{\gamma_U(T)}{\alpha_U(T)}$$

$$Cp_U(T) := \alpha_U(T) \cdot y_{ufl} + \beta_U(T) \cdot y_{uflo} + \gamma_U(T)$$

$$y_n(y_o) := -y_o + 1$$

$$y_{stoic}(y_2) := \frac{1}{z} \cdot y_2$$

$$y_{air}(y_2) := 1 - \frac{1}{0.21} y_2 \qquad\qquad 120$$

Solving for Adiabatic Flame Temperature:

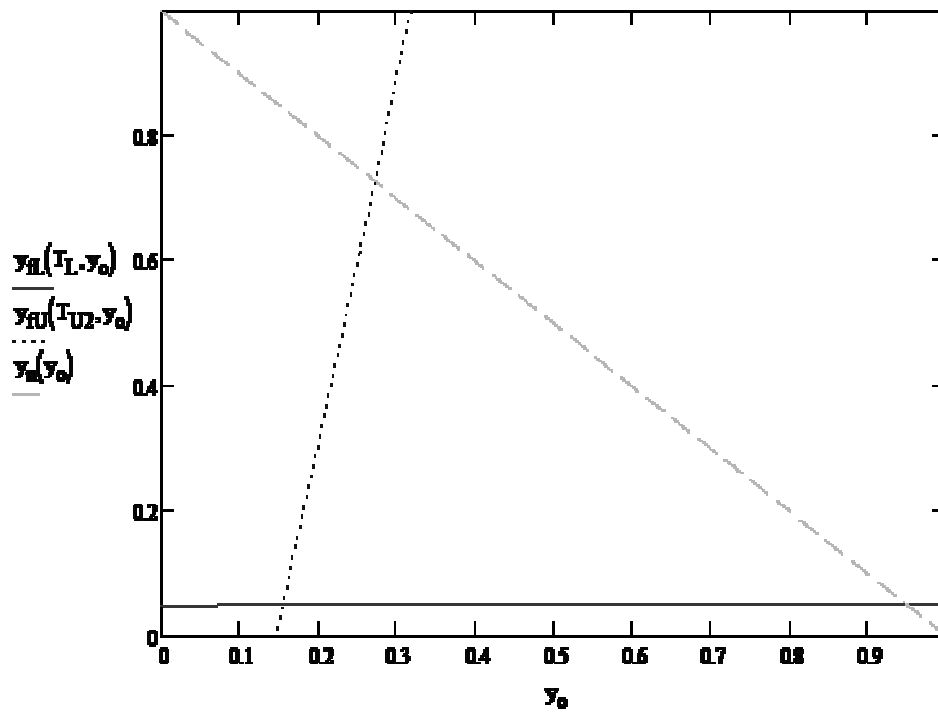$$T_{gU} := 1000 \qquad T_{gL} := 500 \qquad T_{gU2} := 1000$$

Given

$$\left[\frac{1}{z}\cdot\left(1 - y_{ufl}\right)\cdot 0.21\right]\cdot \Delta H_r + Cp_U\left(T_{gU}\right)\cdot\left(T_{gU} - 298\right) = 0$$

$$y_{lfl} = y_{fL}\left[T_{gL}, \left(1 - y_{lfl}\right)\cdot 0.21\right]$$

$$y_{fU}\left[T_{gU2}, \left(1 - y_{ufl}\right)0.21\right] = y_{ufl}$$

$$\begin{pmatrix} T_U \\ T_L \\ T_{U2} \end{pmatrix} := Find\left(T_{gU}, T_{gL}, T_{gU2}\right)$$

$$T_U = 2.085\times 10^3 \qquad T_L = 1.45\times 10^3 \qquad T_{U2} = 2.085\times 10^3$$

···· Upper flammability zone boundary   -- -- Oxygen boundary

———— Lower flammability zone boundary

x-axis: fuel concentration   y-axis: oxygen concentration

Figure A2.1: A quick plot of the upper and lower linear models.

Calculation of limiting oxygen concentration and pure oxygen

limits using linear equation:

$$y_{ggloc} := 0.2 \qquad y_{gguol} := .3 \qquad y_{gglol} := 0.95$$

Given

$$y_{fU}(T_{U2}, y_{ggloc}) = y_{fL}(T_L, y_{ggloc})$$

$$1 - y_{fU}(T_{U2}, y_{gguol}) = y_{gguol}$$

$$1 - y_{fL}(T_L, y_{gglol}) = y_{gglol}$$

$$\begin{pmatrix} y_{loc} \\ y_{uolo} \\ y_{lolo} \end{pmatrix} := \text{Find}(y_{ggloc}, y_{gguol}, y_{gglol})$$

$$y_{uol} := 1 - y_{uolo}$$

$$y_{lol} := 1 - y_{lolo}$$

$$y_{loc} = 0.157$$

$$y_{uolo} = 0.273$$

$$y_{lolo} = 0.95$$

$$y_{uol} = 0.727$$

$$y_{lol} = 0.05$$

The zLFL method for the LOC:

$$y_{zlfl} := z \cdot y_{lf}$$

$$y_{zlfl} = 0.097$$

Appendix III: The Extended Linear Model MathCAD®

Spreadsheet for Methane between the UFL and

the LOC

This spreadsheet is calculating the estimates of the extended linear model for methane.

This spreadsheet is calculating the boundary between the UFL and LOC. Please refer to

Chapter 5 for the equations and theory behind the spreadsheet. MathCAD® was used to

easily calculate the adiabatic flame temperatures through an iterative solution.

Initial Conditions (ideal gas):

$T_1 := 298 \qquad R_{ig} := 8.314$

$T_2 := 1498$

Reaction:

$C_xH_y + z\ O_2 \longrightarrow x\ CO + (y/2)\ H_2O$ Source: C.V. Mashuga 1999

$x := 1 \qquad y := 4 \qquad z := 2$

$y_{ufl} := 0.1614 \qquad\qquad y_{oufl} := 0.651$

$y_{lfl} := 0.0485$

$y_{olfl} := 0.0495$

$y_{uflo} := (1 - y_{ufl}) \cdot 0.21$

System Data

Source: chemical biological and engineering thermodynamics, Sandler 2006

For Carbon:

For Oxygen:

$a1 := -3.9578$

$a2 := 28.167$

$b1 := 5.586 \cdot 10^{-2}$

$b2 := 0.630 \cdot 10^{-2}$

$c1 := -4.5482 \cdot 10^{-5}$

$c2 := -0.075 \cdot 10^{-5}$

$d1 := 1.5171 \times 10^{-8}$

$d2 := 0$

$$Cp_1(T) := \frac{\int_{T_1}^{T} \left(a1 + b1 \cdot T + c1 \cdot T^2 + d1 \cdot T^3\right) \cdot R_{ig}\ dT}{T - T_1}$$

$$Cp_2(T) := \frac{\int_{T_1}^{T} a2 + b2 \cdot T + c2 \cdot T^2 + d2 \cdot T^3\ dT}{T - T_1}$$

For Nitrogen:

$a3 := 27.318$

$b3 := 0.623 \cdot 10^{-2}$

$c3 := -0.095 \cdot 10^{-5}$

$d3 := 0$

$$Cp_3(T) := \frac{\int_{T_1}^{T} a3 + b3 \cdot T + c3 \cdot T^2 + d3 \cdot T^3 \, dT}{T - T_1}$$

For Carbon monoxide:

$a4 := 27.113$

$b4 := 0.655 \cdot 10^{-2}$

$c4 := -0.1 \cdot 10^{-5}$

$d4 := 0$

$$Cp_4(T) := \frac{\int_{T_1}^{T} a4 + b4 \cdot T + c4 \cdot T^2 + d4 \cdot T^3 \, dT}{T - T_1}$$

For Steam:

$a5 := 29.163$

$b5 := 1.449 \cdot 10^{-2}$

$c5 := -0.202 \cdot 10^{-5}$

$d5 := 0$

$$Cp_5(T) := \frac{\int_{T_1}^{T} a5 + b5 \cdot T + c5 \cdot T^2 + d5 \cdot T^3 \, dT}{T - T_1}$$

For Hydrogen:

$a6 := 26.879$

$b6 := 0.435 \cdot 10^{-2}$

$c6 := -0.033 \cdot 10^{-5}$

$d6 := 0$

$$Cp_6(T) := \frac{\int_{T_1}^{T} a6 + b6 \cdot T + c6 \cdot T^2 + d6 \cdot T^3 \, dT}{T - T_1}$$

For Carbon Dioxide:

$a7 := 75.464$

$b7 := -1.872 \cdot 10^{-4}$

$c7 := -661.42$

$d7 := 0$

$$Cp_7(T) := \frac{\displaystyle\int_{T_1}^{T} a7 + b7 \cdot T + c7 \cdot T^{-\frac{1}{2}} + d7 \cdot T^3 \, dT}{T - T_1}$$

For Methane:

$a8 := 19.25$

$b8 := 5.213 \cdot 10^{-2}$

$c8 := 1.197 \cdot 10^{-5}$

$d8 := -1.132 \times 10^{-8}$

$$Cp_8(T) := \frac{\displaystyle\int_{T_1}^{T} a8 + b8 \cdot T + c8 \cdot T^2 + d8 \cdot T^3 \, dT}{T - T_1}$$

$\Delta H_2 := (-241.8 + -110.5 - -74.5) \cdot 10^3$

$\Delta H_2 = -2.778 \times 10^5$

$\Delta H_1 := 2 \cdot -241.8 \cdot 10^3$

$\Delta H_1 = -4.836 \times 10^5$

$\Delta H_r := \left(x \cdot -393.5 + \frac{y}{2} \cdot -241.8 - -74.5 \right) \cdot 10^3$

$\Delta H_r = -8.026 \times 10^5$

$y_n(y_o) := -y_o + 1$

$y_{stoic}(y_2) := \frac{1}{z} \cdot y_2$

$y_{air}(y_2) := 1 - \frac{1}{0.21} y_2$

Linear equation theory:

Lower:

$$\alpha_L(T) := x \cdot Cp_4(T) + \frac{y}{2} \cdot Cp_5(T) - z \cdot Cp_2(T) - Cp_3(T)$$

$$\beta_L(T) := Cp_2(T) - Cp_3(T)$$

$$\gamma_L(T) := Cp_3(T)$$

$$y_{fL}(T, y_2) := \frac{\beta_L(T)}{\dfrac{-\Delta H_r}{T - T_1} - \alpha_L(T)} \cdot y_2 + \frac{\gamma_L(T)}{\dfrac{-\Delta H_r}{T - T_1} - \alpha_L(T)}$$

Upper between the UFL and LOC:

$$\alpha_U(T) := Cp_4(T) + 3 Cp_6(T) - Cp_5(T) - Cp_3(T)$$

$$\beta_U(T) := 2 Cp_5(T) - 2 Cp_6(T) - Cp_3(T)$$

$$\gamma_U(T) := Cp_3(T)$$

$$y_{fU}(T, y_2) := -\frac{\Delta H_1 + \beta_U(T) \cdot (T - 298)}{\Delta H_2 - \Delta H_1 + \alpha_U(T) \cdot (T - 298)} \cdot y_2 - \frac{\gamma_U(T) \cdot (T - 298)}{\Delta H_2 - \Delta H_1 + \alpha_U(T) \cdot (T - 298)}$$

Solving for Adiabatic Flame Temperature:
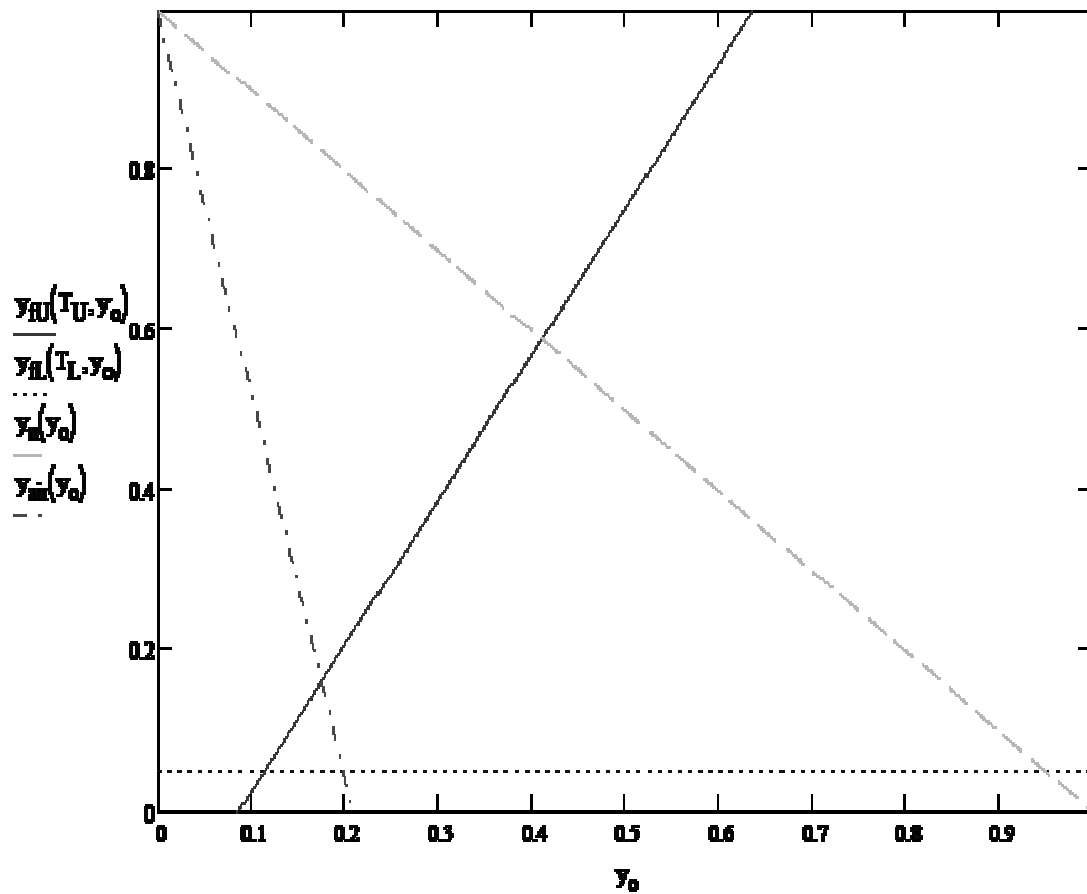
$$T_{gU} := 1000 \qquad T_{gL} := 500$$

Given

$$y_{lfl} = y_{fL}\left[T_{gL}, \left(1 - y_{lfl}\right)\cdot 0.21\right]$$

$$y_{fU}\left[T_{gU}, \left(1 - y_{ufl}\right)\cdot 0.21\right] = y_{ufl}$$

$$\begin{pmatrix} T_U \\ T_L \end{pmatrix} := \text{Find}\left(T_{gU}, T_{gL}\right)$$

$$T_U = 1.646 \times 10^3 \qquad T_L = 1.481 \times 10^3$$

$\dfrac{y_{fU}(T_U, y_o)}{y_{fL}(T_L, y_o)}$

$y_a(y_o)$

$y_{air}(y_o)$

y_o

···· Lower flammability zone boundary   -- -- Oxygen boundary

———— Upper flammability zone boundary   -- · -- · -- Air line

x-axis: fuel concentration   y-axis: oxygen concentration

Figure A3.1: A quick plot of upper flammability limit boundary between the UFL and the LOC

Calculation of limiting oxygen concentration

and pure oxygen limits using linear equation:

$y_{ggloc} := 0.2$ $\qquad$ $y_{gguol} := .3$ $\qquad$ $y_{gglol} := 0.95$

Given

$$y_{fU}(T_U, y_{ggloc}) = y_{fL}(T_L, y_{ggloc})$$

$$1 - y_{fU}(T_U, y_{gguol}) = y_{gguol}$$

$$1 - y_{fL}(T_L, y_{gglol}) = y_{gglol}$$

$$\begin{pmatrix} y_{loc2} \\ y_{uol2} \\ y_{lol2} \end{pmatrix} := Find(y_{ggloc}, y_{gguol}, y_{gglol})$$

$y_{uofl2} := 1 - y_{uol2}$ $\qquad$ $y_{lofl2} := 1 - y_{lol2}$

$y_{loc2} = 0.114$ $\qquad$ $y_{uol2} = 0.411$ $\qquad$ $y_{lol2} = 0.95$

$\qquad\qquad\qquad$ $y_{uofl2} = 0.589$ $\qquad$ $y_{lofl2} = 0.05$

Appendix IV: The Extended Linear Model MathCAD® Spreadsheet for Methane between the UFL and the UOL

This spreadsheet is calculating the estimates of the extended linear model for methane. This spreadsheet is calculating the boundary between the UFL and UOL. Please refer to Chapter 5 for the equations and theory behind the spreadsheet. MathCAD® was used to easily calculate the adiabatic flame temperatures through an iterative solution.

Initial Conditions (ideal gas):

$T_1 := 298$

$R_{ig} := 8.314$

$T_2 := 1498$

Reaction:

Source: C.V. Mashuga 1999

$C_xH_y + z\ O_2 \longrightarrow x\ CO + (y/2)\ H_2O$

$y_{ufl} := 0.1614$

$y_{oufl} := 0.651$

$x := 1 \qquad y := 4 \qquad z := 2$

$y_{lfl} := 0.0485$

$y_{olfl} := 0.0495$

$y_{uflo} := (1 - y_{ufl}) \cdot 0.21$

System Data

Source: Chemical Biological and Engineering Thermodynamics, Sandler 2006

For Carbon:

$a1 := -3.9578$

$b1 := 5.586 \cdot 10^{-2}$

$c1 := -4.5482 \cdot 10^{-5}$

$d1 := 1.5171 \times 10^{-8}$

$$Cp_1(T) := \frac{\displaystyle\int_{T_1}^{T} \left(a1 + b1 \cdot T + c1 \cdot T^2 + d1 \cdot T^3\right) \cdot R_{ig}\ dT}{T - T_1}$$

For Oxygen:

$a2 := 28.167$

$b2 := 0.630 \cdot 10^{-2}$

$c2 := -0.075 \cdot 10^{-5}$

$d2 := 0$

$$Cp_2(T) := \frac{\displaystyle\int_{T_1}^{T} a2 + b2 \cdot T + c2 \cdot T^2 + d2 \cdot T^3\ dT}{T - T_1}$$

For Nitrogen:

$a3 := 27.318$

$b3 := 0.623 \cdot 10^{-2}$

$c3 := -0.095 \cdot 10^{-5}$

$d3 := 0$

$$Cp_3(T) := \frac{\displaystyle\int_{T_1}^{T} a3 + b3 \cdot T + c3 \cdot T^2 + d3 \cdot T^3 \; dT}{T - T_1}$$

For Carbon monoxide:

$a4 := 27.113$

$b4 := 0.655 \cdot 10^{-2}$

$c4 := -0.1 \cdot 10^{-5}$

$d4 := 0$

$$Cp_4(T) := \frac{\displaystyle\int_{T_1}^{T} a4 + b4 \cdot T + c4 \cdot T^2 + d4 \cdot T^3 \; dT}{T - T_1}$$

For Steam:

$a5 := 29.163$

$b5 := 1.449 \cdot 10^{-2}$

$c5 := -0.202 \cdot 10^{-5}$

$d5 := 0$

$$Cp_5(T) := \frac{\displaystyle\int_{T_1}^{T} a5 + b5 \cdot T + c5 \cdot T^2 + d5 \cdot T^3 \; dT}{T - T_1}$$

For Hydrogen:

$a6 := 26.879$

$b6 := 0.435 \cdot 10^{-2}$

$c6 := -0.033 \cdot 10^{-5}$

$d6 := 0$

$$Cp_6(T) := \frac{\displaystyle\int_{T_1}^{T} a6 + b6 \cdot T + c6 \cdot T^2 + d6 \cdot T^3 \; dT}{T - T_1}$$

For Carbon Dioxide:

a7 := 75.464

b7 := −1.872·10^{-4}

c7 := −661.42

d7 := 0

$$Cp_7(T) := \frac{\int_{T_1}^{T} a7 + b7\cdot T + c7\cdot T^{-\frac{1}{2}} + d7\cdot T^3 \, dT}{T - T_1}$$

For Methane:

a8 := 19.25

b8 := 5.213·10^{-2}

c8 := 1.197·10^{-5}

d8 := −1.132 × 10^{-8}

$$Cp_8(T) := \frac{\int_{T_1}^{T} a8 + b8\cdot T + c8\cdot T^2 + d8\cdot T^3 \, dT}{T - T_1}$$

$$\Delta H_2 := (-2\cdot 241.8 + -110.5 - -74.5)\cdot 10^3 \qquad \Delta H_2 = -5.196\times 10^5$$

$$\Delta H_r := \left(x\cdot -393.5 + \frac{y}{2}\cdot -241.8 - -74.5 \right)\cdot 10^3 \qquad \Delta H_r = -8.026\times 10^5$$

135

$$y_n(y_o) := -y_o + 1$$

$$y_{stoic}(y_2) := \frac{1}{z} \cdot y_2 \qquad y_{air}(y_2) := 1 - \frac{1}{0.21} y_2$$

Linear equation theory:

Lower:

$$\alpha_L(T) := x \cdot Cp_4(T) + \frac{y}{2} \cdot Cp_5(T) - z \cdot Cp_2(T) - Cp_3(T)$$

$$\beta_L(T) := Cp_2(T) - Cp_3(T)$$

$$\gamma_L(T) := Cp_3(T)$$

$$y_{fL}(T, y_2) := \frac{\beta_L(T)}{\dfrac{-\Delta H_r}{T - T_1} - \alpha_L(T)} \cdot y_2 + \frac{\gamma_L(T)}{\dfrac{-\Delta H_r}{T - T_1} - \alpha_L(T)}$$

Upper between the UFL and UOL:

$$\alpha_U(T) := Cp_8(T) - Cp_3(T)$$

$$\beta_U(T) := \frac{1}{1.5} \cdot Cp_4(T) + \frac{2}{1.5} Cp_5(T) - \frac{1}{1.5} \cdot Cp_8(T) - Cp_3(T)$$

$$\gamma_U(T) := Cp_3(T)$$

$$y_{fU}(T, y_2) := -\frac{\dfrac{1}{1.5} \Delta H_2 + \beta_U(T) \cdot (T - 298)}{\alpha_U(T) \cdot (T - 298)} \cdot y_2 - \frac{\gamma_U(T)}{\alpha_U(T)}$$

Solving for Adiabatic Flame Temperature:
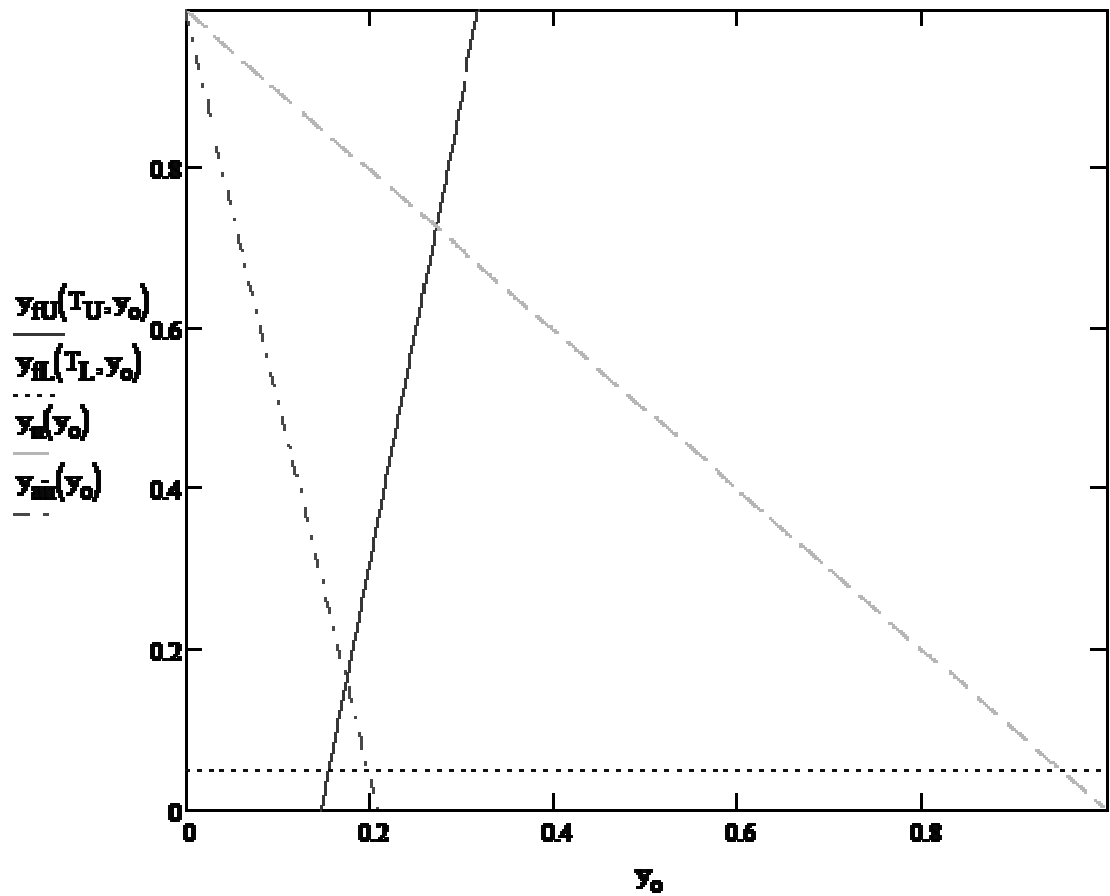
$T_{gU} := 1000 \qquad T_{gL} := 500$

Given

$y_{lfl} = y_{fL}\left[T_{gL}, (1 - y_{lfl}) \cdot 0.21\right]$

$y_{fU}\left[T_{gU}, (1 - y_{ufl}) \cdot 0.21\right] = y_{ufl}$

$\begin{pmatrix} T_U \\ T_L \end{pmatrix} := Find\left(T_{gU}, T_{gL}\right)$

$T_U = 1.88 \times 10^3 \qquad T_L = 1.481 \times 10^3$

··· Lower flammability zone boundary -- -- Oxygen boundary

——— Upper flammability zone boundary -- · -- · -- Air line

x-axis: fuel concentration   y-axis: oxygen concentration

Figure A4.1: A quick plot of the estimate of the upper flammability limit boundary between the UFL and UOL.

Calculation of limiting oxygen concentration and

pure oxygen limits using linear equation:

$y_{ggloc} := 0.2 \qquad y_{gguol} := .3 \qquad y_{gglol} := 0.95$

Given

$$y_{fU}(T_U, y_{ggloc}) = y_{fL}(T_L, y_{ggloc})$$

$$1 - y_{fU}(T_U, y_{gguol}) = y_{gguol}$$

$$1 - y_{fL}(T_L, y_{gglol}) = y_{gglol}$$

$$\begin{pmatrix} y_{loc} \\ y_{uolo} \\ y_{lolo} \end{pmatrix} := Find(y_{ggloc}, y_{gguol}, y_{gglol})$$

$y_{uol} := 1 - y_{uolo} \qquad y_{lol} := 1 - y_{lolo}$

$y_{loc} = 0.157$

$y_{uol} = 0.727$

$y_{uolo} = 0.273$

$y_{lol} = 0.05$

$y_{lolo} = 0.95$